Design, construction and evaluation of a vacuum evaporation system for the concentration of aqueous whey protein solutions

by

Munir Khetni

Thesis presented in partial fulfilment
of the requirements for the Degree

of

MASTER OF ENGINEERING
(CHEMICAL ENGINEERING)

in the Faculty of Engineering
at Stellenbosch University

Supervisor

Dr. Neill Goosen

March 2018

DECLARATION

By submitting this thesis electronically, I declare that the entirety of the work contained therein is my own, original work, that I am the sole author thereof (save to the extent explicitly otherwise stated), that reproduction and publication thereof by Stellenbosch University will not infringe any third party rights and that I have not previously in its entirety or in part submitted it for obtaining any qualification.

March 2018

ABSTRACT

Vacuum evaporation is an old and established technology for the industrial concentration of high water content streams. It is a clean, safe and versatile technology with low management costs. The aim of this study was to design, construct and evaluate a vacuum evaporation system, to increase the concentration of aqueous whey protein solution from 5 wt% to the highest possible solution concentration. The system functions to concentrate aqueous whey protein in order to reduce the volume of transportation and storage, thereby minimising costs. The raw material is pre-heated in the feed tank using a heating jacket at temperatures between 65^{o}C and 70^{o}C. It is then pumped by a centrifugal pump to a flash separator at 160 kPa abs through a throttling valve to obtain a pressure drop of up to 149 kPa abs, forming a two-phase mixture of vapour and liquid. The concentrated solution is recirculated until a required concentration is achieved. The vapour is condensed and the condensate, which may itself be a useful product in some applications, leaves the process.

The variables affecting the product composition include operating temperatures of between 65^{o}C and 70^{o}C, vacuum level (12 – 15 kPa abs), type of separator internals (half pipe or multi-cyclone), feed flow rate (275 to 350 ml/min), liquid retention time inside the flash separator (2 to 4 minutes) and cooling water flow rate (about 750 ml/min).

The design for the two-phase vertical flash separator was done at a ratio (L/D) of 4.8. It was found that the half-pipe internal device was not applicable to the WPC solution since it was foaming. By substituting the half-pipe for the multi-cyclone, the efficiency of the evaporator improved but still foaming persisted due to the laminar flow regime of the solution (inlet momentum of 38 kg/m-sec^{2}). The foaming was finally eliminated by adding antifoam.

The initial design of the VES employed direct preheating of the solution in the feed tank with a heating element. This resulted in fouling of the element as the WPC burnt and stuck to the element in the first hour of evaporation, thereby reducing the solids concentration from 10.8 wt% to 8.6 wt%. A modification was done to the preheating system by introducing a heating jacket for indirect heating. This modification managed to eliminate the fouling. The correlation between condensate recovery and solids concentration during evaporation improved with the modification from a coefficient of determination (R^2 = 0.6404 to R^2 = 0.9942) for direct and indirect preheating respectively.

The viscosity measurement was done at temperatures between 59^{o}C to 70^{o}C at a constant shear rate of 23/s. For WPC solutions with concentrations between 4.2 and 14.5 wt%, the viscosity remained constant with increasing temperatures until 62^{o}C, when it started increasing. For 17 wt% solutions of WPC, the viscosity increased with temperature from 59^{o}C.

The designed VES managed to concentrate the WPC solution to a maximum concentration of approximately 17 wt% at 65^{o}C and vacuum pressure of 13.3 kPa abs. The viscosity then began to increase and the solution became difficult to recirculate whilst attempting to further evaporate it beyond 17 wt%. Evaporating at 70^{o}C, although giving a higher evaporation ratio than 65^{o}C, caused burning of the solution when the concentration reached 11 wt%.

The heat transfer coefficient of the WPC solution with similar initial concentrations (around 5 wt%) was found to be higher at 70^{o}C (433.6 W/m^{2}.K) than at 65^{o}C (431.8 W/m^{2}.K). It was also found to be reduced with increasing solution concentration. When compared to sugar solution with similar initial concentration at 65^{o}C and 13.1kPa abs, the WPC solution was found to have a higher heat transfer coefficient (431.8 W/m^{2}.K and 396.3 W/m^{2}.K for WPC and sugar solution respectively). Due to the differences in heat transfer coefficient, the WPC solution had a higher evaporation ratio than the sugar solution at similar conditions.

OPSOMMING

Vakuum verdamping is 'n ou en gevestigde tegnologie vir die industriële konsentrasie van hoë-water-inhoud strome. Dit is 'n skoon, veilige en veelsydige tegnologie met lae bestuurs koste. Die doel van hierdie studie was om 'n vakuum verdamping stelsel te ontwerp, bou en evalueer, en om die konsentrasie van ‘n waterige wei proteïen-oplossing van 5 wt% na die hoogste moontlike oplossings konsentrasie te verhoog. Die stelsel funksioneer deur waterige wei-proteïene te konsentreer om die volume vir vervoer en stoor te verminder, en so ook koste. Die rou materiaal is vooraf verhit in die voertenk deur 'n verwarmingsbad by temperature tussen 65°C en 70°C. Dit word dan deur 'n sentrifugale pomp na 'n spoel skeier by 160 kPa abs deur 'n klep gestuur om ‘n druk daling van tot 149 kPa abs te verkry en 'n twee-fase mengsel van vloeistof en dampe te vorm. Die gekonsentreerde oplossing hersirkuleer tot 'n vereiste konsentrasie bereik word. Die dampe kondenseer en die kondensaat, wat opsig self ‘n gebruikbare produk is, verlaat die prosedure.

Die veranderlikes wat die produk samestelling beïnvloed sluit in ‘n temperatuur van tussen 65°C en 70°C, die vakuum vlak (12 – 15 kPa abs), tipe interne skeiding (halwe pyp of multi-sikloon), stroomsnelheid van die voering (275 – 350 ml/min), vloeistof retensie tyd binne-in die spoel skeier (2 tot 4 minute), en verkoelings water vloei tempo (ongeveer 750 ml/min).

Die ontwerp vir die twee-fase vertikale spoel skeier is teen ‘n verhouding (L/D) van 4.8 gedoen. Dit was gevind dat die halwe pyp interne toestel nie van toepassing op die WPC oplossing was nie as gevolg van skuiming. Deur die halwe pyp vir die multi-sikloon te verruil, was die doeltreffendheid van die verdamper verbeter maar skuiming het volhard as gevolg van die laminare vloei van die oplossing (inlaat momentum van 38 kg/m-sec^2). Die skuiming was uiteindelik uitgeskakel deur die toevoeging van antiskuimingsmiddel.

Die aanvanklike ontwerp van die VES het gebruik gemaak van direkte voorverhitting van die oplossing deur ‘n verhittingselement in die voertenk. Dit het gelei tot aanpakking van die element as gevolg van die aanbranding van WPC in die eerste uur van verdamping, en lei tot vermindering van die vastestof konsentrasie van 10.8 wt% tot 8.6 wt%. ‘n Verbetering van hierdie sisteem was gevind in 'n verwarmingsbad vir indirekte verwarming. Hierdie verandering het daarin geslaag om aanpaksels te elimineer. Die korrelasie tussen kondensaat

herstel en vastestof konsentrasie was verbeter met 'n koëffisiënt van bepaling (R^2 = 0.6404 na R^2 = 0.9942) vir direkte en indirekte voorverhitting onderskeidelik.
Viskositeit was by temperature tussen 59°C en 70°C gemeet teen 'n konstante wrywings spoed van 23/s. Vir WPC oplossings met konsentrasies tussen 4.2 en 14.5 wt%, het die viskositeit byna konstant gebly met toenemende temperature tot 62°C. Vir 17 wt% oplossings van WPC, het die viskositeit verhoog vanaf 59°C.

Die ontwerpde VES kon die WPC oplossing konsentreer tot 'n maksimum konsentrasie van ongeveer 17 wt% by 65°C en ‘n vakuum druk van 13.3 kPa abs. Die viskositeit het begin toeneem en die oplossing het moeilik geword om te sirkuleer terwyl daar gepoog is om verder te verdamp verby 17 wt%. Alhoewel daar 'n hoër verdamping verhouding by 70°C as 65°C was, het die hoër temperatuur verbranding van die oplossing veroorsaak vanaf ‘n konsentrasie van 11 wt%.

Die hitte oordrag koëffisiënt van die WPC oplossing met soortgelyke aanvanklike konsentrasies (ongeveer 5 wt%) was hoër by 70°C (433.6 W/m^2. K) as by 65°C (431.8 W/m^2. K). Dit is ook gevind om af te neem met toenemende oplossing konsentrasie. In vergelyking met suiker oplossings met soortgelyke aanvanklike konsentrasies by 65°C en 13.1 kPa abs, is daar gevind dat die WPC oplossing 'n hoër hitte oordrag koëffisiënt bevat (431.8 W/m^2.K en 396.3 W/m^2.K vir WPC en suiker oplossings onderskeidelik). As gevolg van die verskille in hitte oordrag koëffisiënt, het die WPC oplossing 'n hoër verdamping verhouding as die suiker oplossing in soortgelyke toestande gewys.

ACKNOWLEDGEMENTS

Firstly, my immeasurable gratitude goes to my Allah for inspiration and the ability to commence and complete this work.

Then to my supervisor: thank you Dr. Neill Goosen for academic guidance and input throughout the whole project. It was a great learning experience working under your supervision.

To workshop staff at Stellenbosch University for timeous fabrications, guidance and assistance through the design phase of the project. I am equally grateful to the laboratory staff, especially Mr Alvin for guidance and support.

To Glasschem Company, thank you for attending on time and taking your time to enlighten me on the operation of equipment.

I would also like to extend my gratitude to Dr. Fozi for general guidance and research expertise advice.

To friends, especially Witness, thank you for assistance and support in compiling this document. To Ayman, it was good to have you by my side throughout the long journey, from long back in Libya to Stellenbosch.

I am highly grateful to the Ministry of Higher Education and Scientific Research for research funding received from the Libyan government.

Finally, I tank whole heartedly my wife (Safa) and my daughter (Sadeem) for being my source of inspiration. You guys refreshed my mind when I was down. My father and mother, I cherished your support and consistent prayers to the great Allah. Thank you very much.

TABLE OF CONTENTS

LIST OF FIGURES

LIST OF TABLES

ACRONYMS

VES	Vacuum Evaporation System
FFE	Falling Film Evaporator
WFE	Wiped Film Evaporator
ATFE	Agitated Thin-Film Evaporator
FCE	Forced Circulation Evaporator
CFD	Computational Fluid Dynamics
GLR	Gas Liquid Ratio
WPC	Whey Protein Concentration

1. INTRODUCTION

1.1 BACKGROUND

Evaporation is often employed in industry to decrease the water content in a liquid stream. It can be employed as a stand-alone process, or to concentrate a solution before the removal of the remaining water. Evaporation is an attractive drying method as high-efficiency evaporation is significantly cheaper than other methods, as presented in Table 1-1. Evaporation is a key unit operation usually employed to remove the water from dilute liquid foods to obtain concentrated liquid products (Smith, 2011).

Table 1-1: Costs comparatives of water removal

Method of water removal	**Separation costs per unit volume of water removed (arbitrary units)**
Spray drying	17-50
Drum drying	10-25
Centrifugation	0.1-10
UF/RO	0.2-7
Evaporation	0.2-5

1.2 CONCENTRATION OF WHEY PROTEIN SOLUTIONS

Evaporation can be employed to concentrate food waste streams to recover valuable nutrients. Four major categories of food wastes can be identified from food processing (seafood, meat and poultry; fruit and vegetables; beverages and bottling; and dairies) (Ammar, 2014). Most of these operations consume large amounts of water, which require treatment before disposal to the environment. However, these waste streams still contain considerable amounts of valuable organic compounds like proteins, carbohydrates and lipids (Litchfield, 1987). Bough and Landes (1978) reported recoveries of proteins from waste streams of poultry chillers, fruitcake, egg washer wastes, cheese whey as well as meat processing, curing and packing.

Whey is a waste stream that is produced in large volumes from the dairy processing industry. It is the remaining liquid after the recovery of curds in the production of cheese and casein

from milk. Whey contains functional components (mainly proteins) which have nutritional value for humans (Renner and Abd-El-Salam, 1991; Smithers *et al.,* 1996). Its disposal therefore is both a loss of a potential food source, and an environmental burden. The world annual production of whey is over 160 million tonnes, of which 94% comes from cheese making and 6% from casein manufacture (Božanić *et al.,* 2014; Guimarães *et al.,* 2010). Other authors like Smithers (2008) estimate the annual global increase in whey production to be equivalent to 2%, increasing proportionally with milk production.

Of the total whey production, 70% is processed into a variety of products, whilst 30% is used for pig feeding, used as fertiliser or dumped into rivers (Božanić *et al.,* 2014). Using whey protein for agricultural applications is however low value and therefore not preferred. Efforts have been intensified in recent years to use whey proteins as replacement for other proteins and in improving the functional properties in other food products (Jeewanthi *et al.,* 2015; Spellman *et al.,* 2005). Smithers and colleagues (2007) reported approximately 700 000 tonnes of whey to be used globally as an ingredient in many foods and dairy products (Sminbbsathers *et al.,* 1996; De Wit, 1998). Foegeding and colleagues (2002) reported whey proteins to be mostly used as ingredients in medically active components.

Whey processing includes pre-treatment processes (filtration, separation and pasteurisation), ion exchange extraction, membrane filtration and evaporation before final concentration by drying processes. Pasteurisation leads to denaturation of whey proteins, as well as their association with casein micelles (Singh and Creamer, 1991). Some researchers (Oldfield *et al.,* 1998; Dannenberg and Kessler, 1988) reported denaturing of minor whey proteins (immunoglobulins and serum albumin) at about 65^{o}C, whilst the major ones (β-lactoglobulin (β-LG) and α-lactalbimin (α-LA)) begin to denature significantly above 70 to 75^{o}C. Singh and Newstead (1992) further suggested that evaporation of milk could be done at temperatures between 50 - 70^{o}C with minimal whey denaturation. The findings by Newstead (1992) were consistent with Singh and Creamer (1991).

Oldfield (1996) reported that whey proteins, due to their heat sensitivity, undergo permanent denaturation at temperatures above 60^{o}C depending on the protein content, temperature, pH and retention time inside the evaporator. However, when evaporating skim milk (concentration up to 49 wt% total solids) using a multiple effect evaporator, with further heat treatment at temperatures between 64 to 74^{o}C, Oldfield *et al.* (2005) found no substantial influence on the denaturation of β-LG and α-LA.

A variety of whey evaporation equipment exists in the dairy industry, their suitability depending on many factors such as costs, the liquid feed characteristics and its concentration (Minton, 1986; Todaro and Vogel, 2014). Evaporators like forced circulation, calandria and agitated film evaporators are more appropriate with heat sensitive material like whey proteins whilst the falling film and the natural circulation evaporators cannot handle heat-sensitive solutions. For low-cost operations, the natural circulation evaporator would be the most appropriate to use provided the solution does not scale, crystallise and does not carry solids in suspension (Minton, 1986; Todaro and Vogel, 2014; Parker, 1963; Glover, 2004). The agitated-film evaporator, although providing the best operating efficiency in all selection criteria, is a costly evaporator to use. For whey concentration, a suitable evaporation system must be able to operate at low temperatures (70^{o}C) and retention times, as well as be able to handle foaming liquids (Glover 2004, Parker 1963).

This study was undertaken to design a vacuum evaporation system (VES) to concentrate whey protein solution at temperatures lower than the boiling point of water, in order to limit the destruction of biological activity of the whey. The different types of evaporation systems, their advantages and disadvantages are discussed in Section 2. Also included in the discussions are the whey protein properties, especially its heat sensitivity, which determines the evaporation temperatures.

After proper selection of the evaporation, equipment followed the initial design of a laboratory scale vacuum evaporation (VES) system in Section 3. The designed VES was evaluated for suitability to concentrate foaming and fouling solutions using whey protein solutions. Foaming of the solution and fouling of the heating element were observed; therefore, some modifications were made to eliminate these two phenomena in Section 4. Physical and chemical methods for foam elimination, as well as the preheating methods were evaluated and the results are discussed in Section 4.

Having eliminated fouling and foaming in the evaporation system, the VES was then tested to determine if it could concentrate different types of solutions. Comparisons were made between solutions of whey protein concentrate and sugar with respect to rate of evaporation and the increase in solids concentration, as functions of feed temperature and initial concentration. The solutions' heat transfer coefficients were also compared under the same conditions. All the results and discussion are reported in Section 4. Section 5 discusses the conclusions and

recommendations drawn from the study, Section 6 is a reference list, and Section 7 contains the appendices.

1.3 PROBLEM STATEMENT

Problem in context

Whey is typically produced at low protein concentrations, (averaging 5%) and there is need to concentrate the product to a higher protein content so as to reduce the transporting and storage costs, as well as to improve its shelf life. Recovering and concentrating the whey proteins is also a way of preventing environmental contamination in cases where the whey is discarded into the environment. Other potential uses like crop fertilisation and pig feeding are low value applications. It is therefore more valuable to concentrate it and use it as a functional additive in human diet and medically active compounds.

Whey is denatured by high temperatures (higher than 70^{o}C), therefore the entire concentrating process should occur at 70^{o}C or lower. Whey is, however, a challenging material to concentrate as it is prone to foaming when heated, and precipitating amino acids and forming scaling on equipment surfaces. Since there exist a wide range of possible evaporator configurations and evaporation equipment, a system is required that would achieve the highest possible protein content at temperatures that preserve the protein functionality and bioactivity, whilst preventing equipment fouling and foaming, as the solids build up in the solution.

1.4 PROJECT AIMS AND OBJECTIVES

Given the context, the aim of the study was to design, construct and evaluate a vacuum evaporation system, to increase the concentration of aqueous whey protein solution from 5 wt% to the highest possible solution concentration.

The specific objectives were as follows:

i. To select a suitable circulation pump for the system through analysis of the preliminary system head loss and determine the system curves.

ii. To design a two phase vertical flash separator.

iii. To establish the effect of different flash separator internals and demisters on the efficiency of the vacuum evaporator.

iv. To determine the physical properties of whey protein concentrate (WPC) solution (viscosity, thermal conductivity, density and heat capacity) at different conditions (temperatures and solid concentration) in order to estimate the heat transfer coefficient for whey protein solutions in the particular equipment.

2. LITERATURE REVIEW

2.1 WHEY PROTEIN

Whey is a valuable by-product resulting from cheese and casein manufacture. Up to 80% of the milk processed for casein and cheese manufacturing leave the process as whey, accounting for about 50% of the original milk's solids content (Asghar *et al.*, 2007; Bylund, 1995). The whey solution contains water and some valuable compounds like proteins, lactose, milk fat, minerals and lactic acid (Morr, 1989).

Protein constitutes about 3.6% of cow's milk, of which 20% is whey and 80% casein (Bylund, 1995). According to Smithers (2008), whey protein was discovered over 3000 years ago and plays a critical role in the food industry as a functional ingredient (Pintado *et al.*, 1999; McIntosh *et al.*, 1998; Frid *et al.*, 2005; Ha and Zemel, 2003). The types of whey proteins are α-lactalbumin (α-LA), immunoglobulins (Igs), bovine serum albumin (BSA), β-lactoglobulin(β-LG), lactoferrin (LF), as well as lactoperoxidase and glycomacropeptides (GMPs) (Bonnaillie and Tomasula, 2008; Whitney, 1988; Miller *et al.*, 2000).

Whey is processed into many commercial products such as whey protein isolate (WPI), whey protein concentrate (WPC) and whey protein hydrolysates (WPH). Other products include mineral whey, whey powder, whey permeate and demineralised whey (Foegeding and Luck, 2011; Jovanović *et al.*, 2005; Mulvihill, 1992).

2.1.1 Whey protein denaturation

The globular native protein structure determines the functional properties (e.g. solubility, emulsification and gelation) of the whey protein. To preserve the functionality, it is therefore critical to avoid protein denaturation during whey processing. By definition, protein denaturation is any changes to the protein structure (secondary and tertiary structure) without rupturing the peptide covalent bonds (Swaisgood and Fox, 1992). It can also be defined as the breaking of hydrogen bonds and hydrophobic interactions, which result in the unfolding of a protein (Jovanović *et al.*, 2005).

Donovan and Mullvihill (1987) described proteins as heat sensitive, with sensitivity decreasing in the order: α-lactalbimin > β-lactoglobulin > BSA > immunoglobulins. They reported denaturation to occur in a two-phase process, beginning with the unfolding, which is then

followed by aggregation. Klarenbeek (1984) and Maćej (1983) reported that although whey proteins will start denaturing at 65^{o}C, most of the denaturing occurs at temperatures above 80^{o}C. Duranti and colleagues (1989) reported critical heating of whey protein for denaturation to be 85^{o}C, 5^{o}C above Maćej (1983)'s 80^{o}C, whilst Hillier and Lyster (1979) put the temperature interval at 70-80°C.

Temperature and pH influence the rate of denaturation (Paramalingam, 2004). The denaturation is known to be increasing exponentially with increasing temperature. Solution concentration is also reported to influence whey protein denaturation, with high concentration tending to break the hydrogen bonds. Pierre *et al.* (1977) and later McMahon *et al.* (1993) reported that the denaturation level of total whey protein increases with total protein concentration by using the ultrafiltration process. The result resonates with the findings of Oldfield (1996) who also found the degree of denaturation to depend on the protein component, pH, temperature, total protein content as well as time of exposure.

Due to the significant dependence of denaturation on evaporation temperature, it is critical that the temperature is selected such that there is minimum whey protein degradation. Since higher temperatures increase the rate of evaporation, a balance has to be maintained between the increase in evaporation rate and the sensitive nature of whey proteins. Other measures, like introduction of vacuum systems, can also be taken to mitigate denaturation and achieve a high rate of evaporation at the same time. Vacuum evaporation systems allow boiling of the solution at temperatures below the denaturing level of whey proteins.

2.1.2 Whey protein processing

Cheese whey processing begins with pre-treatment (separation, filtration and pasteurisation) to remove fat and fines, as well as improving its bacteriological quality (Zeman, 1996; Brans *et al.,* 2004; Rektor and Vatai, 2004; Saxena *et al.,* 2009). After the pre-treatment, it then undergoes extraction in ion exchangers to minimise fat and lactose content (Stanic *et al.,* 2012). The membrane filtration process then follows where the aqueous whey stream is split into a protein concentrated permeate and retentate fraction of low molecular weight molecules (Atra *et al.,* 2005). Final concentration of the whey protein is then undertaken using the evaporation process, before drying, to produce whey protein concentrate (Paramalingam, 2004). However, the process of evaporation is discussed in more detail in the subsequent sections.

2.1.3 Physical properties of the whey protein solution

The physical properties of the whey protein solution are critical in the design of evaporation equipment, since most models used for design depend on them. The properties (including density, heat capacity, thermal conductivity and viscosity) are in turn dependent on the composition of the whey and the temperatures at which they are measured. Different researchers described the physical properties of dilute solutions of whey (Bylund, 1995; De Wit, 1989; Vélez-Ruiz and Barbosa-Cánovas, 1998; Middleton, 1996; Bloore and Boag, 1981; Snoeren *et al.*, 1982; Fernandez-Martin, 1972).

The literature is rich with semi-empirical and theoretical models of the physical properties of milk (Snoeren *et al.*, 1982; Bloore and Boag, 1981; Murakami and Okos, 1989; Fernandez-Martin, 1972; Jeurnink and De Kruif, 1993; Bertsch, 1983; Housˇka *et al.*, 1994; Middleton, 1996), whereas a few describe the whey protein solution (Housˇka *et al.*, 1994; Buma, 1980). These models cannot be applied to whey proteins because they are appropriate for protein concentrations of between 25 – 37% whereas the whey protein in this study has lower concentrations (5 - 20 wt%). However, some semi- empirical models developed by Murakami and Okos (1989) for foodstuffs can be applied to whey protein solutions, since they do not have restraints to protein content.

Density

The density of the whey protein solution is a critical factor in the design of evaporation systems. Density is significantly influenced by the solution concentration, increasing roughly by 26 wt% under increased concentrations (Schwartzberg, 1989). Models in literature for whey products (Murakami and Okos, 1989; Singh and Heldman, 2001; Buma, 1980) show that the density of the solutions increase as the total solids concentration increases. Other researchers like Choi (1986) and Murakami and Okos (1989) developed models for food solutions (protein, carbohydrates, fat) applicable in the temperature range of -40°C – 150°C (Equation 2-1).

$$\frac{1}{\rho} = \sum \frac{w_i}{\rho_i} \qquad \text{Equation 2-1}$$

Where;

w_i - Mass fraction of the component in the solution (Kg/kg)

ρ_i - Density of component in the Solution (Kg/m^3)

ρ - Density of the total solution (kg/m^3)

Viscosity

Different authors like Tang and colleagues (1993), Hermansson (1975) and Herceg *et al.,* (2002) studied the rheological behaviour of WPC solutions. Tang *et al.* (1993) reported Newtonian behaviour for WPC solutions of a concentration with less than 10 wt%. Investigations by Hermannson (1975) and Herceg *et al.* (2002) also found dilute WPC solutions of up to 10 wt% to have Newtonian behaviour. Tang *et al.* (1993) further reported that WPC solutions with apparent viscosity between 15 - 20 wt% and a pH of 6 decreased marginally with shear rate lower than 50/s. The viscosity ceased to be influenced at shear rates above 50/s. WPC solutions of between 40 – 50 wt% were found to be pseudo plastic (Alizadehfard and Wiley, 1996).

The behaviour of WPC solutions can therefore be concluded to depend on the concentration and shear rate. Lower concentrations (below 10 wt%) have been shown to have Newtonian behaviour. Increasing the concentration of the WPC solutions to between 10 – 20 wt% however changes their behaviour to pseudo plastic if the shear rate is low (at most 50/s), finally becoming independent of shear rate when the shear rate is increased beyond 50/s.

Viscosity is considered to be one of the critical input variables in the concentration of protein solutions (Mackereth *et al.,* 2003). The protein solutions viscosity is generally influenced by their concentration and shape of the protein molecules (Cohn and Edsall, 1965), their size (Kirkwood *et al.,* 1949), as well as their molecular weight, flexibility and the intermolecular interactions (Blake *et al.,* 1965; Kendrew *et al.,* 1961). Viscosity is further dependent on external factors such as pH, temperature, composition and heat treatment among others (Bloore and Boag, 1981; Snoeren *et al.,* 1982).

Viscosity significantly increases during evaporation as concentration increases, and it does so in a non-linear fashion. Rapid changes in viscosity are observed with small changes in concentration at high concentrations (Snoeren *et al.,* 1982). Such increases may result in

reduced flow rates, decreases in turbulence and high fouling rates. Lewis (1993) reported a sharp rise in viscosity above 35% solids content for skim milk concentrate.

Thermal conductivity

Lewis (1987) and Schwartzberg (1989) reported thermal conductivity to be strongly influenced by the moisture content for most foods, and generally decreasing by at least 35% during evaporation. Murakami and Okos (1989) as well as Singh and Heldman (2001) using Equations 2-2 and 2-3, found the thermal conductivity of whey protein solutions to decrease with increasing total solids concentration, given by Equation 2-2.and 2-3 within the temperature of -40-150 ^{o}C.

$$K = \sum \emptyset_i \, K_i \qquad \text{Equation 2-2}$$

$$\emptyset_i = \frac{w_i}{\rho_i \sum \frac{w_i}{\rho}_i} = \frac{w_i \, \rho}{\rho_i} \qquad \text{Equation 2-3}$$

Where;

K_i - Thermal conductivity of the component (W/m.K)

$\emptyset_i$ - Volume fraction of the component (kg/kg)

K - Thermal conductivity of the solution (W/m.K)

ρ_i - Component's density (Kg/m^3)

ρ - Density of the total solution (Kg/m^3)

Heat capacity

The overall heat capacity of whey protein depends on the different components in the solution, so its estimation requires the knowledge of the heat capacities of constituent components. Schwartzberg (1989) and Bertsch (1983) when investigating the heat capacity of milk, found it to be decreasing with temperature by 38 wt% over a temperature range of 50-140^{o}C.

The semi- empirical models for whey products were given by Equation 2-4 (Singh and Heldman, 2001; Housˇka *et al.*, 1994; Murakami and Okos, 1989):

$$C_p = \sum w_i \, C_{pi}$$ Equation 2-4

Where;

C_p - Heat capacity of the solution (kJ/(kg·K))

C_{pi} - Heat capacity of the component (kJ/(kg.K))

w_i - Component mass fraction.

2.2 EVAPORATION

Evaporation is a thermal process utilised for the concentration of aqueous solutions, emulsions or suspensions by boiling off and removing the volatile solvents in an evaporator (Harker *et al.*, 2013), and it is a common water removal technique in the dairy industry (Fergusson, 1989). The evaporation process consumes huge amounts of energy and has been used in many processes, including food processing, chemicals, pharmaceuticals, sugar industries, and paper and pulp industry (Al-Najem, Ezuddin et al. 1998, McCabe, Smith et al. 1993). In some instances, the evaporated, volatile component is condensed and collected as the main product (Standiford, 2005).

In the dairy industry, manufacturing of powdered whey products employs evaporation as a final concentration stage before drying. Evaporation improves the whey quality and reduces the costs involved in the drying process. Since whey proteins are heat sensitive, it is usually evaporated under negative pressure to obtain the boiling point of the solution at lower temperatures (Fergusson, 1989).

Some applications of evaporation are listed below;

i. Reduction of the product volume to economise on packaging, handling and storage costs (Brennan, 2006; Nelson and Tressler, 1980; Ashurst, 2013).
ii. Manipulating the form of a product, e.g., sugar from cane or NaCl from brine. (Brennan *et al.*, 1990; McGinnis, 1971; Meade and Chen, 1977).
iii. Removing impurities, e.g., NaCl from sugar (Standiford, 2005).
iv. Precipitation of main contaminants from products, e.g., the precipitation of NaCl from caustic soda (Standiford, 2005; Lopez-Toledo, 2006).

v. Recycling of resources, e.g., spent cooking liquor in a pulp mill can be concentrated and used as a source of energy (Standiford, 2005; Lopez-Toledo, 2006).
vi. Concentrating waste before disposal, e.g., nuclear reactor waste and cooling tower blowdown streams (Pabby *et al.*, 2008).
vii. Recovering by-product streams for as products, e.g., the concentration of spent distillery slop into animal feed (Standiford, 1983; Standiford, 2005).
viii. Distilling impure streams of water to recover distilled water, e.g., seawater and brackish water (Frankel, 1960).

2.2.1 Evaporator types

Evaporators designs and modes of operation vary widely according to the requirements of the solutions under evaporation (Billet and Fullarton, 1989; Minton, 1986; McCabe *et al.*, 2001). The various evaporator types can be classified using different criteria, one method being how the heating medium and the evaporated liquid are separated while still allowing thermal contact (Todaro and Vogel, 2014; Green and Perry, 1973). Methods of separation of the heating media and the liquid include the following:

- Using tubular surfaces to separate the evaporating liquid from the heating medium.
- Using jackets to confine the heating medium.
- Heating medium brought into direct contact with evaporating liquid (e.g., a submerged combustion evaporator).
- Using solar energy for heating.

Evaporators can further be subdivided into those using natural circulation or forced circulation, or whether they employ rising or falling films (Al-Najem *et al.*, 1998; McCabe *et al.*, 1993; Standiford, 2005). The majority of evaporators available in industry are fitted with tubular heating surfaces. They can further have the heating liquid inside or outside the tubes. These evaporators use forced circulation of the heating liquid in heating surfaces (mechanical methods) (Minton, 1986).

The time required to attain a set concentration can be reduced by either raising the evaporation temperatures or by exposing it to higher surface areas (Todaro and Vogel, 2014; Minton, 1986; McCabe *et al.*, 1967). However, high temperatures and high residence times thermally degrade some solutions (e.g. whey proteins); therefore, it is critical in such instances to keep the

residence time and operating temperature as low as possible (Parker, 1963; Glover, 2004; Sinnott, 2005; Todaro and Vogel, 2014).

The evaporators like the forced circulation, rising falling film, plate and agitated thin film as well as the falling film evaporators are suitable for fouling, foaming, high temperature sensitive and viscous solutions like whey protein (Fergusson, 1989; Minton, 1986). These evaporators will therefore be discussed further in the succeeding sections.

Film-Type Evaporators

The long-tube falling film evaporator (FFE) is presented in Figure 2-1. The liquid product is introduced from the top of the evaporator and is evenly distributed to the heating tubes in the head. Upon entering the heating tube, the liquid is partially evaporated, and the liquid and the vapour both move downward in a parallel flow. The heat exchanger and the separator at the bottom part of the evaporator separate the liquid and its vapour. The FFE is popular for heating sensitive material due to its low holdup time. Its other advantages are its superior heat transfer, even at low temperature differences, cost effectiveness as well as superior vapor-liquid separation characteristics (Glover, 2004). The major drawbacks of the FFE are its high space requirements, need for recirculation and unsuitability for scaling materials. The FFE is mostly applicable for concentration of dairy products, sugar solutions, black liquor and phosphoric acid (Glover, 2004; Todaro and Vogel, 2014).

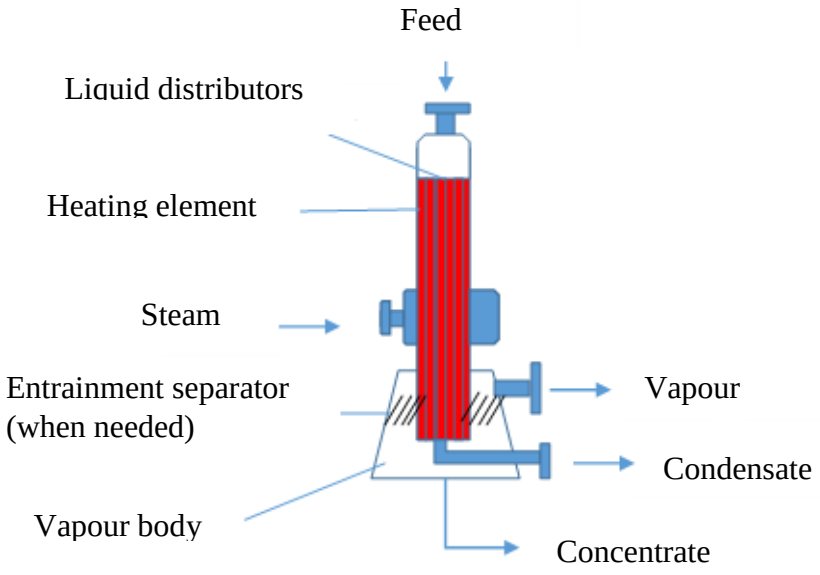

Figure 2-1: Falling-film evaporator (redrawn from Glove, 2004)

Wiped Film Type Evaporator

The wiped film evaporator (WFE), also referred to as the agitated thin-film evaporator (ATFE) is usually employed to concentrate high viscosity liquids (up to 10^5 poise), heat-sensitive solutions as well as materials that require short heating times (Glover, 2004). The WFE evaporators are usually found in vertical orientations (Figure 2-2). The liquid feed material flows downwards, with axially arranged blades constantly mixing it and turning it into a thin film. The WFE can run on low pressures, and can have low pressure drops when compared to other types of evaporators. The WFE evaporators are preferred for their short heating times, high heat transfer coefficients as due to turbulence induced by the rotor, their plug flow behaviour and the ability to evaporate concentrated, viscous solutions. They also cause less product decomposition (Hyde and Glover, 1997; Freese and Glover, 1979). Their major drawbacks are however their high cost and inability to recompress vapour for energy recovery. They are commonly employed in food and pharmaceutical (e.g. enzymes, and biological

solutions) concentration procedures as well as in recovery of valuable compounds from waste streams (e.g. reduction of inorganic NaCl streams volumes).

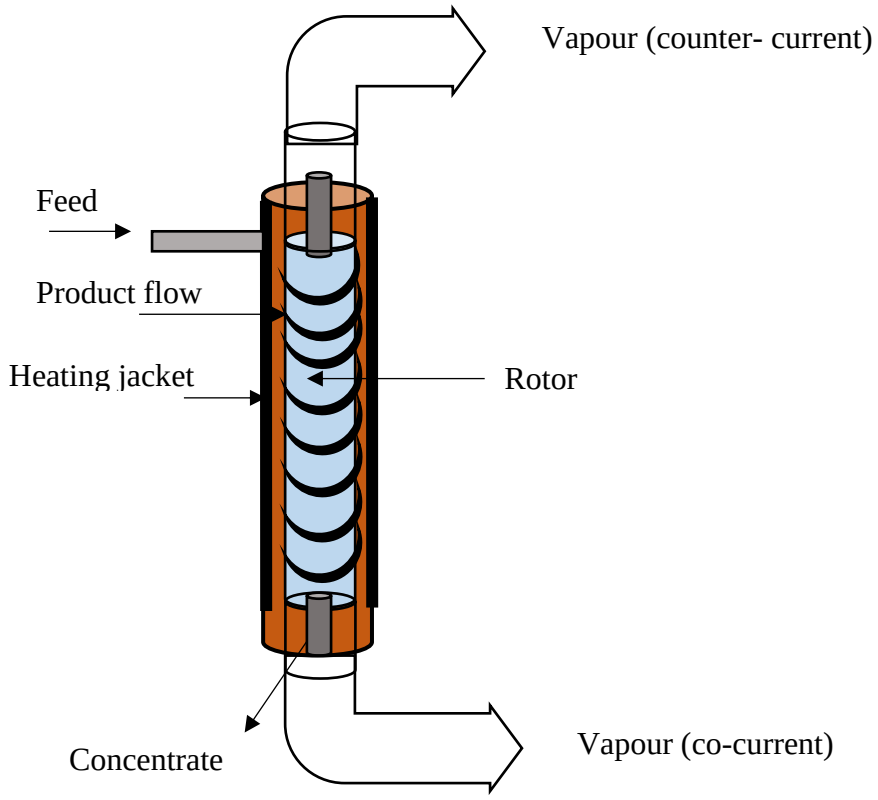

Figure 2-2: Agitated thin-film evaporator (redrawn from Glover, 2004)

Rising film evaporator

The rising film evaporator is also called a long tube vertical evaporator (Figure 2-3). This evaporator type is widely used in industry (Minton, 1986). It is made up of a shell-and-tube heat exchanger combined with a liquid-vapour separator. The evaporator, although occupying little floor space, requires a high headroom. Recirculating systems are performed as either a batch or continuous operations. Boiling induces circulation of fluid across the heat transfer surface (Glover, 2004). A further advantage of these evaporators is their ability to handle foamy solutions as well as their high heat transfer coefficients owing to their partial two-phase flow. They however denature sensitive solutions due to their high hydrostatic heads at the bottom, which may case high product temperature.

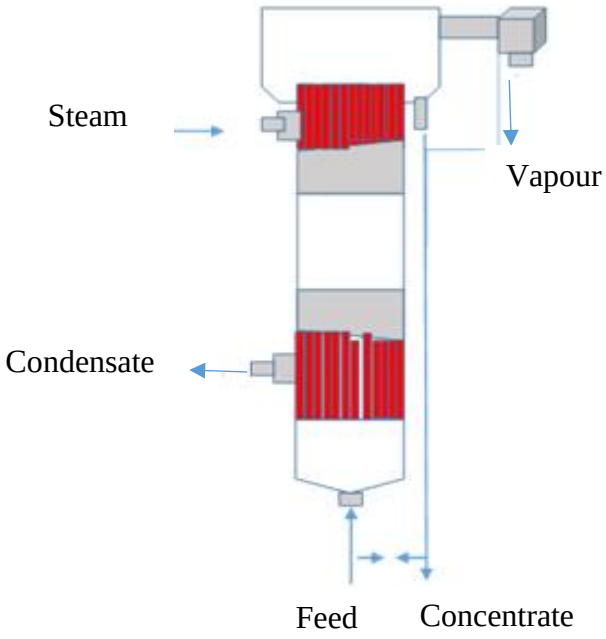

Figure 2-3: Long-tube rising-film vertical evaporator (redrawn from Glover, 2004)

Rising/ falling film evaporators

The two evaporators (rising-film and the falling-film) are often combined as shown on (Figure 2-4) in order to benefit from the advantages of each type of evaporator. A single tube bundle is divided into two sections, a rising film and a falling film. This results in a high evaporation to feed ratio, suitable for viscous solutions (Minton, 1986; McCabe *et al.*, 1993). The rising film evaporator is diagrammatically presented on Figure 2-4. The rising/falling film evaporator's residence times are low, has high heat transfer rates, is relatively economic and has low hold up. Its disadvantages include the requirements for large space and unsuitability to fouling solutions like whey proteins (Minton, 1986, Glover, 2004).

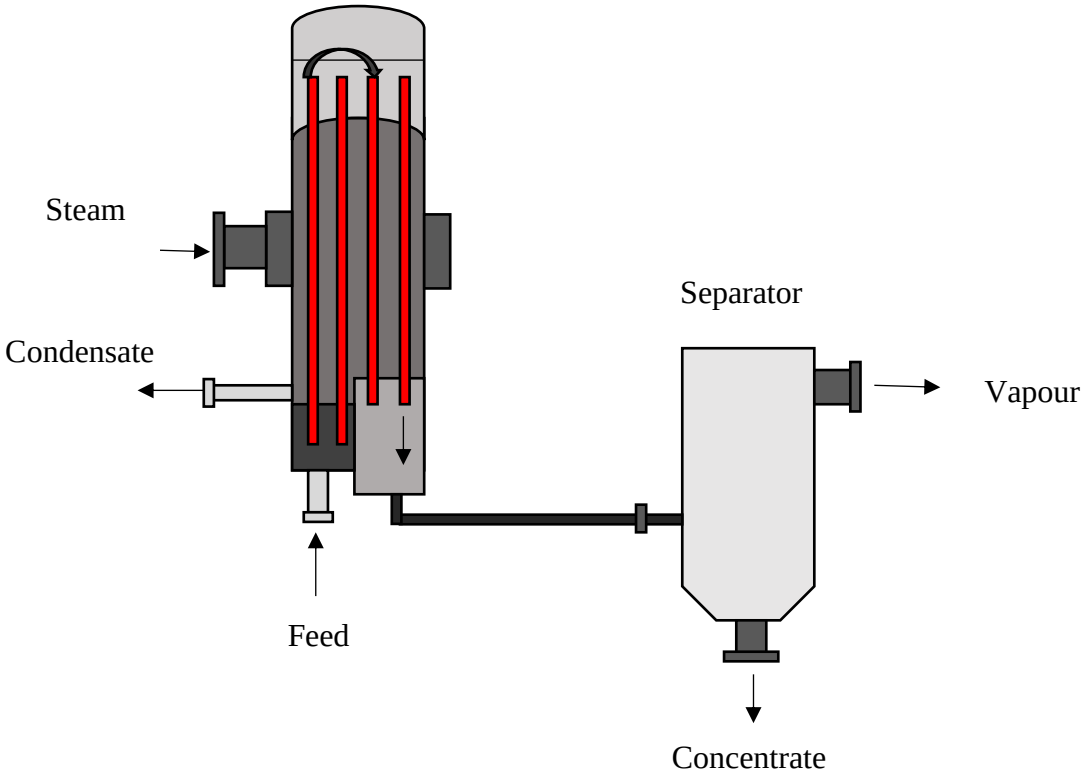

Figure 2-4: Rising/failing-film evaporator combines (redrawn from Glover, 2004)

Gasketed Plate Evaporator

The gasketed-plate evaporator is also referred to as the plate evaporator due to its similarity in design to the plate heat exchanger as shown in Figure 2-5. Many embossed plates with openings at the four corners are mounted on a top and bottom carrying bar. The interfering gaskets on adjacent plates separate the fluid and guide it to the respective corner openings. Both series and parallel liquid flow are known to exist as per the gasket design. The evaporator's high turbulent flow through small passages improves the heat transfer coefficient. The gasket plate evaporator is popular with high viscosity, foaming, fouling and heat-sensitive solutions, usually of food products, pharmaceuticals, emulsions, glue, etc, (McCabe *et al.*, 1993). It also requires low headroom. Its disadvantage is its large gasketed area, which makes it prone to leaking (Minton, 1986). The gasket plate evaporators are commonly used in removing monomers from polymers, stripping applications and deodorisation (Glover, 2004).

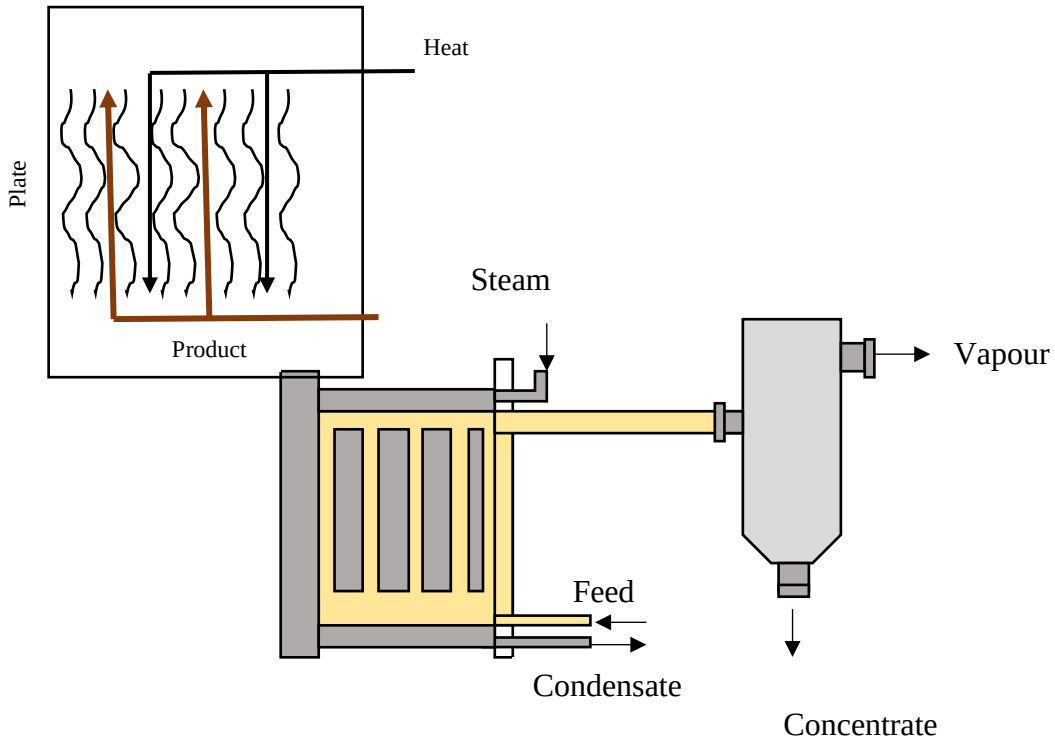

Figure 2-5: A gasketed plate evaporator (redrawn from Glover, 2004)

Forced Circulation Evaporators

The forced circulation evaporator (FCE) is the most expensive evaporator, although it has the widest applicability. Its major component is a shell and tube heat exchanger (either horizontal or vertical) (Minton, 1986). The flash chamber is fitted above the heat exchanger with a circulating pump provided to circulate the liquid (Figure 2-6), (Standiford, 2005). The recirculation of the concentrate back to the feed stream however increases the heat transfer, leading to a reduction in the size of the evaporator, thus lowering the costs. The forced evaporators are mostly used for solids containing solutions (Glover, 2004). Their major advantages are the high heat transfer coefficients, positive circulation and their ability to reduce fouling. Disadvantages include high costs, high power consumption and longer product hold ups. The forced circulation evaporators are typically used for citric acid, caustic potash, urea and magnesium chloride among other uses.

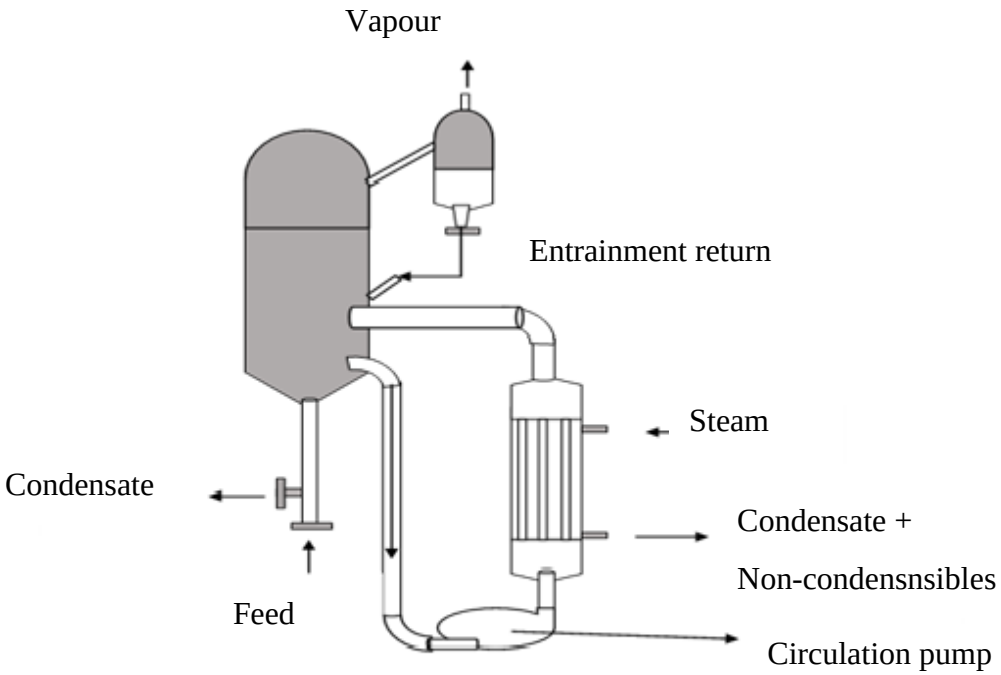

Figure 2-6: Forced circulation evaporator (redrawn from Standiford, 2005)

2.3 EVAPORATORS AND EVAPORATOR SYSTEMS.

The evaporator's primary function is to increase the concentration of a solution. There are three principal components of evaporator design; heat transfer, energy efficiency and vapour-liquid separation. An evaporator system is usually employed where a series of different types of evaporators are installed. Since all evaporators work on the principle of addition of thermal energy across a heat transfer surface, they are considered to be functionally heat exchangers. The following factors must be considered when designing an evaporator to make it efficient (Todaro and Vogel, 2014):

i. Ability to significantly heat the solution using a small heating surface area: This is a critical factor in evaporator design as the type, cost, and size of the system depends on it.

ii. Obtaining the specified liquid and vapour separation using the simplest devices available: Separation of evaporated vapour and liquid may be necessary for some reasons, e.g. to recover valuable components in the vapour or the fluid which would otherwise be lost.

iii. Energy efficiency: Evaporator performance is usually rated by its steam economy, or the amount of energy required to achieve the evaporation of an amount of solvent. Making provisions for heat exchange between the unheated starting fluid and the relatively high-temperature fluid leaving the condenser may improve energy efficiency (Minton, 1978).

iv. Considering the solution specifications: critical specifications include the quality of the product, product denaturation, foaming and hold up, as well as whether the product is corrosive, salts or scales. These factors are further discussed in the subsequent sections.

2.3.1 Factors affecting evaporator design

Major factors to be considered when designing an evaporation system include the characteristics of the liquid feed and its concentration. These characteristics can significantly influence the mechanical design, geometry, and type of evaporator. The major properties are listed below (Todaro and Vogel, 2014; Minton, 1986; McCabe *et al.*, 1967):

Concentration: Most physical characteristics of dilute solutions are dependent on the solvent used. However, as the solution increases in concentration, its properties may significantly change. Whey protein solutions properties, such as viscosity and density normally increase with increasing concentration, thereby reducing the heat transfer performance. Some liquids may form crystals at higher concentrations, with the potential to plug the heat transfer surface. Increasing the solution concentration also increases its boiling point, thus reducing the evaporation efficiency. This limits the evaporation to low concentrations (Singh, 2007).

Foaming: Foam can be defined as colloidal systems that form when gas bubbles cluster together, with thin liquid films separating them (Damodaran, 1997). Whey protein solutions may foam during evaporation as a result of air entrapment by protein (Lakkis and Villota, 1990; USDEC, 2004; Zhu and Damodaran, 1994). They are considered as foaming agents because they can unfold and adsorb at the boundaries between the two phases (dispersed and continuous) (Borcherding *et al.,* 2008; Tamm *et al.,* 2012). The presence of foam in separating vessels results in three major complications to a separating system. Firstly, it results in the addition of another phase (the emulsion phase) to the system, thereby complicating the mechanical control of the vessel liquid level. The second phase also occupies more vessel space and disrupts the normal vessel operation since its volume to weight ratio is much larger than liquids. Lastly, the separation of liquid and vapour phases becomes a difficulty when the foam is uncontrolled. There will be entrainment of foam in both phases (Stewart and Arnold, 2008). To reduce the effects of foaming in evaporators, antifoaming agents can be employed or foam can be mechanically broken by using mechanisms that disrupt the foam structure (e.g. multicyclone internals). Operating at low liquid levels is also one strategy used to limit foaming (Perry *et al.,* 1984).

Temperature sensitivity: Heat sensitive solutions must be either heated at low temperatures or exposed to heat for short residence times to avoid denaturation. Three possible alternatives can preserve the heat sensitive solutions during evaporation. These include minimization of the product volume in the evaporator, time in the evaporator and employing vacuum into the system to reduce the boiling point of the solutions (Glover, 2004). For whey proteins solutions, their sensitivity and denaturation were discussed in Section 2.1.1.

Scaling: Scaling is defined as the growth or piling of materials whose solubility decrease with increasing temperature on evaporator heating surfaces, although it sometimes results from a chemical reaction (Glover, 2004). Solids are deposited on hot evaporator surfaces during evaporation, inhibiting heat transfer and causing tube blockages. There is therefore need to regularly remove the deposits, usually during process shutdowns (Minton, 1986).

Fouling: Fouling is formation of solid deposits on evaporator heating surfaces. During evaporation of whey protein solution, proteins may form deposits on the evaporator surfaces, thereby causing fouling. The major variables influencing fouling are the processing conditions like temperature, fluid velocity and pressure (Bansal and Chen, 2006). Fouling increases resistance to heat transfer and hinders fluid flow (Taborek *et al.*, 1972). It causes losses in cleaning chemicals and reduces plant capacity as a result of maintenance and cleaning shut downs. It also increases costs (both operating and capital) as heat transfer equipment are then over-designed to accommodate fouling (Fryer and Belmar-Beiny, 1991). Dairy processing unit operations might require fouling related downtime every 8 -12 hours (Fryer and Belmar-Beiny, 1991; Delplace *et al.*, 1996). Although the downtime required for evaporator cleaning due to fouling is normally 2 hours, it can increase to 4 hours depending on the type of chemicals used for cleaning and extent of the fouling (Woodshead, 1997).

Corrosion: Higher liquid velocities are usually found in evaporators than other equipment, so both corrosion and erosion are common (Minton, 1986). Corrosion is a critical decisive factor in selection of evaporator material of construction (Glover, 2004). Corrosion therefore greatly influences evaporator type selection. Corrosion resistant materials are more expensive and have high heat transfer coefficients (Minton, 1986).

Quality of the product: Increased product quality and purity are usually a result of low holdup and low operating temperatures. Usually, special alloys and other high-grade materials of construction that facilitate high heat transfer rates produce products of high quality (Minton, 1986).

2.3.2 Selection of evaporators

The major requirements for evaporator designing are as follows (Niro Inc, 2005):

i. Operational parameters like solution concentrations, operation temperatures and evaporator capacity.
ii. The characteristics of the solutions, including thermal sensitivity, viscosity, foaming tendency, etc.
iii. Available utilities (steam, cooling water, electric power, etc).
iv. The costs of operation and capital expenditure.
v. Manufacturing conditions and standards.
vi. Construction materials and adopted types of finishes to surfaces.
vii. Prevailing conditions at site, like climate, infrastructure and space availability.
viii. Regulations pertaining to health and safety and environmental concerns.

A selection guideline for industrial evaporator design is given in Table 2-1 (Parker, 1963; Glover, 2004; Sinnott, 2005):

Table 2-1: Selection guide of evaporator (Parker, 1963; Glover, 2004; Sinnott, 2005)

Evaporators type	**Feed condition**							**Suitable for heat sensitive material**	**Retention time (s)**
	Viscosity, cP			**Foaming**	**Scaling or fouling**	**Crystals producing**	**Solids in suspension**		
	High viscosity > 1000	**Medium viscosity 100 to 1000**	**Low viscosity <100**						
Calandria (short-tube vertical)		—	—	—	—	—	—	No	168
Forced circulation		—	—	—	—	—		Yes	41.6
Falling film			—					No	Not available
Natural circulation			—	—				No	16
Agitated film (single pass)	—	—	—	—	—	—	—	Yes	1.0
Long-tube falling film			—					Yes	Not available
Rising-Falling			—	—				Yes	Not available

2.3.3 Heat transfer in evaporators

The heat transfer coefficient is an important factor in evaporator design, knowledge of which can reduce equipment cost and improve the design of evaporators (Kandlikar, 1990; Miranda and Simpson, 2005). Factors influencing the heat transfer coefficient include the liquid viscosity, thermal conductivity, its density, as well as surface tension. Fluid temperature and feed flow velocity also play a part. There are also process conditions like heat flux and pressure at boiling point as well as the design of the heating surface that influence the heat transfer coefficient (Adib *et al.*, 2009; Bergman *et al.*, 2011).

Energy transfer through heat transfer occurs along a temperature gradient within any system. Heat transfer is the major factor to be considered when designing an evaporator since the evaporator heating surface is the largest cost driver. Comparisons between evaporators are done using an index of the ratio of the heat transferred as a function of unit time and unit temperature difference for a unit investment. The evaporator with the highest ratio is the most efficient given the same operating conditions (Todaro and Vogel, 2014). Typical overall heat transfer coefficients for different types of evaporators are presented in Table 2 -2.

Table 2-2: Overall heat transfer coefficients for different evaporators (Dutta, 2006)

Types of evaporators	**Overall heat transfer coefficient ($W/m^2 .^oC$)**
Long-tube vertical evaporator	
Natural circulation	1000-2700
Forced circulation	2000-7500
Short-tube vertical or calandria evaporators	750 -2500
Agitated - film evaporators	
Low to medium viscosity (< 1 P)	1800 – 2700
High viscosity (>1P)	1500
Falling film evaporators (viscosity < 0.1 P)	500 -2500
Rising film evaporators	2000 -5000

Components making up the evaporation systems include a heat source, a separator, a condenser and a vacuum device. The heat source supplies sensible heat that, raises the solution to its boiling point, and provides the latent heat of vaporisation whilst the separator removes vapour from the concentrated liquid phase. The condenser serves to condense the vapour and remove it from the system and finally, the vacuum device lowers the boiling point of the solution and maintains a lower evaporation temperature.

Since separators are the major components of evaporator systems, the design and selection of a separator for whey protein solutions concentration is further discussed in the subsequent section.

2.4 FLASH SEPARATION DESIGN

2.4.1 Background

Liquid/vapour separators are a common type of process equipment. Information on their design is readily available in technical papers and corporate process engineering design guidelines (Svrcek and Monnery, 1994). Separator technology is invaluable in gas-liquid processes to remove the liquid from the gas stream. Three principles: gravity settling, momentum and coalescing work to effect the physical separation in separators. Figure 2-7 is a diagrammatic representation of a flash separator, showing its major components (Bothamley, 2013a). Phase separation plays an integral part in most chemical engineering processes, for separation of products from by-products, protecting sensitive equipment from moisture and releasing hazardous gases (Wenten and Chandranegara, 2008). Separators are categorised by their geometrical configuration, as either vertical or horizontal (Mokhatab and Poe, 2012). They can also be classified by their functionality, as either two-phase or three-phase separators, according to their operating pressure (high [6500 – 10300 kPa], medium [1500 – 4800 kPa] or low [70 – 1200 kPa] pressure), or according to their application e.g. production, metering, low temperature, test and stage separators, as well as by their principles of operation (gravity settling, coalescing and centrifugation).

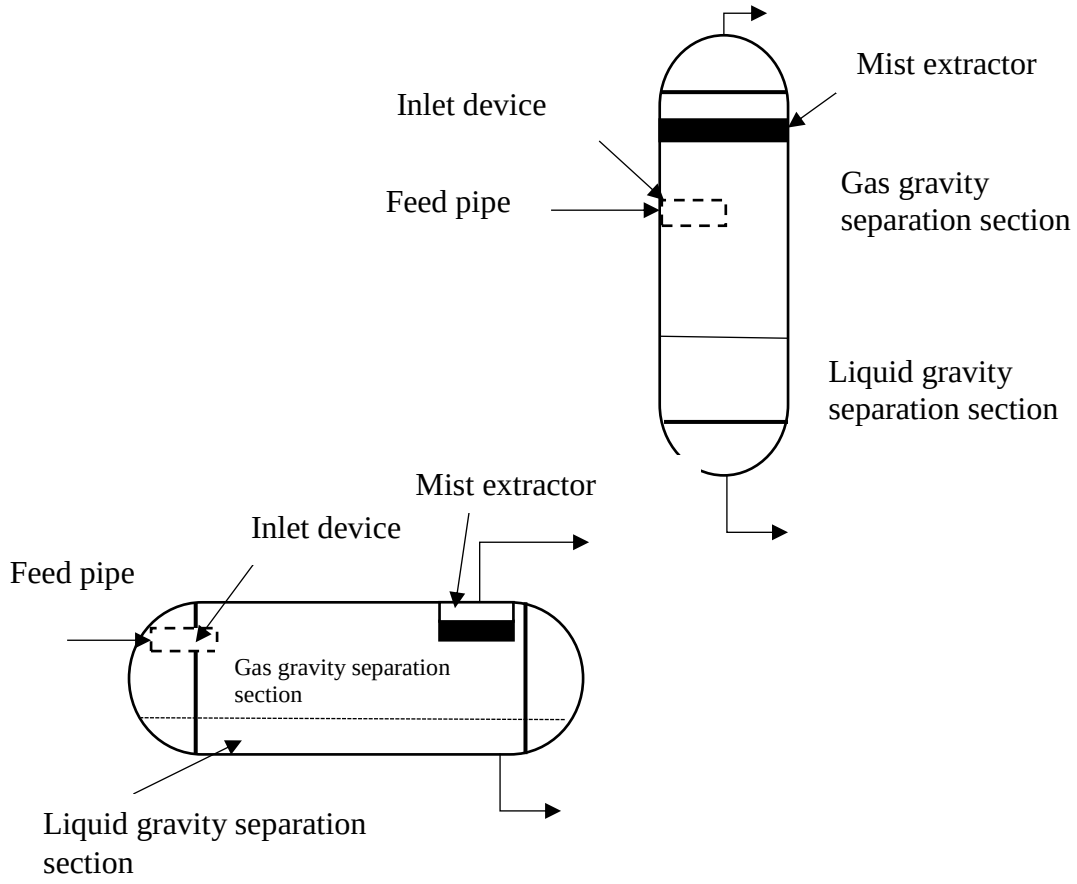

Figure 2-7: Parts of a vertical and horizontal flash separator (redrawn from Bothamley, 2013)

2.4.2 Gas-liquid systems

Combined gas-liquid systems are split into separate gas and liquid streams, relatively free of each other for subsequent disposal or further processing. Gas-liquid systems are categorised as gas phase or liquid phase depending on the continuous phase. When the gas phase is continuous, the small droplets of liquid are dispersed within the gas stream while the gas bubbles are distributed within a liquid when the liquid is in continuous phase.

In a liquid stream, the gas can be dispersed either in an unstable or stable form. In an unstable form, buoyancy separates the phases easily when the dispersing force is removed. In stable dispersions, the gas remains dispersed even after the elimination of an external force, making them harder to separate. Foam is an example of a stable dispersion, formed through concentrating of an additional stabilising substance on the interface of the liquid and vapour

phases (Perry *et al.*, 1984). Over the years, developments have been made in the design and selection of phase separators suitable for various applications. This section's main focus is on the equipment suitable for the separation of whey protein solutions.

2.4.3 Gravity separators

In gas/liquid separation, gravity separators are defined as pressure separators that employ gravitational forces to separate the two phases (liquid and gas). The gas velocity is lowered to increase the efficiency of the separation. Gravity separators are usually designed to remove droplets larger than 0.25 mm (Talavera, 1990) since they require large vessel sizes to achieve settling. The gravity separator designs can either be vertical or horizontal configuration depending on the operating conditions. However, factors like costs and space requirements always have to be considered.

Gravity separators consist of the following components (Mokhatab and Poe, 2012):

i. A segment for primary gas/liquid separation housing an inlet diverter
ii. A segment for gravity settling which provides sufficient retention time for settling to take place.
iii. A gas outlet with a mist extractor which captures the entrained liquid droplets
iv. Control strategies for pressure and liquid levels.

The vapor-liquid separation process consists of three stages. The first stage, referred to as the initial separation, interrupts the large droplets using an inlet diverter so that they drop by gravity. The second stage is called secondary separation. This stage has distribution baffles to enhance gravity separation of smaller droplets in disengagement area. The baffles create an even velocity distribution in the fluid. The third stage is mist elimination. In this stage, the tiniest droplets conjoin on an impingement device, usually a mist pad, forming larger droplets which then settle by gravity (Mokhatab and Poe, 2012).

2.4.3.1 Vertical separators

The vertical separator is commonly used for gas separation processes of relatively large liquid volume, and is commonly installed on oil wells. It is different from the horizontal in that it performs better when dealing with slugging problems (Younger and Eng, 2004). It can handle comparatively huge slugs of liquid without holdover into the gas outlet, thus giving greater surge control. It is also popular with low Gas-liquid ratio (GLR) wells and instances where large liquid slugs and sands are anticipated. It is critical that flash vertical separators are fabricated in a way that directs the flow stream to the top and flow through a gas-liquid separating area.

Level control is a critical factor in vertical separators, it can fluctuate substantially whilst the operating efficiency is maintained (GPSA, 2004). However, pressure drop in the down comer is affected by fluctuating levels, which cause a reduction in the demisting device drainage. The vertical separator uses all of its cross-sectional area in droplet separation, thus making it suitable for high gas to liquid ratio systems (Svrcek and Monnery, 1994; Soares, 2002). A typical vertical phase separator is presented graphically on Figure 2-8.

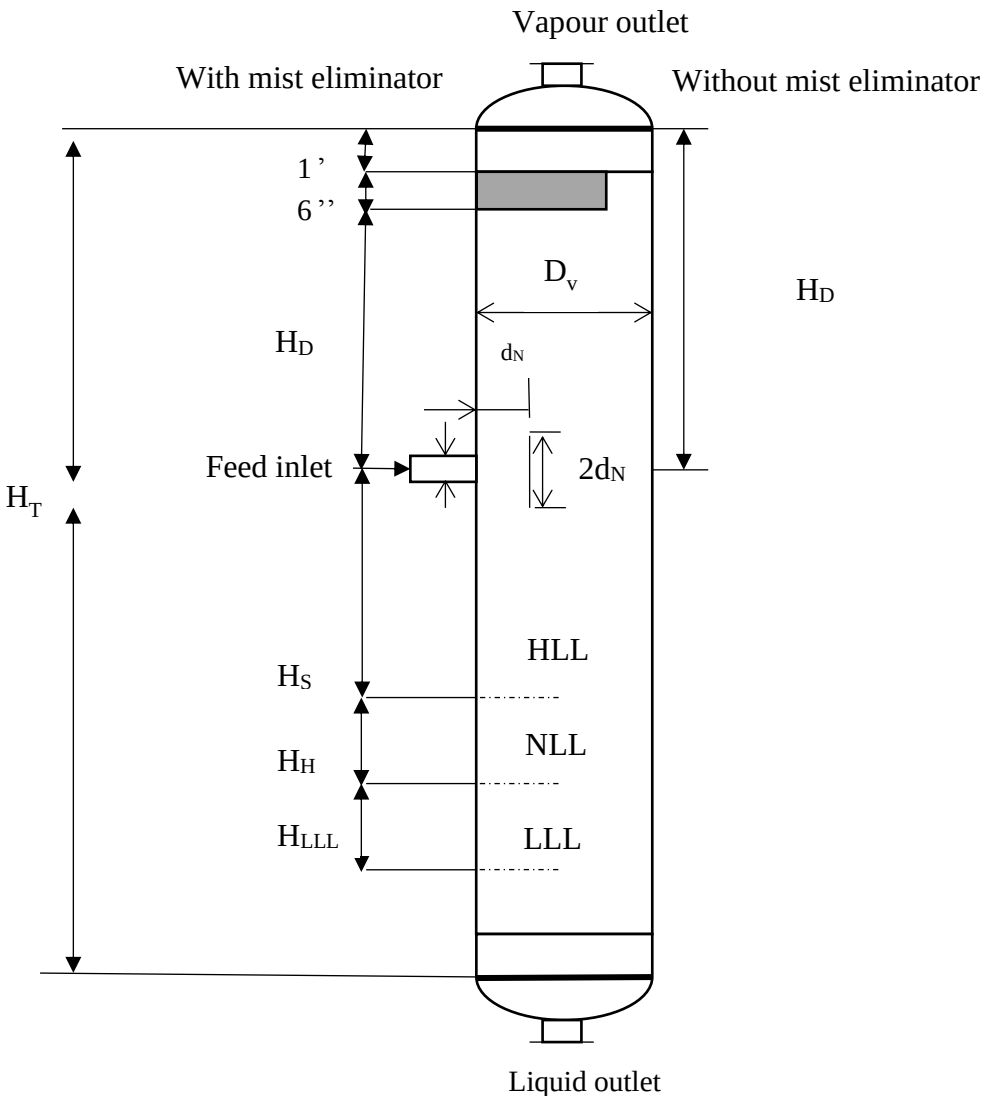

Figure 2-8: A typical vertical phase separator and its dimensions (redrawn from Svrcek and Monnery, 1994).

Where :

H_T is the total vertical separator height (m), D_v is the vessel diameter (m), d_N is the nozzle diameter (m), H_D is the disengagement height (m), H_S is the surge height (m), H_H is the holdup height (m), H_{LLL} is the low liquid level height (m), HLL is the high liquid level, NLL is the normal liquid level and LLL is the low liquid level.

The vertical separator's gas inlet is typically configured normally to the vessel axis. It is commonly fitted with an inlet internal, which serves to distribute the flow uniformly over its cross-section. If the vertical separator is constructed without a distributor, the first separating force exerted on the liquid particles affects the vessel wall on the opposite side of the inlet. Placing the channel opposite to the separator axis forcibly changes the direction of the gas flow as it moves to the outlet. Such a scenario results in exertion of centrifugal forces on the liquid and impingement of droplets to the separator walls or touching the liquid surface at the lower level of the separator (Soares, 2002). Entrained liquid droplets are removed from the gas stream as it travels through the separator to the gas outlet. The gravitational pull is stronger on larger drops than on smaller ones, causing larger droplets to be pulled to the liquid chamber of the separator (Soares, 2002).

2.4.3.2 Horizontal separators

When the feed gas to liquid ratio is low, a horizontal separator vessel is a suitable choice because of its large surge volume (Hall, 2012). Horizontal separators prevent upsets to the process from liquid level fluctuations.

Some drawbacks of the horizontal separator are listed below (Stewart and Arnold, 2008):

- It is more difficult to remove solids in horizontal vessels than vertical vessels.
- Horizontal vessels occupy more space.
- Horizontal separators do not have enough room to space instrumentation like level indicators and other instruments, resulting in process control problems if turbulence occurs on the gas-liquid interface.

A typical horizontal separator is shown in Figure 2-9.

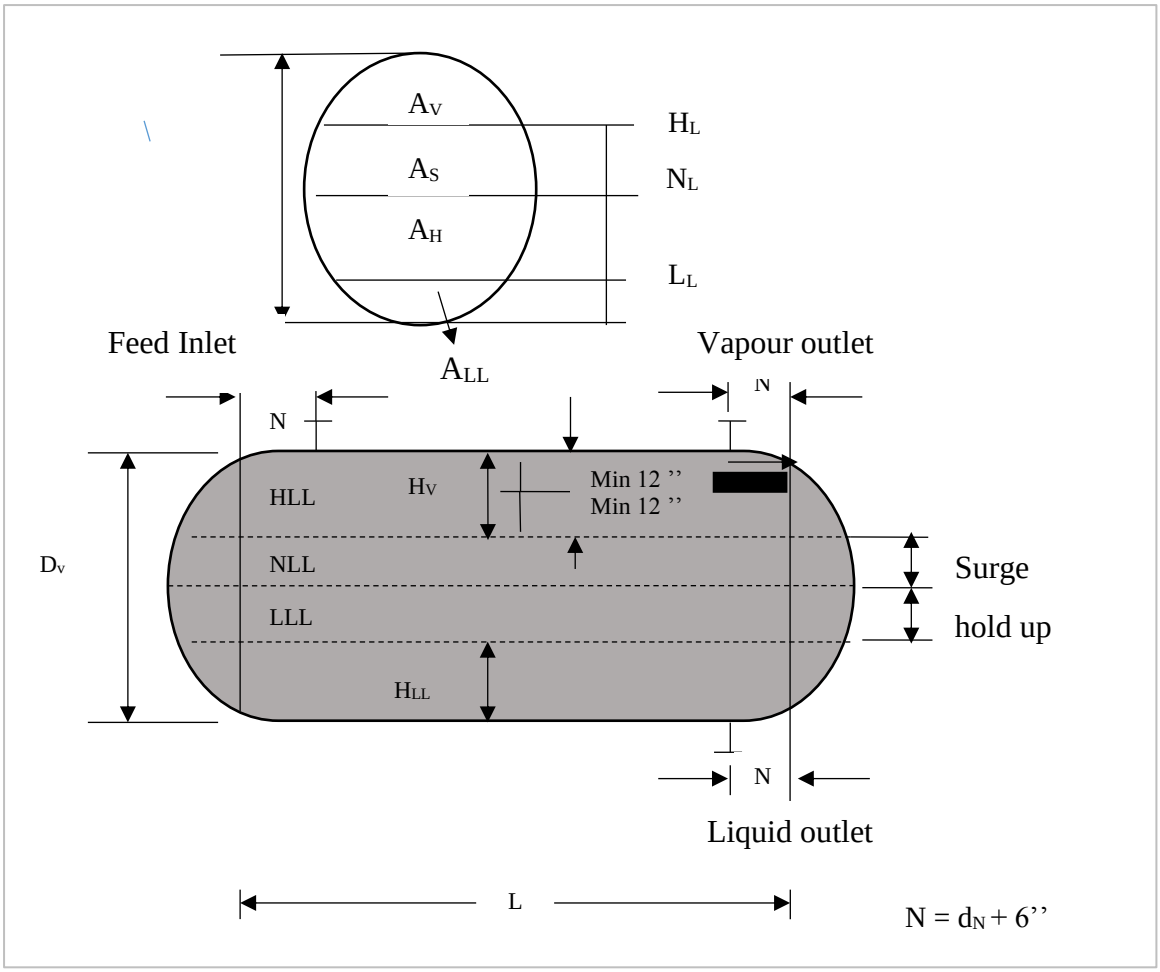

Figure 2-9: A typical horizontal phase separator and its dimensions (redrawn from Svrcek and Monnery, 1994).

Where :

H_V is the vapour disengagement area height (m), L is the vessel length (m), H_{LL} is the low liquid level height (m), A_H is the cross section for HLL in horizontal vessel (m^2), A_S is the cross section for NLL in horizontal vessel (m^2), A_V is the vapour disengagement area required (m^2) and A_{LLL} is the cross section for LLL in horizontal vessel (m^2)

In the simple design (Figure 2-9), a multiphase flow enters the separator from the top left and is separated into two flows, which exit at the right end, with vapour at the top and the liquid at the bottom. Since a small portion of the separator is available for vapour disengagement as indicated by the upper part of Figure 2.10, there is need for a large vessel diameter to cater for large gas flow rates (Svrcek and Monnery, 1994). One significant advantage of horizontal flash separators is their provision of a long surface for removal of liquid droplets.

2.4.4 Separator selection

The horizontal flash separators are advantageous in that they require smaller diameters than vertical separators for the same gas flow rates. They also have large surge volumes and large surface areas, which facilitate foam dispersion. There is also no counter flow in horizontal separators.

Vertical separators are mostly applicable in processes with small flowrates and high gas/liquid ratios, as well as areas where there is space limitation. They are also suitable where easy level control is desired. Their advantages are that they are easy to clean, can handle more solids without plugging and can reduce re-entrainment.

2.4.5 Vessel Internals

Vessel internals improve the process of droplet coalescence in separators. Gas-liquid separators which are not fitted with enhancement internals only remove liquid entrainments of which the sizes are above 0.1 mm. With efficient internals, the corresponding droplet sizes are reduced to between 0.005 and 0.01 mm (Lu *et al.*, 2009). A number of different inlet devices of varying efficiencies and complexities are available. These inlet devices significantly affect the overall separator efficiency. The functions of inlet devices in separators are as follows (Akpan, 2013; Stewart and Arnold, 2008):

Separation of bulk liquids

Improving the efficiency for liquid/gas separation is one of the major functions of inlet devices as they reduce the load on the rest of the separator. The inlet devices are also critical in combination with mist extractors such as vane pads in enhancing the liquid droplet separation. By reducing the amount of droplets in the gas stream, the inlet devices enhances the performances of the demisters.

Improvement of the gas liquid distribution

The inlet device must be properly sized to be able to significantly reduce the momentum of the feed stream and ensure its smooth distribution into the vessel separation compartment for improved separation efficiency. Poor distribution of the liquid results in high residence times,

whereas poor gas distribution to the mist extractor overloads the demister and causes high liquid carryovers.

Prevention of re-entrainment

Re-entrainment occurs when a gas flows at high velocities above a liquid surface. Re- entrainment usually occurs in vessels with deflector baffles or half pipes. Liquid shattering, resulting from the smashing of the liquid into baffle plates and breaking up into smaller droplets than were present decreases the separation efficiency of the separator. A properly designed inlet device minimises the effects of re-entrainment.

Facilitation of de-foaming

Some feed streams may have a high likelihood to foam, therefore will require an inlet device to break down the foam and improve the separator efficiency. The inlet device will also reduce the use of chemicals (antifoaming agents)

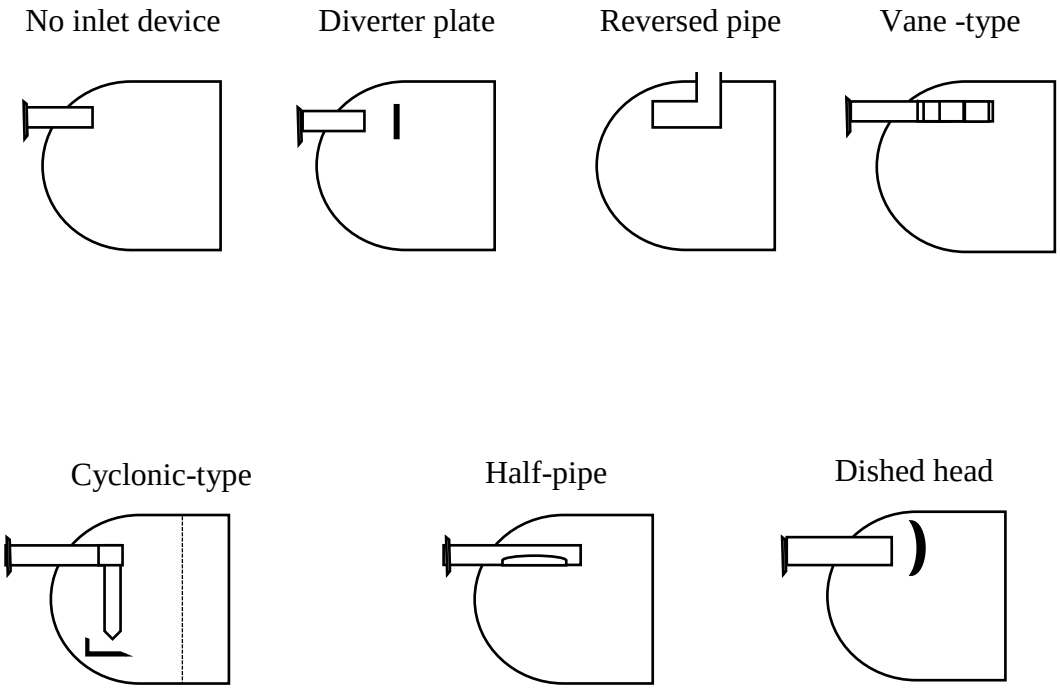

Figure 2-10: Different types of inlet devices (redrawn from Bothamley, 2013a)

There are seven types of inlet devices as shown on Figure 2-10, which are diverter plate, half-pipe, inlet vane and inlet cyclone device. The devices are further discussed in the succeeding sections.

Diverter plate

The diverter plate rapidly changes the flow direction and velocity, resulting in separation of the liquid and gas phases. The energy level in the liquid stream is higher than that of the gas stream with the same velocity since it is the denser phase. The liquid phase therefore changes its direction at a lower rate than the gas phase (Bothamley, 2013a). It thus impacts on the diverter and falls to the bottom section of the separator, whilst the gas phase encircles the diveter. Thus the diverter design must consider the forces resultant from the impact of the liquid stream. Two different diverter plates are shown in Figure 2-11 for horizontal and vertical separators (Slettebø, 2009).

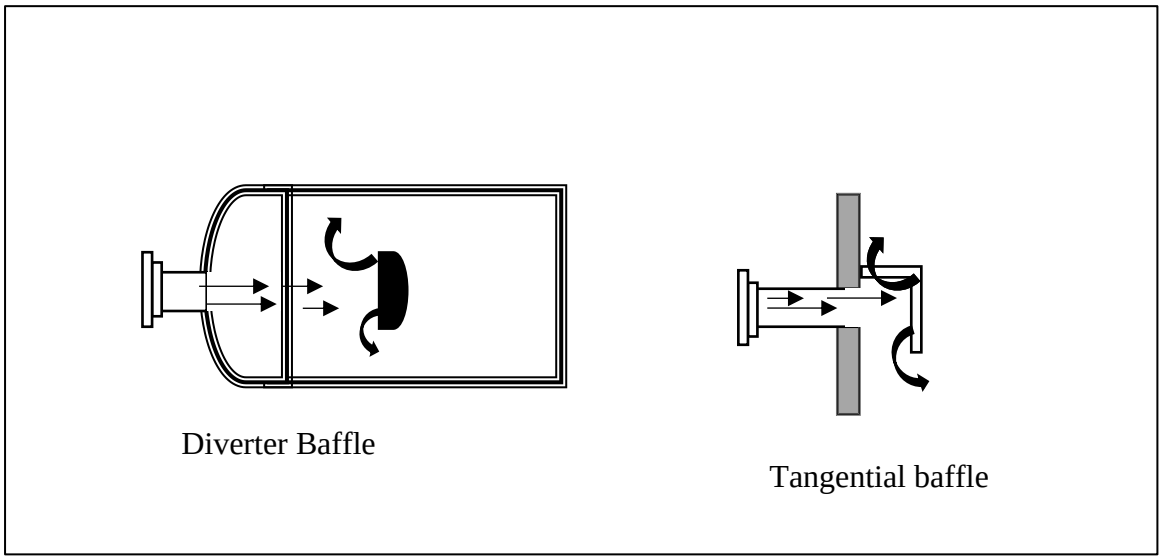

Figure 2-11: Examples of diverter plates (redrawn from Slettebø, 2009)

Half-pipe

When a horintal cylinder's bottom half is removed along its length, a half pipe device is created (Figure 2-12). The half-pipe directs both the gas and the liquid down into the separator (GPSA, 2004). It can also be produced by transforming 90° elbows. The half-pipe internals are slightly more efficient and possess better gas distribution capacities than diverter plates (Bothamley, 2013a; Slettebø, 2009).

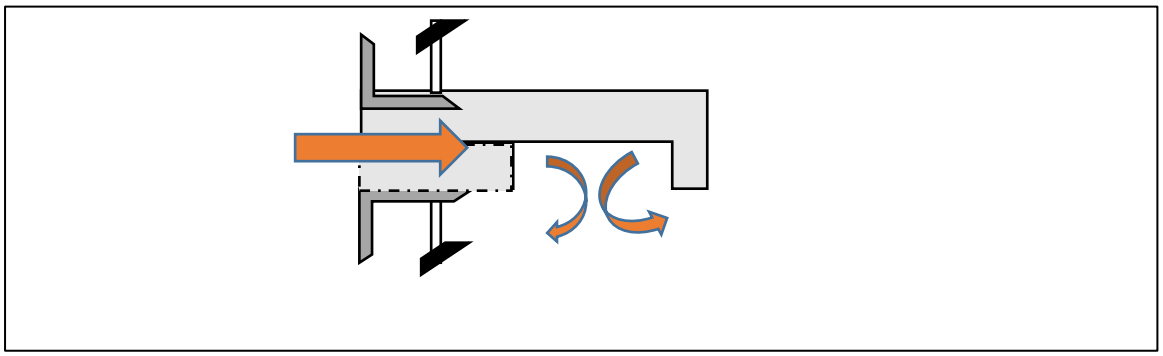

Figure 2-12: Half-pipe internals of a vertical separator (redrawn from Slettebø, 2009; HAT_international, 2008).

Inlet vane

An inlet vane distributor is a complex type of inlet device. Inlet vanes are employed in circumstances where the gas load is higher than the liquid. They are therefore the most common inlet devices in separators (GPSA, 2004). The vanes are also suitable for foaming solutions and streams that contain solids. Inlet vanes reduces the flowrate of the gas and liquid streams into the separator and distribute them at low pressure drops. They also reduce droplet shattering by reducing agitation (Bothamley, 2013a). Inlet vanes perform much better than half-pipe and diveter platedevices by distributing the phases in a more controlled way, as well as giving a more stabilised level control (Slettebø, 2009).

Inlet cyclones

Inlet cyclones perform much better than all other inlet devices. However, they are the most complex devices. Centrifugal forces in cyclones are used separately and distribute the gas/liquid streams. Inlet cyclones can also handle solids (GPSA, 2004). A provided spin device sets the feed into a rotation where it is moved to the cyclone walls by centrifugal forces. Separation results in the feed being drained to the bottom of the separator, while the gas exits the cyclone at the top. Single cyclones and multi-cycolnes where several small cyclones are connected in series are known to exist (Bothamley, 2013a).

If the gas and liquid outlet pressures are incorrectly balanced, there will be liquid carry over or gas carry under. Cyclones are suitable for steady flow rate systems as they are sensitive to flow fluctuations.

2.4.5.1 Inlet device performances

Carryovers occur when the demisting devices are overloaded due to poor inlet separation. A suitable inlet device reduces the inlet momentum and separates the bulk liquid without creating or shattering droplets. It also must create proper distribution of vapour. Table 2-3 provides a summary of the different functions of the inlet devices (Bothamley, 2013a; Norsok, 2001).

Table 2-3: Inlet devices performances (Bothamley, 2013a; Norsok, 2001)

Inlet device functions	**No device**	**Diverter plate**	**Half-pipe**	**Inlet vane**	**Cyclone**
Momentum reduction	Poor	Average	Good	Good	Good
Bulk separation	Poor	Poor	Average	Good	Good
Prevent re-entrainment	Poor	Poor	Average	Good	Average / Good
Minimize droplet shattering	Poor	Poor	Average	Good	Good
Defoaming	Poor	Poor	poor	Average	Good
Low-pressure drop	Good	Good	Good	Good	Average
Good gas distribution	Poor	Poor	Poor	Good	Average

Table 2-3 shows the performances of different inlet devices. It shows that the inlet vane is the best performing device. Inlet cyclones provide better separation efficiencies than vanes but they have limited operating ranges. Proper practices can however compensate for the operation weaknesses of the inlet cyclones.

The vanes and cyclone inlet devices are more commonly employed in large separators whilst diverter plates are common for smaller and less critical separations. The half-pipe internals, though simple and uncostly, is a device whose performance is relatively good in all separation applications (Bothamley, 2013a). Table 2-4 shows some performance guidelines for inlet devices as a function of the inlet momentum, which determines the selection and sizing of inlet devices.

Table 2-4: Inlet devices and their inlet momentums

Inlet Device Type	ρv^2, kg/m-sec^2
No inlet device	1040.3
Diverter plate	1411.9
Half-pipe	2080.7
Vane-type	8025.5
Cyclone	14862.2

Table 2-4 shows typical design values (limits) for inlet momentums of different inlet devices. To avoid higher entrainment loads and difficult separation conditions, the limits for inlet momentum should be considered when selecting inlet devices during equipment design.

2.4.6 Mist Extraction Equipment

Mist extractors (also referred to as demisters) are commonly used to exclude mist from vapour carrying streams. They remove the entrained liquid particles from gas streams by reducing its velocity (Bothamley, 2013a). Mist extractors boost the droplet sizes and increase the gravitational forces. The choice of a mist extractor depends on droplet sizes, tolerated pressure drop, presence of solids, as well as the liquid handling in the separator (Slettebø, 2009).

Laws of fluid mechanics govern the rate of droplets entrained in the gas stream. As gas flows upwards, two opposing forces act on the droplet: the gravitational force and a drag force. As gas velocity increases, the drag increases and when the two forces equal, the droplet attains terminal velocity. If its velocity increases further than the terminal velocity, the droplet will get entrained into the gas stream and exits the separator with the gas.

Gas velocities are determined by K-factors. Low K-factors keep the liquid droplets in the gas stream, whilst too high factors results in re-entrainment as the droplets breakup. The K-values are normally in the range of 0.09 to 0.3 m/s. K-value guidelines for different devices are given by standards (Norsok, 2001).

The mist eliminator must be designed to remove the droplets already in the system. Therefore it is critical to determine the droplet size. In the initial selection process, the most suitable mist eliminator media must be selected to avoid liquid hold-up in the pad after the mist eliminator

is installed. It is also important that the environment the mist eliminator will operate in be defined to minimise maintenance requirements and reduce operation costs. There are three major types of mist extractors: mesh pads, van packs and demisting cyclones (GPSA, 2004).

2.4.6.1 Meshpad

Mesh pads are made by tightly knitting wire, metal or plastic into packed layers and then crimp and stack them into the required thickness (GPSA, 2004). The mesh pad is the most common mist extractor in chemical process industries. It is mounted near the separator's gas outlet. The entrained droplets coalesce when they contact the wire surfaces of the mesh pad due to inertia. The mesh pads are usually constructed with wires of diameters ranging between 0.10 to 0.28 mm, with a void fraction of 0.95 to 0.99. The thickness of the mesh pads usually varies from 100-300 mm whilst the pressure drop ranges from 0.01 to 0.3 kPa (Fabian *et al.*, 1993; Norsok, 2001).

A good design of a separator which uses a mesh pad can have a K-value of less than 0.1 m/s. A K-value above 0.1 m/s causes flooding of the mesh and loss of separation efficiency. In such scenarios the mesh then coalesces the smaller droplets to give larger ones. Typical minimum droplet removal sizes are 0.01 mm for a metal mesh and (0.003 -0.005 mm) for a plastic or fibre mesh (Norsok, 2001). Mesh pad performance can be measured by the droplet removal efficiency and gas handling capacity (GPSA, 2004).

Table 2-5: Mesh pad K value factors as a function of pressure (Fabian et al., 1993; GPSA, 2004).

Pressure, kPa	Percent of design value
100	100
500	94
1000	90
2000	85
4000	80
8000	75

A well-designed mesh pad that is also well operated removes droplets larger than 0.003-0.005 mm from the gas stream with a corresponding pressure drop of less than 0.25kPa. Mesh pads' normal operation range is between 30-110% of the design gas capacity (GPSA, 2004).

The gas approach the pad from the bottom in the upwards direction. K_S-values of the mesh pad deteriorate with pressure as shown in Table 2-5.The K_S-value is assumed to decrease by 10% per 42 L/min/m^2 (Bothamley, 2013a; Bothamley, 2013b) if the velocity of the approaching liquid to the mesh pad exceeds the values given in Table 2-6.

Table 2-6: K-value of mesh pads and performance parameters (Campbell, 2014; Bothamley, 2013b)

Description	**K-value (m/sec)**	**Separable droplet size, 90% removal, (mm)**	**Liquid load before capacity deteriorates, (l/min/m^2)**
Standard" mesh pad	0.107	0.005	31.5
High capacity" mesh pad	0.12	0.008-0.01	63
High efficiency." co-knit mesh pad	0.07	0.002-0.003	21

Where; K- value - Demister capacity factor, m/s

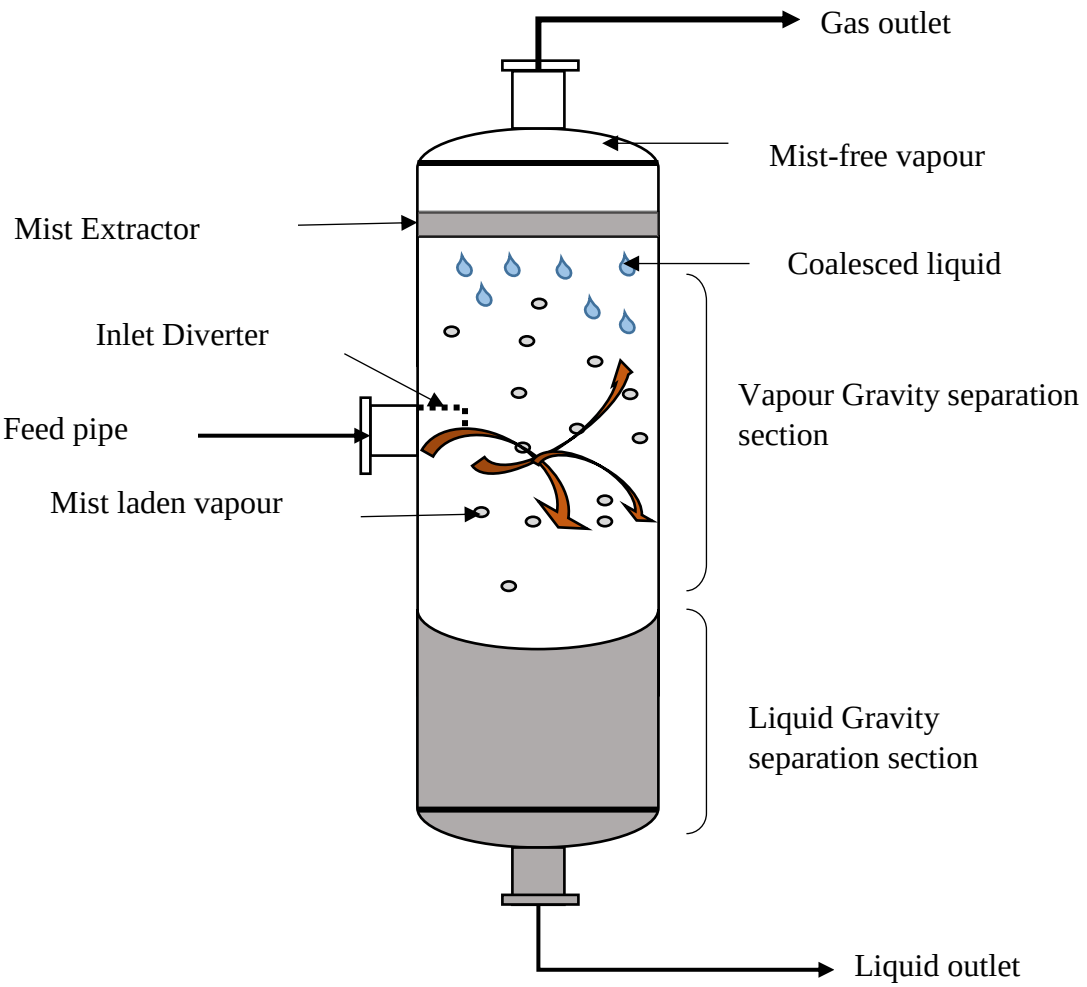

Figure 2-13: Typical mist extractor in a vertical separator (redrawn from Campbell, 2014)

2.4.6.2 Vane packs

Droplets are also captured by inertial impaction in vane packs. The gas is forced to change its direction by the vane bend angles, while liquid droplets, due to their higher density, travel in a straight-line. The droplets then impact the vane surface and are gathered and removed from the gas stream. Table 2-7 displays vane pack performance characteristics (Campbell, 2014; Bothamley, 2013b), while Figure 2-14 shows a typical vane pack which is suitable for a horizontally flowing gas. The collected liquid is directed from the gas stream through channels. The double pocket design isolates the liquid from the gas stream, thereby decreasing the probability of re-entrainment of the droplets.

Table 2-7: Typical vane-pack characteristics (Campbell, 2014; Bothamley, 2013b)

Vane type	Flow direction	K-value, (m/s)	Droplet removal Efficiency	Liquid load before capacity deteriorates, (L/min/m^2)
Simple Vane	Up flow	0.15	90+% > 0.020 mm	84
Simple Vane	Horizontal	0.20	90+% > 0.020 mm	84
High Capacity Vane	Up flow	0.25-0.35	95+% > 0.010 mm	210
High Capacity Vane	Horizontal	0.3-0.35	95+% > 0.010 mm	210

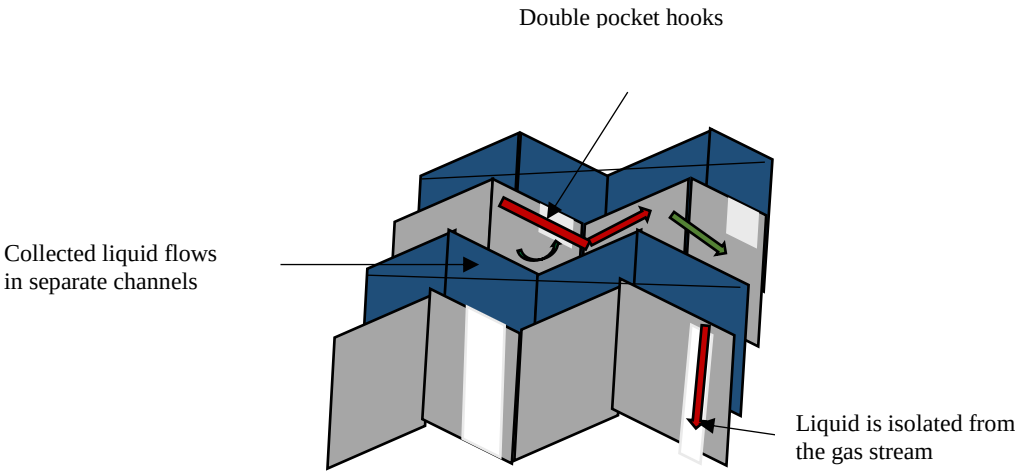

Figure 2-14: Horizontal gas flow in a vane pack (redrawn from Slettebø, 2009; Koch-Glitsch-LP, 2007).

Vane packs are applicable for liquid droplets whose diameter range from 0.010 - 0.040 mm. The K-value range for the double pocket vane pack is wider than normal: 0.04 to 0.35 m/sec, giving it a broader working area and a reduced clogging risk, which is desirable especially for subsea operation when the flow is unsteady (Campbell, 2014; Bothamley, 2013b).

2.4.6.3 Cyclone mist extractors

Cyclone tubes may be mounted in singles or in multiples in a cyclone demister. The cyclone demisters have the capacity to handle high gas volumes, and are more efficient in droplet removal than mesh pads and vane packs, as well as less prone to clogging. Figure 2-15 is a

diagram of a cyclone mist extractor (Slettebø, 2009; Koch- Glitsch-LP, 2007). The gas stream with mist enters the cyclone and is swirled, where high centrifugal forces push the liquid droplets outwards. The pushed droplets form liquid films on the cylinder wall and eventually removed through gaps in the wall. The main gas exits the cyclone from the top whereas the liquid is discharges from the bottom.

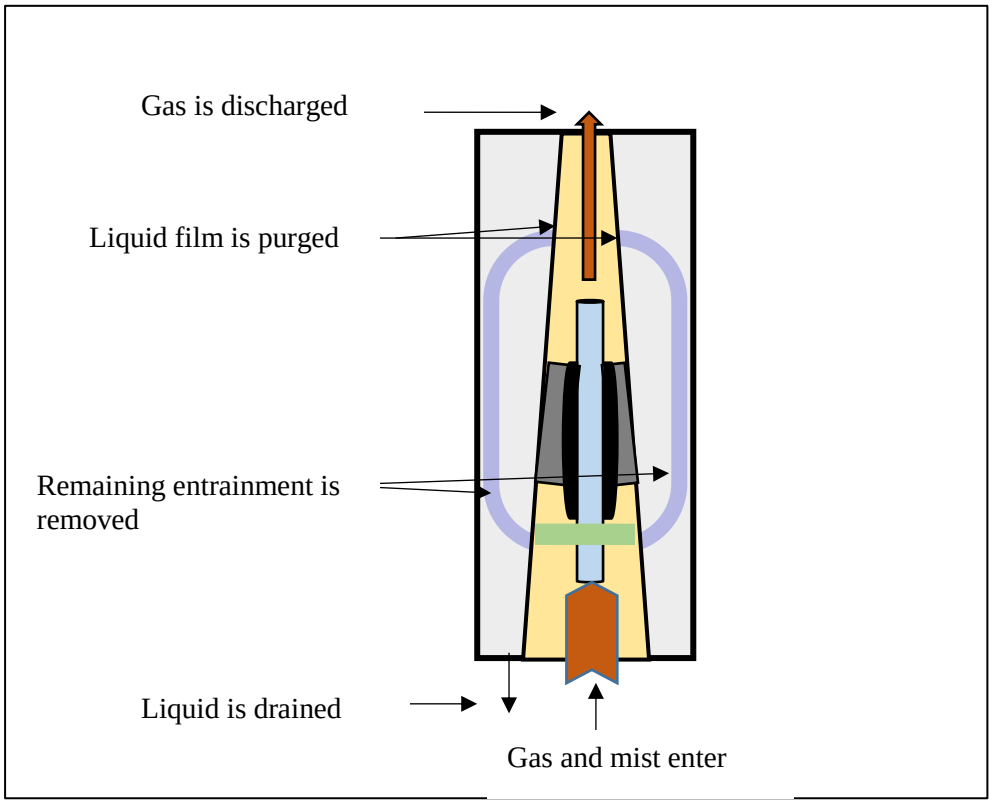

Figure 2-15: Cyclone mist extractor (redrawn from Slettebø, 2009; Koch-Glitsch-LP, 2007)

Cyclone configuration can be either horizontal or vertical. They are usually made to correspond to the gravitational separator. Droplets of 5μm in diameter can be removed by cyclone mist extractors. Installing cyclonic devices has potential benefits of cost reduction since the total separator size required is greatly reduced.

2.4.7 Comparison of mist extractors

From Table 2-8, the cyclone mist extractor has the best overall performance. For subsea, the applicable extractors are the vane and cyclones since they are the only ones which can handle large gas and liquid capacities and remove solids. Cyclone demisters are more efficient than

vane packs owing to their high acceleration forces. Increasing operating pressures reduces efficiency in vane packs whilst maintaining cyclone efficiency.

Table 2-8: comparing the different types of mist extractors (Slettebø, 2009; Koch-Glitsch-LP, 2007)

Types of mist extractors	Knitted mesh	Fibered	Vane	Cyclone
Cost	1	10	2-3	3-5
Gas capacity	5	1	6-15	15-20
Liquid capacity	5	1	10	10
Particle size (mm)	0.003-0.010	<0.0001	0.008-0.040	0.005-0.010
Pressure drop (kPa)	< 0.245	0.49-4.9	<0.09-0.88	1.96-2.35
Solid Handling	3	1	10	8

Relative scale based on 1 as the lowest. Others are scaled.

Mesh fouling

Sometimes fouling of mesh mist eliminators causes liquid carryover in the exit gas stream. Figure 2-16a is a diagram showing a normal demister fitted with a spray system. Spraying prevents fouling and plugging of the mesh pad by removing deposits. When fouling substances are present in the process, the mesh unit can be placed downstream of the vane unit in a two-stage demister (Figure 2-16b). Figure 2-16b is a typical retrofit design where a demister is placed vertically in a vertical vessel to increase its effective surface area (Kalis, 2004).

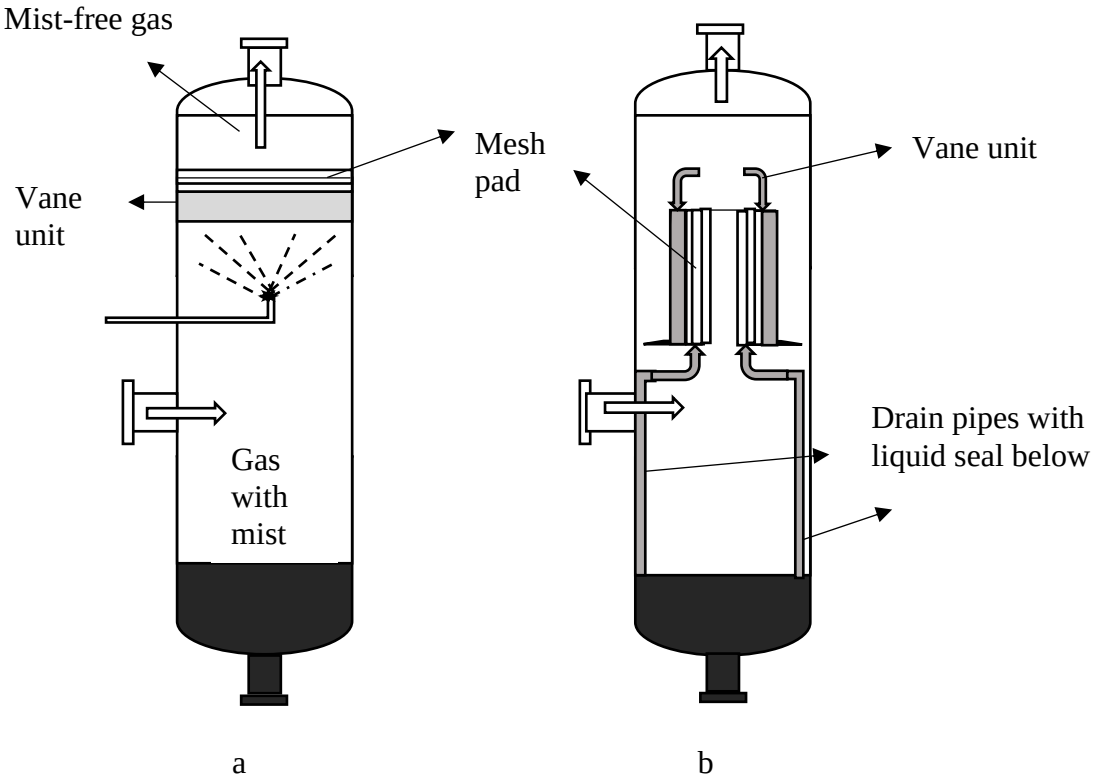

Figure 2-16: Demister configurations in a vertical phase separator (redrawn from Kalis, 2004).

It is important to ensure a unified flow profile so as to maximise the separating potential of a demister or a coalescer. Differences in velocities result in re- entrainment of the dispersed phase in some sections, whilst in other regions droplets will be too small for the unit to handle (Fabian *et al.*, 1993; Kalis, 2004). Velocities of 30% -110% of the optimal speed usually result in good unit performance. Droplets cannot impinge on the demister surface when the velocities are lower than the 30%, whilst too high velocities result in re-entrainment of already separated droplets (Couper, 2012). A thin plastic or metal wire (0.08 - 0.40 mm) is used for the construction of demisters. By comparing the nominal surface areas, the performances of different pad designs are evaluated. Typical values range from 160 to 2000 m^2/m^3 inlet distributors and outlet geometry (Moss and Basic, 2013).

2.4.8 Sizing of phase separators

Factors affecting separation

The following factors must be determined before separator design (Stewart and Arnold, 2008):

- Flowrates of both liquid and gas streams
- Temperatures and pressure (both design and operating)
- The tendencies of the feed streams to surge
- Fluid physical properties (compressibility, viscosity and density)
- Design specifications
- Type and degree of impurity
- The solution's tendency to foam
- Corrosive nature of solution.

Sizing considerations

The feed point to the separator, which lies just above the vapour/liquid interface, should be 610 mm from the separator bottom and 1220 mm from its top. For horizontal separators, it is not a prerequisite that the interface be at the centerline of the vessel. When the interface location is made off-centre and a design variable, it is possible to obtain a smaller-diameter vessel. The feed enters the separator from the end, just above the interface of the vapour/liquid phases, which should be 250 mm from the bottom and 410 mm from the top.

Younger (1955), evaluated seven separators with the L/D ratio between 1.7 to 3.6 and found that they were all vertically installed. This resonates with Branan (1994)'s rule which determines that horizontal separators should be used for L/D ratios which exceeds 5. Scheiman (1963) suggested a settling length of 0.75D, or at least 305 mm, whereas Gerunda (1981) suggested equal diameters and lengths or a minimum length of 914 mm. Scheiman (1963) further specified a height of at least 152 mm from the liquid outlet to the liquid surface. Branan (1994) suggested using 305 mm plus half of the external diameter of the inlet nozzle or at least 457 mm. Gerunda (1981) specified at least a 0.5D or a minimum of 610 mm. A surge time in the range of 2 to 5 minutes was recommended by Scheiman (1963), whilst Younger (1955) recommended 3 to 5 minutes.

The separator design must also include a vortex breaker, and it should be covered by the minimum liquid level, as well as an additional liquid height. Patterson (1969) conducted experiments and showed that variations between the lower liquid level and the liquid velocity in the outlet nozzle were minimal. For a liquid level of 127 mm and a velocity of 2.13 m/sec in the outlet piping of a tank which does not have a vortex breaker, a vortex is likely to occur, which will be difficult to break. Gerunda (1981) recommended a 610 mm minimum liquid level to eliminate vortices.

The thickness of the mist eliminator should be sufficient to trap the majority of the liquid droplets in the gas stream. Its thickness is usually 152 mm, with an additional 305 mm above the eliminator for uniform flow distribution across the eliminator. The separator's total length is calculated by summing up its dimensions.

Sizing procedures

Descriptions by different researchers (Lyons and Plisga, 2005; Wiencke, 2011; Couper, 2012; Evans, 1974; Hall, 2012) provide some basic steps into determining the dimensions of separator vessels based on the feed stream characteristics and the design separation efficiency. Evans (1974) and Hall (2012) gave the following guidelines.

Vessel orientation

When determining vessel orientation, two critical factors should be considered: the phases' volumetric ratio and surge volume. For large liquid fractions and surge volumes, a horizontal vessel should be considered. Horizontal vessels, unlike vertical vessels, give stability to the liquid level in the tank and have larger available cross-sectional areas for vapour disengagement in streams with high gas to liquid ratios. Horizontal vessels are normally employed in the separation of water and hydrocarbons (Hall, 2012) since they have shorter distances from vessel edges to the phase interface (Couper, 2012).

Liquid surge volume

Hall (2012) described half full as half the vessel's total volume or half the maximum allowable volume in case of a high-level shut off. Using old rules of thumb (Couper, 2012), stated that

the capacity of knockout drums before compressors should be such that when half full, their liquid holdup time should be 10-20 minutes while that for fired heater surge drums should be 30 minutes. 5-10 minutes will normally suffice for other uses. For gas-liquid separators, typical liquid retention times are normally between 30 seconds to 10 minutes (Laleh *et al.*, 2012). In systems where the gas is the dominant phase, gas retention times will be considerably shorter.

Gas velocity

A droplet's terminal velocity determines the maximum allowable gas velocity $(u_g)_{max}$ whilst flooding of the demister pad determines the maximum gas velocity. The flooding point of demister pads is in turn determined by its free volume. For vessels fitted with demisters, Equation 2-5 is used to calculate the gas velocity (Hall, 2012):

$$u_{g(max)} = K\sqrt{\frac{(\rho_l - \rho_g)}{\rho_g}} \qquad \text{Equation 2-5}$$

Where:

K is the maximum allowable velocity coefficient (m/sec).

With suitable K-values, Equation 2-5 can be employed when sizing separators without demisters. Demister properties, operating conditions and desired separation determine the K-values. Table 2-9 shows a list of K-values for demister equipped separators (Couper, 2012).

Table 2-9: Typical K-values for separator vessels fitted with mesh pad demister (Couper, 2012)

Efficiency, %	Density, kg/m^3	Specific surface area, m^2/m^3	K, m/sec	
			Under pressure	Vacuum
Low (99.0%)	80-112	213	0.122	0.061-0.082
Standard (99.5%)	144	279	0.107	0.061-0.082
High (99.9%)	192	377	0.107	0.061-0.082
Very high (>99.9%)	208-224	394	0.076	0.061-0.082

Vessel and demister dimensions

The minimum cross sectional area of a demister and a separator is determined by the gas flow rate Q_g and its maximum velocity $(u_g)_{max}$ (Evans, 1974).

$$A_{min} = \frac{Q_g}{(u_g)max}$$ Equation 2-6

Where A_{min} is the minimum vessel cross-sectional area or demister (m^2), and Q_g is the inlet gas flow rate (m^3/sec).

The vessel diameter is calculated considering the liquid surge volume. It may be bigger than the diameter of the demister. To determine the minimum diameter, a simple geometrical calculation is used (Evans, 1974).

$$D_{min} = \sqrt{4(A_{min})/\pi}$$ Equation 2-7

Where:

D_{min} is the minimum vessel or demister diameter in meters.

The average density variable ρ_{mix} (Evans, 1974) is used to calculate nozzle sizes;

$$\rho_{mix} = \frac{Q_L+Q_g}{(\frac{Q_g}{\rho_g})+(\frac{Q_L}{\rho_L})}$$ Equation 2-8

Where: ρ_{mix} is the average density in kg/m^3.

Using empirical correlations (Equations 2-9 and 2-10), the maximum and minimum velocities for the inlet nozzle can be estimated (Evans, 1974).

$$u_{max(nozzle)} = 30\sqrt{\rho_{mix}}$$ Equation 2-9

$$u_{min(nozzle)} = 18\sqrt{\rho_{mix}}$$ Equation 2-10

Where:

$(u_{min})_{nozzle}$, $(u_{max})_{nozzle}$ are the minimum and maximum inlet nozzle velocities respectively in m/sec.

Equation 2-11 can be used to calculate the inlet nozzle cross-sectional area (Hall, 2012).

$$A_{nozzel} = \frac{Q_g + Q_L}{\rho_{mix}\, u}$$ Equation 2-11

Where A_{nozzle} is the inlet nozzle cross-sectional area (m^2) and u the inlet velocity $(u_{min})_{nozzle} < u < (u_{max})_{nozzle}$ in m/sec.

The selected velocity should allow calculation of a practical inlet nozzle size (Hall, 2012). Figure 2-17 illustrates the position of the inlet nozzle.

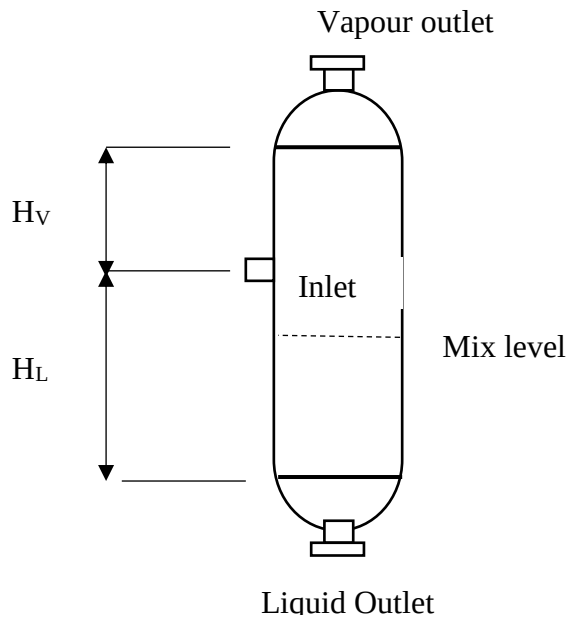

Figure 2-17: Inlet nozzle spacing in a vertical separator vessel (redrawn from Hall, 2012)

According to Hall (2012), the following criteria should be used for vertical separator inlet nozzle spacing:

- The height between the feed inlet and the gas outlet should be 910 mm plus half the external diameter of the inlet pipe. The minimum height can be 1220 mm.
- The height between the feed inlet and the maximum liquid level should be 300 mm plus half the external diameter of the inlet pipe and cannot be less than 460 mm

Lastly, the ratio of the separator height ($H_v + H_l$) to the diameter must be between 3 and 5. To increase the total height and raise the ratio to 3, an addition of the surge volume can be done. Horizontal separators have to be used for ratios larger than 5 (Evans, 1974). Since the liquid droplets experience no net upward lift, the maximum design gas velocity $(u_g)_{max}$ of a horizontal separator will be slightly higher than that of a vertical separator (Couper, 2012). The terminal velocity (u_t) as calculated in Equation 8 is an indication of the absolute maximum value.

Equation 2-9 describes the minimum available cross-sectional area for vapour disengagement. At least 20 % of the separator volume and 300 mm of its top space must be occupied by the gas when full. Therefore, according to Hall (2012) and Evans (1974), to calculate the minimum cross-sectional area for a horizontal vessel, Equation 2-12 can be used:

$$A_{total(min)} = \frac{A_{min}}{0.2} \qquad \text{Equation 2-12}$$

Where;

$A_{total\,(min)}$ - Minimum total cross-sectional area for a horizontal separator (m^2).

To determine the minimum diameter D_{min}, Equation 2-7 is solved, also considering the 20% gas volume in the tank requirement (Hall, 2012).

$$V_H = \frac{v}{0.8} \qquad \text{Equation 2-13}$$

Where:

V_H - Total vessel volume for horizontal separator (m^3).

Equation 2-14 is used to calculate the length of the horizontal vessel (Evans, 1974).

$$L_H = \frac{V_H}{\frac{\pi}{4} D_H{}^2} \qquad \text{Equation 2-14}$$

Where

L_H - Length of the horizontal separator (m)

D_H - Diameter of the horizontal separator(m).

2.5 CONCLUSION FROM THE LITERATURE

Some fundamental conclusions can be made from the literature review which shall form the basis of the further work undertaken. The solution characteristics (density, thermal conductivity, heat capacity and viscosity) were found to be influential in the design of evaporation equipment. The whey protein solution, owing to the heat sensitivity of its constituent proteins (Section 2.1.1), requires vacuum evaporation at low temperatures (below 70^{o}C) since denaturation was found to be increasing with increasing temperatures. This can be achieved by incorporating a vacuum system, set to allow lower solution boiling than that of water. This approach will not be critical with non-heat sensitive solutions. Evaporator designs for whey protein solutions will also need to consider its foaming and fouling properties. Indirect heating and application of antifoaming agents or physical foam breakers will have to be considered.

It was also established that many types of evaporators are available for selection in the dairy industry (Section 2.2.1). Their selection depends mainly on their cost and solution properties. Separators efficiency was also found to be dependent on the internals (diverters, half pipes, vane or cyclone), which also depend on the solution being processed and their cost.

From Section 2.4.4, the vertical design is more suitable for small liquid flow rates, as this configuration occupies less space and can prevent re-entrainment. These were the prerequisites for the concentration of the WPC. The design also offers easy level controlling for efficient gas-liquid separation.

From Section 2.4.6 and Table 2-8, the mist extractor of choice was the mesh due to its applicability to small designs. The mesh mist extractor is also the most common device and simplest to use. Although the cyclone and the vane would give superior performances, they are highly expensive and not applicable to small operations.

Most of the pre-requisite separator design properties of whey protein are unknown. Therefore to fill that gap in the literature, this work will attempt to answer the following research questions:

i. At what operating conditions (temperature and pressure) will the whey protein evaporate without denaturation?

ii. Will the solution foam, and at what temperature?

iii. What is the relationship between rate of evaporation, heat transfer coefficient and concentration for whey protein solution?

iv. How does the evaporation characteristics of the whey protein solution compare to that of non-heat sensitive materials like sugar solutions?

3. EXPERIMENTAL SECTION

3.1 INTRODUCTION

The main objective of this section was to design a vacuum evaporation system as well as to evaluate the effects of operating variables (the flash separator internals, initial solution concentration, vacuum pressure and solution feed temperature) on the efficiency of the evaporation system, by initially using pure water as the experimental liquid, before the WPC, NaCl and sugar solutions.

In this study, a lab scale VES was applied to concentrate WPC solution. The FCE is less costly when compared to agitated thin film evaporator. From Table 2-1, evaporators like falling film, natural circulation and calandria are not suitable for heat sensitive material, so they were not be considered. The long-tube falling film, although suitable for sensitive material, cannot be used for foaming, scaling and solids in suspensions. The evaporator whose performance surpasses the rest is the agitated-film evaporator, but it is highly expensive. The FCE, although performing poorly with liquids carrying solids in suspension, was the most suitable choice since it is less expensive and the material to be used in this study was not likey to contain solids. The forced circulation evaporator was also a preferred choice when compared to natural circulation since it could be applied to smaller scale operations.

All the equipment, comprising the complete lab-scale vacuum evaporation system was mounted within a square stainless steel standing frame. The different pieces of equipment were a centrifugal pump, heating jacket, feed tank, heating coil, vertical flash separator, a condenser, vacuum pump, temperature measurement systems, cooling finger, and control unit. The whole apparatus is shown in Figure 3-1.

3.1.1 Flow sheet development

From the literature review, it was concluded that the components of an evaporation system must include a heat source, a separator, a condenser and a vacuum device. A feed tank was also provided to store the whey protein solution and collect the recycled concentrated liquor. Heat is mostly provided by heat exchangers in industry, but due to the miniature scale of the laboratory equipment, an alternative source in form of a heating element in the feed tank (pre heating) was opted for. A heating coil further heated the solution after pressure drop in

the throttling device to enhance flashing in the evaporator. To improve the efficiency of the evaporator, a throttling device (needle valve) was also provided on the inlet line to the evaporator. The separator, concluded to be the main part of the evaporator, was also included in the equipment list. To reduce the boiling point of the water and preserve the heat sensitive whey protein, a vacuum unit was also incorporated. A centrifugal pump was selected to pump the solution from the feed tank to the separator, through the throttling device and the heating coil, due to its easy applicability in less viscous materials and high delivery pressure. Finally, a condenser was included to condense the vapour and allow quantification of the liquid evaporated, and to allow easy removal of the evaporated water from the system.

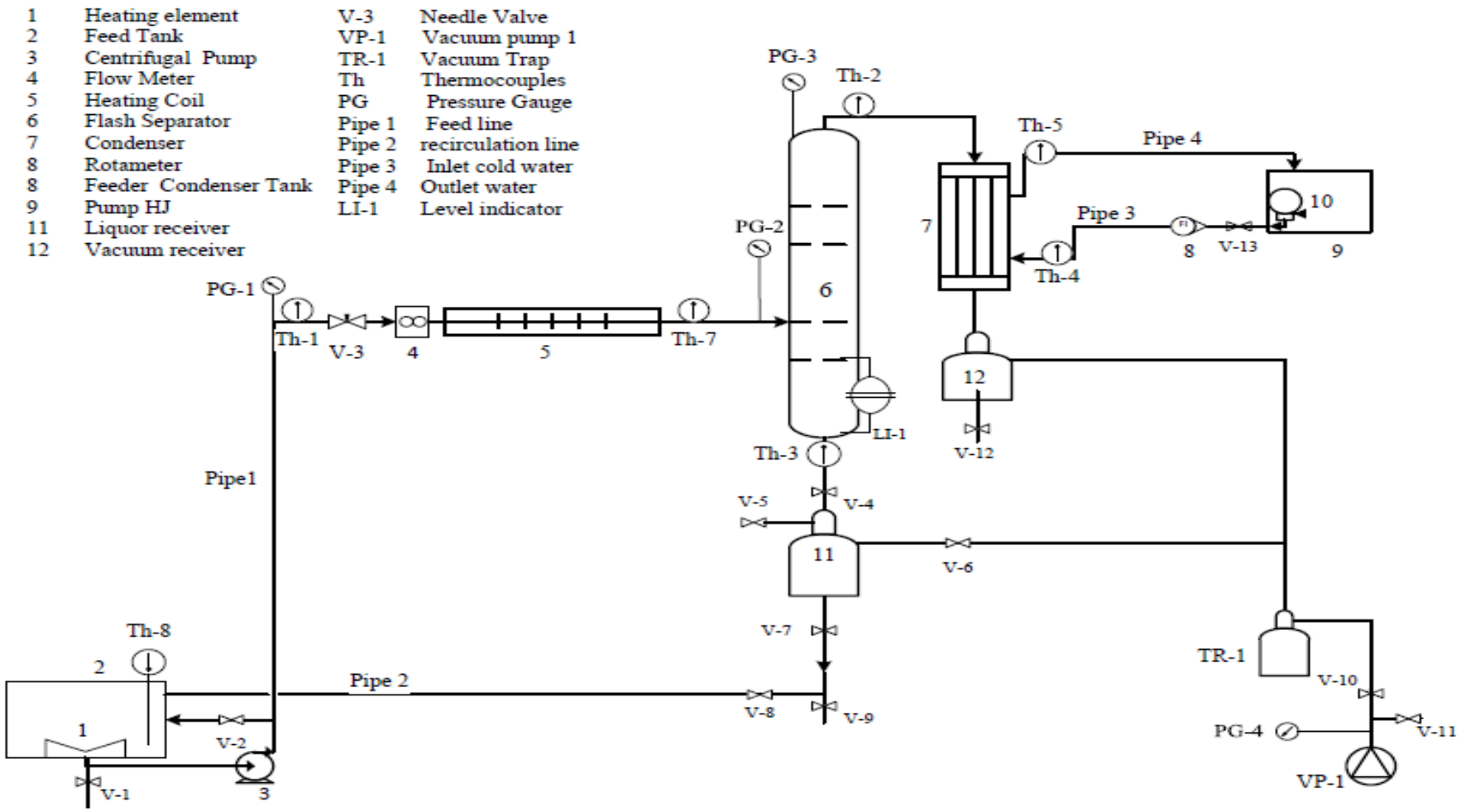

Figure 3-1: The initial vacuum evaporation system.

3.2 EQUIPMENT DESCRIPTION

3.2.1 Feed tank

The feed tank (number 2 on Figure 3-1): a cylindrical stainless steel tank was fabricated in the Processing Engineering Stellenbosch University workshop. It is 210 mm inside diameter with a height of 525 mm and a capacity of approximately 18 L. A metal pipe with an inside diameter of 12.3 mm was connected to the tank through a socket and fed the centrifugal pump (3) with the whey solution. The tank bottom was fitted with a single circuit heating element for heating the feed solution material. The circuit element is 180 mm in diameter and power rated 3 kW.

3.2.2 Feed pump

The feed pump (TMP 35 model) is a centrifugal pump manufactured by Magnetic Centrifugal Pumps (number 3 on Figure 3-1). According to Campbell and colleagues (2015), centrifugal pumps are preferred since they have low installation and maintenance costs. They are also simple to operate and operate under different conditions whilst maintaining a smooth, continuous flow without pulsation. Other advantages of centrifugal pumps include their simple design, with few moving parts, as well as their applicability in small spaces. It is single stage, with a horizontal input connection and vertical discharge connection. The pump is rated 1 HP and 3 phase, with a constant speed motor running at 2900 rpm. It is rated at 0.7 m^3/hr against a total head of 3.6 m. Feed pipes were made of copper with an inside diameter of 12.3 mm. The system curve and pump curve, and calculations can be found in Appendix A.

3.2.3 Vacuum device

The system also comprises of a vacuum trap (TR-1), vacuum receiver (12) and liquor receiver (11). The vacuum pump (VP-1) (Model S10), a single stage rotary vane with a capacity of 10 m^3/hr was supplied by Speedivac South Africa. The vacuum trap was a modified 1 L glass Schott media bottle, whilst the liquor receiver (11) was a 3 L, also of Schott bottle type, supplied by Glasschem, South Africa. The vacuum receiver was fabricated using a 5 L glass bottle (Schott). Vacuum lines connecting the vacuum system to the vacuum trap and the equipment were made of 8 mm silicon tubes.

3.2.4 Control Unit

A 30 ampere energy controller was supplied by Glasschem, South Africa. The controller had two outputs (15 A each) controlled with a regulator on each channel. The regulators were rated 25 A at 240 V and were connected to both the heating coil and the heating element. The controller's main purpose was to regulate and record the temperature for the heating element (1) and the heating coil (5). The unit was connected to five different thermocouples (Th1-Th5) which measured temperature and a further two thermocouples (Th7–Th8) for heating elements temperature control and measurement (accuracy; ±3^{o}C). The thermocouples are shown on the diagram (Figure 3-1) and are further described in Section 3.2.8. It was also connected to a flow meter to measure and record the flowrate of the feed solution.

3.2.5 The heating coil

The heating coil (number 5 on Figure 3-1) was manufactured by Glasschem South Africa. It was constructed by coiling a 1 mm copper wire around a 22 mm ceramic tube and insulated with standard fibreglass around the wires, then covered by a steel tube of 64 mm outside diameter and 300 mm long (Figure 3-2). The coil had a rated capacity of 1 kW. The feed tube (12.3 mm inside diameter and 15 mm outside diameter) was then fitted inside the ceramic tube, and normal sand was added to fill in the space between the feed and ceramic tubes for enhanced heat transfer by conduction, as radiation heat transfer lead to overheating of the heating coil. The heating coil therefore maintained the temperature of the two-phase mixture of liquid and vapour just before entering the flash separator.

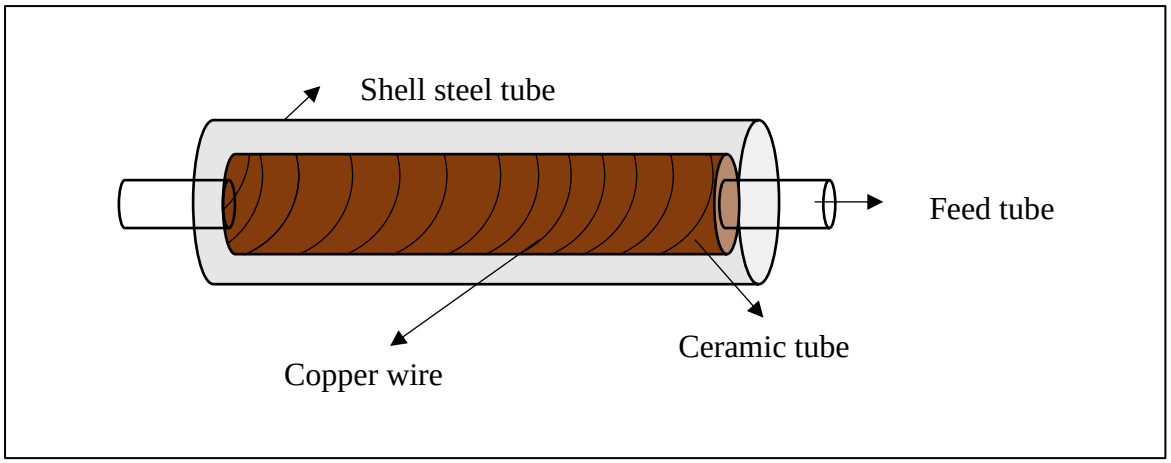

Figure 3-2: A schematic diagram of heating coil.

3.2.6 The flash separator

The stainless steel flash separator (number 6 on Figure 3-1) was fabricated in the Stellenbosch University Workshop. Its dimensions were an outside diameter (O.D) of 129 mm, a thickness of 4 mm and 601 mm in length. The base geometry of the final separator differed slightly from the general design guidelines presented in Section 2.4.8. The total height was reduced to give the main design part (the L/D ratio) of 4.8 (therefore lying between 3 and 5) as recommended in (Section 2.4.8) for a vertical separator design. The main reason for the height reduction was to reduce the equipment cost without affecting the separator efficiency. Details of design calculations for the vertical flash separator are presented in the Appendix B.

3.2.6.1 Flash separator internals and mist extraction devices

The flash separator design was fitted with a half pipe internal device since it was considered the most economical of the three suitable devices. The multi-cyclone, one of the best performance devices beside the inlet vane, was also experimentally compared to the half pipe device.

The mist extractor of choice was the mesh due to its applicability to small designs. The mesh mist extractor is also the most common device and simplest to use. Although the cyclone and the vane would give superior performances, they are highly expensive and not applicable to small operations

Half-pipe inlet

The Stellenbosch University Workshop fabricated the stainless steel half pipe internal (Figure 3-3). The dimensions of the pipe were an inside diameter (I.D) of 24 mm and length 125 mm. The bottom half of the pipe was cut centrally (5 mm from the edges) and 12 mm diameter, to produce a grove of length 115 mm and 12 mm deep.

Figure 3-3: The half-pipe inlet device.

The mesh pad

The mesh pad was supplied by the Specialities in knitted Mesh Products (SMI) Company, South Africa. The stainless steel wire mesh pad was 500 mm thick and 125 mm diameter with 0.28 mm mesh holes (Figure 3-5).

Figure 3-4: The Mashhad

3.2.7 The condenser

A water-cooled Graham type condenser (number 7 in Figure 3-1) consisting of a 10 mm inner coil running through a 45 mm inside diameter cooling chamber was considered. It was fabricated by Glasschem South Africa. The vapour inlet and condenser outlet were fitted with glass tubing of 12 mm inside diameter and connected to the flash separator and vacuum receiver respectively. The condenser water inlet and outlet were fitted with a glass tubing of 4 mm inside diameter. Cold water was pumped by means of a submersible pump; model HJ-Series (HJ-941) with a capacity output of 800 l/hr. The cold water was controlled by 1000 WOG BSP model ball valve.

3.2.8 Measuring Instruments

Temperature measurement

Temperatures were measured with steel thermocouple digital probes (type PT100) applicable up to 120^{o}C, which were connected to the LCD (control Unit). The thermocouple probes were monitored at seven different points, i.e;

- Th 1 measured the feed temperature just before entering the throttling process.
- Th 2 measured the vapour temperature.
- Th 3 measured the recirculating liquor temperature.
- Th 4 and 5 measured the water supply temperature at inlet and outlet of condenser.
- Th 7 measured the temperature of the two-phase mixture of liquid and vapour just before entering the flash separator.
- Th 8 measured the temperature solution in the feed tank.

All these are shown in Figure 3-1. Before starting the experiments, all thermocouples were calibrated in a constant temperature bath at the boiling and freezing points of water.

Pressure gauges

Bourdon tube pressure gauges, stainless steel series were supplied by WIKA (model 232.50). The pressure gauges cover ranges of 1.3 kPa abs to 251.3 kPa abs. They are used on the low-pressure (PG 2 - PG5) and high-pressure sides (PG1) as shown on Figure 3-1. The pressure gauges were calibrated to read 1.3 kPa abs to 251.3 kPa abs with a vacuum pump, centrifugal pump and compressed air. The pressure gauges were installed to monitor pressures at five different points, i.e.

PG 1 measured the pressure of the fluid immediately prior to the fluid entering the throttling process, PG 2 measured the two-phase mixture of liquid and vapour pressure just before entering the flash separator, PG 3 measured the pressure inside flash separator and PG 4 measured the vacuum pump pressure. All these are indicated on Figure 3-1.

The electromagnetic flowmeter

The total fluid flow rate fed to the heating coil was measured by means of an electromagnetic flow sensor meter (number 4 in Figure 3-1)(model SNS-FLOW401), which is mainly made of a plastic body, with 6.35 mm external threads and a flow range of 0.3-6 L/min. A pinwheel sensor measured the amount of liquid that moved through it. The flowmeter's maximum operating temperature was 80^{o}C, and was connected to the unit controller for flow recording.

The rotameter

The flow rate of cooling water into the condenser was measured using a 25 mm plastic variable area rotameter (GEMU ID-DE-88003029-7505275)(number 8 in Figure 3-1), with a capacity of 0-60 L/hr of water at 20^{o}C (number 7 on Figure 3-1). The rotameter was calibrated by discharge weight versus time measurements at operating temperature.

3.2.9 General system insulation

The entire apparatus was insulated to minimize heat losses. All small pipe feed lines were covered with standard fibreglass with aluminium foil insulation, approximately 10 mm thick. The heating coil was covered with 20 mm aluminium foil insulation, as well as the flash separator, and any other hard to insulate parts, such as the throttling valve. To minimise heat losses from the heating jacket, standard fibreglass and aluminium foil insulation approximately 30 mm thick was used to wrap it from top to bottom.

3.3 VACUUM EVAPORATION SYSTEM DESIGN

The initial VES process flow diagram is shown on Figure 3-1. It included a centrifuge pump, the throttling valve, heating coil, the flash separator, condenser, vacuum pump and the feed tank (heated by a direct heating element). The VES was tested with water to confirm its functionality and compare the evaporation characteristics of running at different conditions, namely without an inlet device, with a half pipe internal as well as half-pipe with a mesh pad.

3.4 EXPERIMENTAL DESIGN

3.4.1 Initial experimental design

From the literature review, many variables were confirmed to affect the performance of the vacuum evaporation system. The variables investigated in this study were the evaporating temperature, internals type inside flash separator (with or without half-pipe), with or without a mesh pad device, vacuum pressure and the initial concentration.

Three experiments were then run at the same conditions of temperature (70^{o}C), pressure (12.3 - 23.3 kPa abs), flowrate (300 -350 ml/min) and condenser water supply (750 ml/min) to evaluate the evaporation characteristics of three different factors as follows:

i. Using half-pipe internal without mesh pad (Experiment1).
ii. Using half-pipe with mesh pad (Experiment 2).
iii. No device (Experiment 3).

3.4.2 Experimental procedure

The VES was tested for leaks, thoroughly cleaned and then flushed with demineralised water before the experimental work began. Power supply thermocouples and other instruments were then connected and calibrated.

The vacuum evaporation system was started after setting the feed tank temperature (Th8), feed flow rate, heating coil temperature (Th7) and vacuum levels (PG-2 and PG-3) at the desired values as described in appendix G. During the course of the run, all temperatures (Th1-Th8) and flow rates were recorded at 10-minute intervals on the controller LCD.

The feed solution was heated to the required set point in the feed tank (2) using a heating element in a heating jacket (1), its solution temperature (Th8) being controlled by the temperature controller unit. A centrifugal pump (3) pumped the feed solution from the feed tank (2) at 160 kPa absolute pressure (PG-1). Some solution was recycled through a gate valve (V-2) located on the discharge side of the pump. Copper tubes (12.3 mm internal diameter), assembled with removable clamps were used as feedlines. The feed was pushed to the flash separator through a throttling device, 6.35 mm brass integral bonnet needle valve, 0.37 CV, (Model B-1RS4, 792962001).

The needle valve (V-3 in Figure 3-1) controlled the raw material flow rate as well as drop the pressure. Then from the throttling device, the flow became turbulent due to a high-pressure drop, which stabilised to steady state (laminar flow) after some time. The feed then passed through the flow meter (4) for flow measurement and then the heating coil (5) where it was heated to evaporating temperature, forming a mixed liquid and gas stream. The two-phase mixture then entered the flash separator (6) where it separated into a bottoms liquid fraction and a tops vapour fraction. The bottom fraction was recycled to the feed tank (2) through the liquor receiver (11) and the process of heating, throttling and flash evaporation repeated until a required solution concentration was achieved. The liquor receiver (11) was drained every 2 to 4 minutes. When the required concentration was attained, the bottoms product was then collected into a final products tank. The top vapour fraction was sucked by vacuum pump (VP- 1) to a vacuum receiver (12) (5 l Schott bottle)). The condensate was measured and recorded on an hourly basis. A vacuum trap TR-1 (1 l Schott bottle), fitted in the vacuum line between the vacuum receiver (12) and vacuum pump (VP-1) to protect the vacuum pump from any condensate coming from the vacuum receiver, was kept in a cold-water bucket.

A vacuum pump (VP-1) was connected to a liquor receiver (11) through TR-1 to facilitate the draining of the flash separator (6) bottoms liquid without disrupting the vacuum system. Silicon tubes (10 mm inside diameter) were used as vacuum unit lines for easy removal. The vacuum system was carefully sealed and checked for air leakage every time before each run. Vacuum pressure inside flash separator was adjusted manually by using the needle valve (V-10) (Type Brass Veriflo Parker. Model WO67544-02SN087878). A 6.35 mm type 1000 WOG BSP bleed ball valve (V-11) was also connected to vacuum pump (VP-1) for safety procedure.

3.4.3 Modification of the initial design

Modification was done by adding a second vacuum pump and a condensate receiver to eliminate fluctuations during liquor drainage increase the accuracy of condensate recovery measurements, respectively. The whole apparatus is shown in Figure 3-5 and the added equipment are described as follows:

Vacuum pump 2

The second vacuum pump (VP-2) (model EDM2) was supplied by Edwards High Vacuum, United Kingdom. It served to reduce the pressure in the liquor receiver (11) and thus facilitate drainage of the concentrated liquid from the separator whilst the system was operating. Vacuum adjustment was done using a 6.35 mm type 1000 WOG BSP bleed ball valve (V-14) and was measured by a pressure gauge (PG-5). One more vacuum trap (TR2) and condensate receiver (13) were also added to the unit.

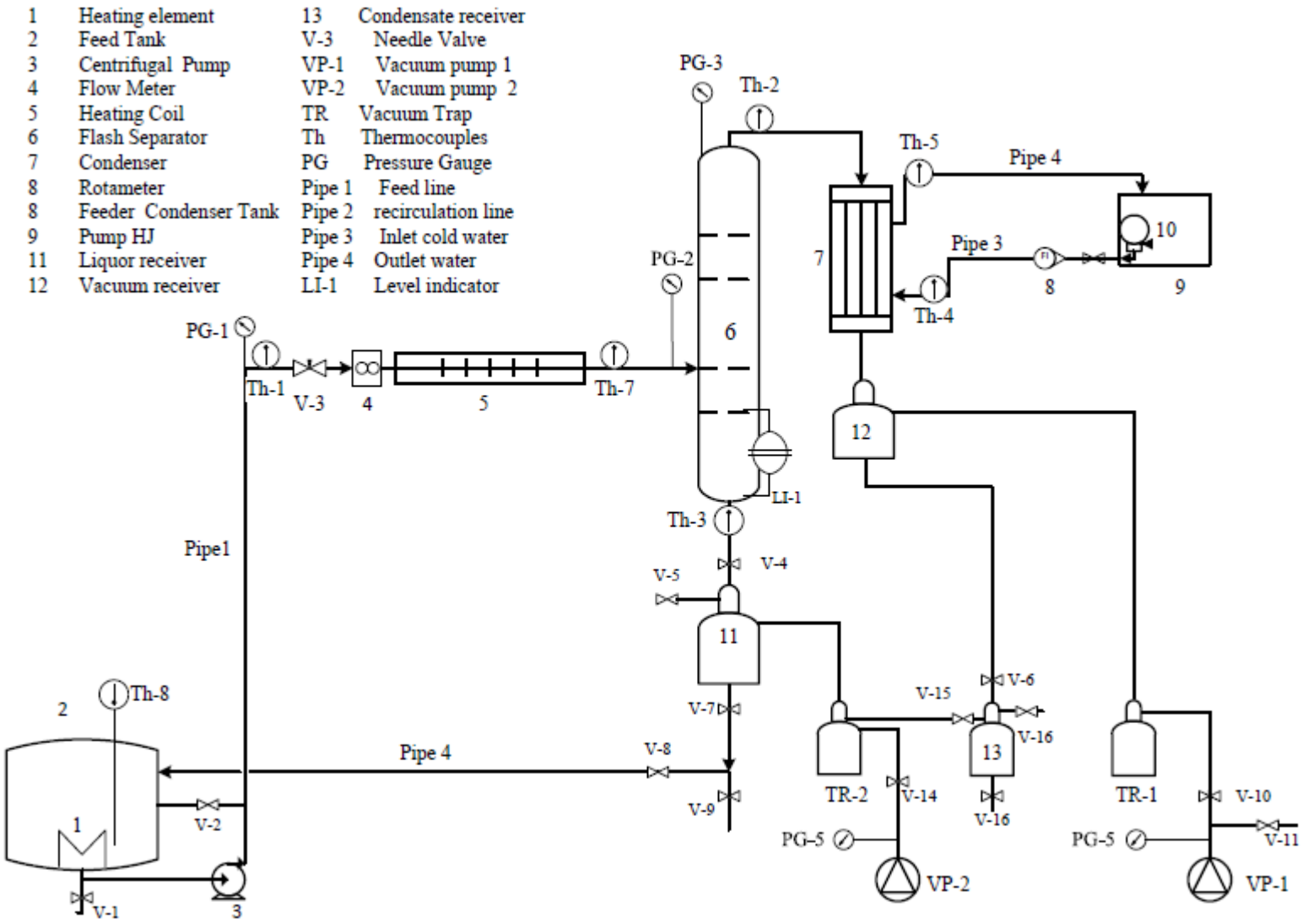

Figure 3-5: Modification of the initial vacuum evaporation system design

3.4.3.1 Evaluation of initial modifications

The three runs described in Section 3.4.1 were repeated on the modified experimental set up (Figure 3-2). The pressure and the flowrate stabilised due to the modifications (21.3 kPa abs and 300 ml/min respectively). The temperature (70^{o}C) and condenser water supply (750 ml/min) remained unchanged. The experimental factors are defined as follows:

i. Using half-pipe internal without mesh pad (Experiment 4).
ii. Using half-pipe with mesh pad (Experiment 5).
iii. No device (Experiment 6).

3.4.3.2 Modified experimental procedure

After modifications to the initial design of a second vacuum pump (VP-2), a condensate receiver (13) as well as the vacuum trap (TR-2) the experimental procedure also changed as follows:

The addition of the condensate receiver (13) allowed the condensate to be drained from the vacuum receiver (12) every ten minutes. Instead of measuring the cumulative volume of condensate in the vacuum receiver, the condensate could now be drained into the condensate receiver, and then into a measuring cylinder for accurate measurement. From the vacuum receiver (12) bottom, the condensate passed through the condensate receiver (13) and a vacuum trap TR-2 (1 l Schott bottles) connected in series to prevent the condensate from reaching the vacuum pump (VP-2). TR-2 was kept in a cold-water bucket to eliminate any remaining condensate from the system.

The second vacuum pump (VP-2) was connected to a liquor receiver (11) (3 l Schott bottle) and the condensate receiver (13) through TR-2 to facilitate the draining of the flash separator (6) bottoms liquor and the condensate from the vacuum receiver without disrupting the vacuum system.

3.4.4 Modification to eliminate foaming

Modification was done to eliminate foaming of the WPC solution. Physical methods were preferred over chemical methods (addition of antifoam) to avoid introduction of silicone into the final consumable product.

The first modification stage was replacement of the mesh pad with five stages of mesh after the mesh pad was blocked by the foam. The next stage was to replace the half pipe with a multi-cyclone to stop eliminate foaming in separator. Finally, when the two modifications could not stop foaming, a window was inserted on the separator to observe the foam at formation stage and facilitate addition of antifoam. The modification details are as follows:

Mesh stages

Since foaming is generally difficult to control, mesh stages were introduced as an attempt to break the foam bubbles, with an evaluation run to determine if they would work. The stages of mesh were fabricated in the Stellenbosch University Workshop using galvanised welded mesh supplied by a local store in South Africa. Five stages, 15 mm thick and approximately 125 mm diameter with 7 mm mesh holes were made.

Multi-cyclone inlet

A multi-cyclone device (Figure 3-4), consisting of four cyclones, was fabricated in the Stellenbosch University Workshop. The multi-cyclone was added as a modification to the original design to eliminate foaming. Due to the limiting size of the flash separator, the multi-cyclone was designed with two large and two small cyclones. The description of the multi-cyclone is as follows:

- Cyclone body inside diameter 32 mm for large and 24 mm for small
- Cyclone total height 110 mm
- Cylindrical part height 70 mm
- Gas outlet diameter 18 mm
- Vortex finder length 40 mm and inside diameter 16 mm
- Cyclone cone-tip inside diameter 21 mm for large ones and 11 mm for small

Figure 3-6: The multi-cyclone inlet device

Addition of antifoam

After an unsuccessful prevention of foaming by using modified internals in the flash separator, the separator was modified to facilitate addition of antifoam when foaming started. Two glass windows (500 mm in diameter and 5 mm thick) were fitted into the separator wall to enable visual detection of foaming. The antifoam addition device was constructed from a 200 ml glass bottle and was also connected to the separator using a 3 mm copper tube with a plastic ball valve to add the antifoam into the separator without disrupting the vacuum conditions.

3.4.4.1 Evaluation of foam elimination modifications

Four experimental runs were conducted to evaluate the effect of the modification on foam elimination. Experiments 5, 6, 7 and 8 were run on conditions stipulated in Table 3-1. All the experiments were run on about 300 ml/min feed flowrate and vacuum pressure of between 12.3–15.3 kPa abs.

Table 3-1: Experiments condition for foam elimination modifications

Factors	Temperature (°C)	Initial concentration (wt%)	Run number
Half-pipe with mesh pad	70	10	5
Half pipe with mesh stages	65	10	6
Multi cyclone with stages mesh	60	10	7
Multi cyclone with anti-foam	65	10	8

3.4.5 Modification to eliminate fouling on heating element

Modification of the pre heating (direct heating) system was done in an attempt to eliminate fouling on the heating element in the feed tank. The first stage was to fit a stirrer in the feed tank to agitate the feed WPC solution. The stirrer was uncontrolled and at high speed, thus it produced foaming in the system. A controller was then connected to reduce and regulate the stirrer speed. Finally, the direct heating was replaced by indirect heating by using a heating jacket around the feed tank. The modification details are as follows:

Stirrer and controller

The stirrer, connected to a single phase motor (model JA2R08ON#) with a rotational speed of 1250 rpm was fitted for agitation. A Yaskawa controller (model VS mini J7) regulated the stirrer speed.

The heat jacket

In order to avoid fouling on the heating element that occurred when employing direct heating of the solution through a heating element located in the feeder tank, a decision was made to introduce indirect heating.. This was done by placing the feeder tank inside a second, larger tank, thus effectively creating a heating jacket. A cylindrical stainless steel tank was fabricated to use as a heating jacket. It had a 300 mm inside diameter and a height of 260 mm with a capacity of approximately 9 L. The jacket was fitted with a 3000 W heating element and temperature probe (Th-6) measured the water temperature. The feeding tank (Section 3.2.1) was then fitted inside the heating jacket and mixing was achieved by use of a stirrer to achieve homogeneity in heat transfer inside the feeder tank.

3.4.5.1 Evaluation of fouling elimination modifications

A total of four experiments were conducted to evaluate the effect of the heat jacket, the stirrer and indirect heating on fouling. Experiments 9, 10, 11 and 12 were run on conditions shown in Table 3-2. The flowrate was about 300 ml/min and vacuum pressure between 12.3 - 15.3 kPa abs.

Table 3-2: Experiments condition for fouling elimination modification.

Factors	Temperature (°C)	Initial concentration (wt%)	Run number
Direct heating	65	10	9
Direct heating with uncontrolled stirrer	65	10	10
Direct heating with controlled stirrer	65	10	11
Indirect heating	65	10	12

3.4.6 Whey protein concentration

Having made some modifications to eliminate feed flow fluctuations, fouling and foaming in the system, the next stage was then to evaluate the system evaporation parameters with the WPC solution and compare them with NaCl and sugar solution. Sugar and NaCl solution were selected as non-protein materials because they are relatively easy to find and neither corrosive nor thermal sensitive (at temperature ranges of 60 to 70°C). They also have known physical properties.

The variable ranges were then selected after some test runs (with water) were done to confirm the capacity of the vacuum evaporating system. The evaporating temperature range was selected to be 60 to 70°C because for a small vacuum flash separator, a lower evaporating temperature would cause excessive entrainment. To suit the capacities of the flow meter, centrifugal pump and the flash separator, the feed inlet flow rate range was limited to between 275 and 340 ml/min. Finally, the vacuum pressure was limited to between 10 kPa abs to 15 kPa abs. The experimental variables are presented in Table 3-3.
The experiments evaluated the following:

- The heat transfer coefficients of the WPC solution, sugar solution and the NaCl solution.
- The viscosity of the WPC and the sugar solutions.
- The maximum achievable concentration of the WPC solution using the designed VES.
- The relationship between rate of evaporation, heat transfer coefficient and concentration for the WPC solution.
- How the evaporation rate of the WPC solution compare to that of non-heat sensitive materials, sugar and NaCl solutions at the same conditions.

The experimental conditions are presented in Table 3-3.

Table 3-3: Experiments conditions

Type of solutions	**Temperature (°C)**	**Initial concentration (wt%)**	**Run number**
WPC	65	5	15
WPC	65	10	16
WPC	70	5	17
WPC	70	10	18
Sugar solution	65	5	19
NaCl solution	65	5	20

3.4.7 Statistical analysis

Statistical analysis was performed using Statistica, STAT 13, 2017. The analysis included regression analysis and multi variable graphical analysis. Regression analysis was done to determine the relationship between the condensate collected and a solid concentration of WPC solutions which were directly and indirectly heated. The regression was done at 95% confidence level. Standard deviations of feed flowrate before and after addition of a second vacuum pump were calculated using excel 2013.

3.5 MATERIALS

Whey protein concentrate (80%) regular (manufactured by Leprino Foods, USA) was supplied by Warren Chem Specialities. It was received in a 20 kg bag and kept tightly closed in a dry area at room temperature. Food grade sugar and coarse NaCl were bought from local stores. Food grade antifoam (20%) (Bio-sil AF720F) was supplied by Silicone and Technical products (Pvt) Ltd, Cape Town. Sodium hydroxide pellets (NaOH) was supplied by AR Chemicals & Laboratory Suppliers South Africa. It was dissolved in water to make a solution of 0.2% strength. Deionised water was used for making all solutions.

3.5.1 Whey proximate composition

The proximate analysis of the WPC is shown in Table 3-4. Analysis was done by Karnala Deviries at Leprino Foods Dairy Product Company in the USA.

Table 3-4: WPC proximate composition

Component	wt%	Method
Protein	80	Kjeldahl
Fat	8.5	Rose-Gottlieb (Ether extraction)
Moisture	6.5	Vacuum oven 149^{o}F (65^{o}C)
Ash	5.0	Residue in ignition

3.5.2 Preparation of whey protein solution

The WPC powder was dissolved in deionised water and mixed with an overhead stirrer (model IKA RW 16 basic). The stirrer was manufactured by IKA-Werke GmbH & Co. KG, in Germany. The agitation speed was maintained at 1200 rpm. Concentrations of the solutions were varied from approximately 5-10 wt% and were prepared immediately prior to each experimental run.

3.6 METHODS

3.6.1 The heat transfer coefficient

The heat transfer coefficient is a critical parameter in evaporation systems since it determines the efficiency of evaporators. It is useful in investigation of the energy consumption by the evaporator. Therefore, for minimising the evaporation system's energy consumption and environmental impact, the heat transfer coefficient must be calculated.

In this study, the heat transfer coefficient was determined inside the heating coil. The heating coil was selected because it was closer to the separator, therefore could be better used to determine the relationship between heat transfer coefficient and the evaporation rate. Only the inside heat transfer coefficient was calculated because the thermal conductivity of the sand and ceramic tube were unknown and the temperatures of the ceramic tube/sand as well as the sand/copper tube interfaces could not be measured (Figure 3-7). The heat transfer coefficients of two liquids (WPC and sugar solution) were investigated. The physical properties of WPC and sugar solution are mainly functions of the temperature and their mass fraction.

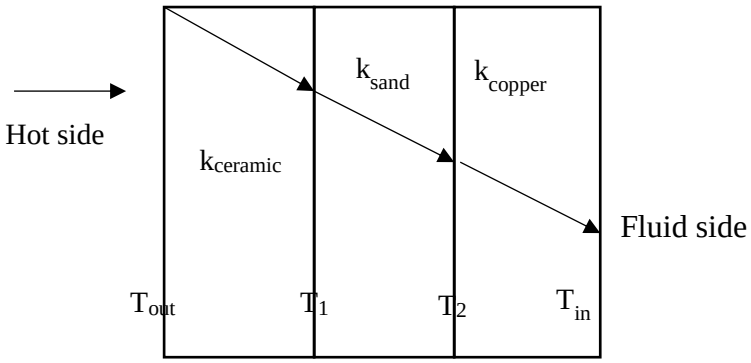

Figure 3-7: Temperature gradient across the heating coil

Where;

T_{out} - Temperature of the wires (Hot side, ^oC)

T_1 - Temperature between the ceramic tube and sand (^oC)

T_2 - Temperature between the sand and copper tube (^oC)

T_{in} - Inside temperature (fluid side,^oC).

$K_{ceramic}$ - Thermal conductivity of ceramic tube (J/s m K)

K_{sand} - Thermal conductivity of sand (J/s m K)

K_{copper} - Thermal conductivity of copper tube (J/s m K)

The heat transfer coefficient, h_i, was calculated using Equation 3-1 (Suryanarayana, 1995):

$$h_i = N_u \frac{K_i}{D_i} \qquad \text{Equation 3-1}$$

Where:

h_i - Heat transfer coefficients ($W/m^2.k$)

Nu - Nusselts number

Ki - Thermal Conductivity (J/s m K)

Di - Inside diameter of tube (m)

3.6.1.1 Thermal properties of solutions

WPC and sugar solutions

A regression model used to calculate the thermal properties of WPC (density, thermal conductivity and heat capacity) was developed from the thermal properties of food (protein, fat, water, carbohydrate and ash) (Choi, 1986; Murakami and Okos, 1989). The model is applicable for a temperature range of -40°C to 150°C.

For calculation of the heat capacity and thermal conductivity of the sugar (sucrose) solution, models by Simion and colleagues (2017) were employed. The models are applicable for solutions at temperatures between 0 to 100°C and concentration between 0 to 90 wt% for heat capacity. Thermal conductivity models applicability was for temperatures between of (0 to 80°C) and concentration of between 0 and 60 wt%. For calculation of the density of sugar solution as a function of temperature and concentration, with an accuracy of more than 5×10^{-5} g/cm^3, a model developed by Darros-Barbosa and colleagues (2003) was used. The thermal properties of the sugar solution as determined by these models were then compared to carbohydrate properties as determined by a model developed by Choi (1986). The data are presented in Appendix D. Calculation procedures of the thermal properties are presented in Appendix C.

3.6.2 Viscosity measurement

Viscosity is considered to be one of the critical input variables in the concentration of protein solutions (Mackereth *et al.,* 2003). Viscosity measurements were necessary for the determination of the heat transfer coefficient. The apparent viscosities of the WPC and sugar solutions were measured using a Rheometer Anton Paar (PhysicaMCR501). Viscosity measurements were obtained at a temperature range of 59 to 70^{o}C using a DG26.7/T200/SS and a cooling bath temperature of 20^{o}C. The apparent viscosity at a constant shear rate of 23/s (calculated during system design) was used for different solutions comparisons. Apparent viscosities of the WPC solutions were determined as functions of the solid concentration and temperature. The mass fraction and temperature dependence measurements were varied between 4.2 wt% to 17.1 wt% and 59^{o}C to 70^{o}C respectively. The temperature was linearly increased from 59^{o}C to 70^{o}C using a heating rate of 0.4^{o}C for 25 sec (with temperature control accuracy of 0.1^{o}C).

3.6.3 Sample preparation

Different samples of WPC solution were prepared by adding WPC powder to deionised water at 40^{o}C (in a water bath) and stirring at low speed (500 rpm) to avoid foaming until dissolved. The solutions were prepared based on weight, using a mass scale with an accuracy of 10^{-4} g and later stored at 4^{o}C to be used within 48 hours.

3.6.4 Moisture analysis

Moisture content was established using the Karl-Fischer titration method (Fischer, 1935). The method involved evaporating samples to constant weight at 180^{o}C using a Kern electronics moisture analyser (DBS 60-3) supplied by Kern & Sohn GmbH, Balingen. Approximately 1 g of each sample was weighed into an aluminium dish and dried until it reached a constant weight. Smaller samples of approximately 1 g were preferred because they create thinner films, which allow faster drying (approx. 15 minutes per sample). The samples were withdrawn by opening the drain valve at the feed tank bottom and collecting 5 ml of solution into a glass bottle on an hourly basis.

4. RESULTS AND DISCUSSION

4.1 PROCESS EQUIPMENT DEVELOPMENT

This section presents results of experiments ran in the process development stage (Experiments 1 – 14). They included elimination of process challenges such as flow fluctuations, foaming inside the separator as well as fouling on the heating element in the feed tank.

Experiments 1, 2 and 3 did not produce satisfactory results due to system fluctuations, mainly the flowrate and vacuum pressure inside the separator. To eliminate the fluctuations, modifications, including addition of a second vacuum pump and a condensate receiver were done. The modifications also allowed accuracy measurement of the condensate removal by draining the condensate every 10 minutes from the vacuum receiver to the condensate receiver for quantification. Evaluations of these modifications were carried out in experiments 4, 5 and 6, and were successful.

Experiments 7 to 10 were run on WPC solution and observations of foaming were made which led to some further modifications, which included the introduction of stages of mesh, the multi- cyclone and the antifoam. The foam was eliminated by addition of antifoam after the other modifications could not stop it.

The next batch of experiments (11 to 14) dealt with fouling elimination. The modifications involved the incorporation of a stirrer at a controlled agitation rate and replacement of direct heating (using a heating element) with a heating jacket (Indirect heating)

4.2 OPTIMIZATION OF THE VES

The system was optimised by using WPC at different operating temperatures (65 and 70^{o}C) with different initial solid concentration (5 and 10 wt%) in experiment 15-18. . The system was further optimised by using different solutions (sugar and NaCl solutions) at 65^{o}C with an initial concentration of 5 wt% in experiment 19 and 20. The WPC solutions were then evaluated to determine the heat transfer coefficient, viscosity, and comparisons were made with non-heat sensitive materials (sugar and NaCl solutions) were done. All these results are presented in this section.

4.3 INITIAL EXPERIMENTS RESULTS

The VES was tested with water to confirm its functionality and compare the evaporation characteristics of running at different conditions. Three experiments: experiment 1 (with half-pipe), experiment 2 (half-pipe with mesh pad) and experiment 3 (no device) were run and their conditions and results are shown in Table 4-1 and 4.2 respectively.

Table 4-1: Experimental conditions of initial design

Condition	Experiment 1	Experiment 2	Experiment 3
Initial quantity of water (kg)	6	6	6
Operating temperature (^{o}C)	70	70	70
Evaporator pressure (kPa abs)	12.3-23.3	12.3-23.3	12.3-23.3
Protein solution flow rate (ml/min)	300	300	300
Condenser water flow rate (ml/min)	750	750	750
Mesh pad	None	Yes	None
Type of internal	Half-pipe	Half-pipe	None

Table 4-2: Condensate removal with the time for initial design experiments.

Time (minutes)	Moisture removal (ml)		
	Experiment 1	Experiment 2	Experiment 3
0	0	0	0
60	900	850	120
120	1900	1650	320
180	2600	2350	550
240	3350	3150	870

Figures 4-1 and Table 4-2 compare the condensate collected with time for the three experiments using different separator internal devices. Figures 4-1 shows the increase in condensate recovered for three experiments (1, 2, and 3) respectively, at the same operating temperature (70^{o}C) and vacuum pressure about (21.3 kPa abs) but different devices (half-pipe, half-pipe with mesh pad and no device) respectively. The evaporation time increased up to 240 minutes for all experiments,. From Table 4-2, the run with only the half pipe device (experiment 1) had the highest condensate recovery (3350 ml), followed by experiment 2 with half-pipe and mesh pad (3150 ml) and lastly the experiment 3 with no device (850 ml). Figure 4-1 illustrates graphically the condensate recovery over time.

Figure 4-2 shows the extent of fluctuations of the feed flowrate in the three experiments (1, 2 and 3), as the pressure inside the separator varied during drainage of solution. The flowrates fluctuation range was 90 ml/min (from 300 to 390). Experiment 3 (with no device) had the highest standard deviation of feed flowrate (32 ml/min), followed by experiment 1 (with a half pipe internal) (29 ml/min) and lastly experiment 2 (with a half pipe and mesh pad) (17 ml/min).

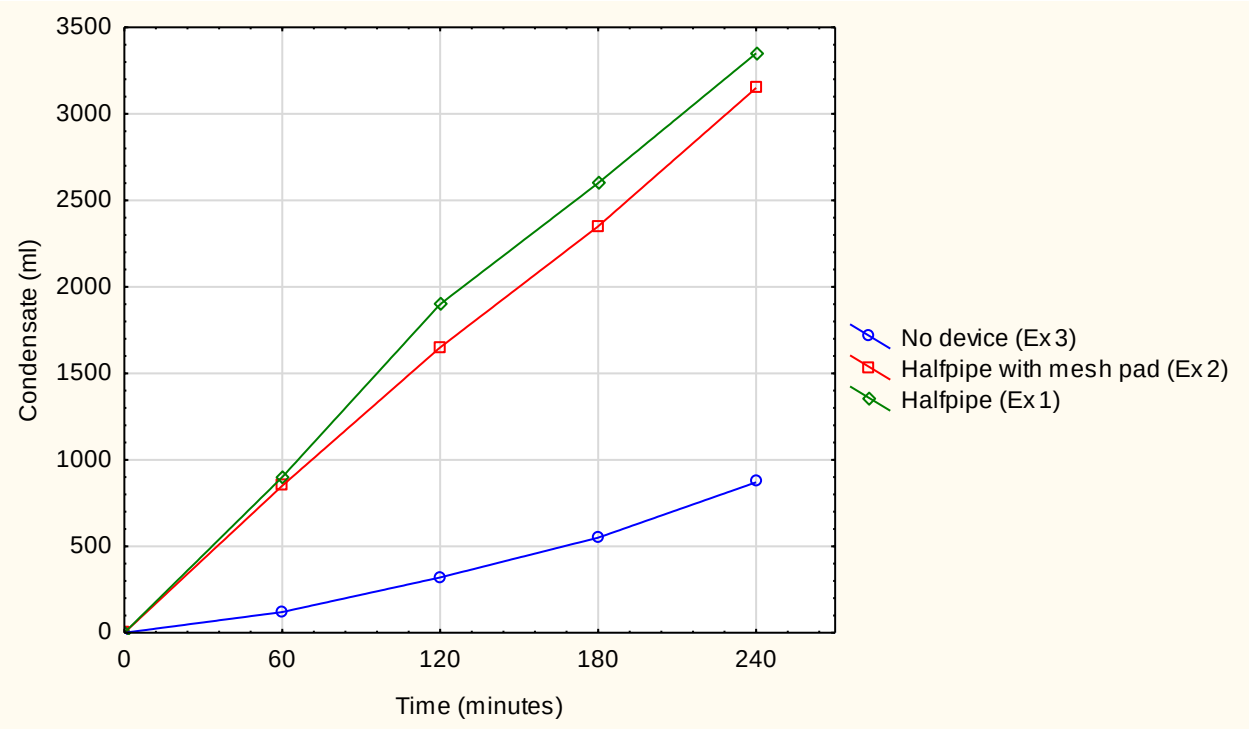

Figure 4-1: Evaporating water of different devise at the same temperature (70^{o}C)for experiments 1, 2 and 3

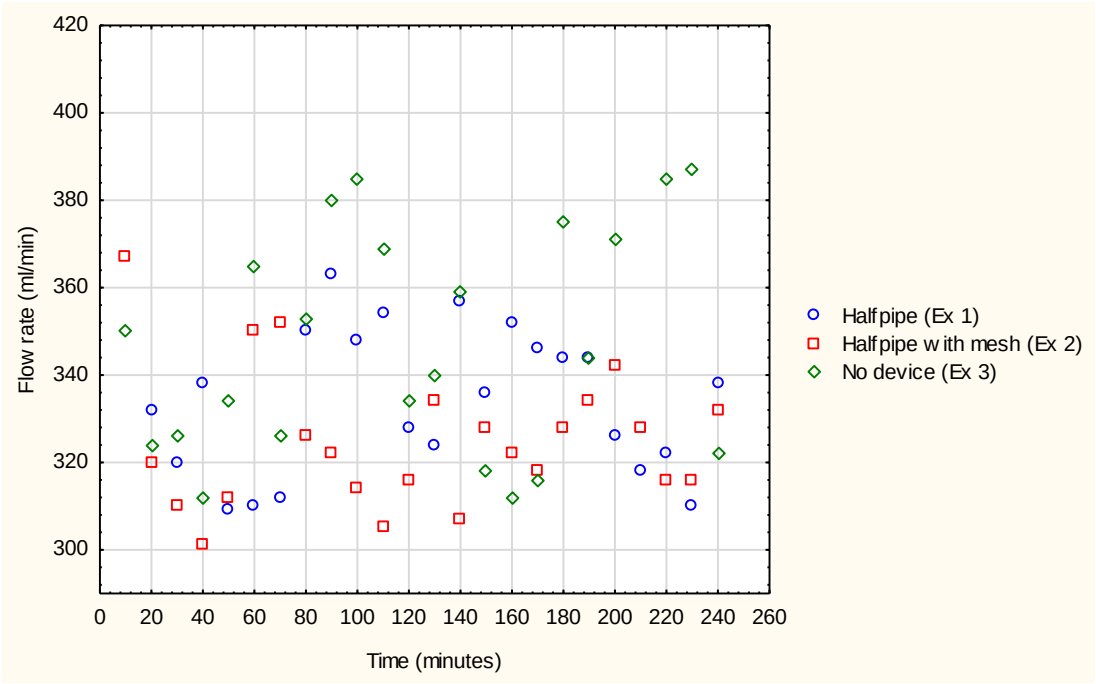

Figure 4-2: Flow rate profile of different devise at the same temperature (70^{o}C) for experiments 1, 2 and 3

Where: Ex is the experiment number

4.3.1 Evaluation of initial modifications

After modification of the initial VES system by addition of the second vacuum pump and the condensate receiver, experiment 4 (with a half-pipe), experiment 5 (with a half-pipe and mesh pad) and experiment 6 (with no device) were run to eliminate the fluctuations of the flow feed flow rate and control of separator pressure. The experimental conditions and results are presented in Table 4-3 and 4.4 respectively.

Table 4-3: Experimental condition of modification initial design

Condition	Experiment 5	Experiment 6	Experiment 7
Initial quantity of water(kg)	6	6	6
Operating temperature (^{o}C)	70	70	70
Evaporator pressure (kPa abs)	21.3	21.3	21.3
Protein solution flow rate (ml/min)	300	300	300
Condenser water flow rate (ml/min)	750	750	750
Mesh pad	None	Yes	None
Type of internal	Half-pipe	Half-pipe	None

Table 4-4: Condensate removal with time

Time (minutes)	Moisture removal (ml)		
	Experiment 4	Experiment 5	Experiment 6
0	0	0	0
60	1046	675	485
120	1894	1740	1160
180	2936	2620	1935
240	3691	3450	2750

Figure 4-3 and Table 4-4 compare the condensate collected in the three experiments (4, 5 and 6). They show that the half-pipe internal had the highest condensate recovery (3691 ml) after 240 minutes, followed by the half-pipe with mesh pad device (3450 ml) and lastly experiment 6 (with no device (2750 ml)).

Figure 4-4 shows the fluctuations of the feed flowrate of the three experiments (4, 5 and 6). The fluctuation range was about 35 ml/ min (from 280 to 315 ml/min). Flow rate standard deviations were 11, 9 and 8 ml/min for experiments 4 (with half a pipe), 5 (half a pipe and mesh) and 6 (no device) respectively.

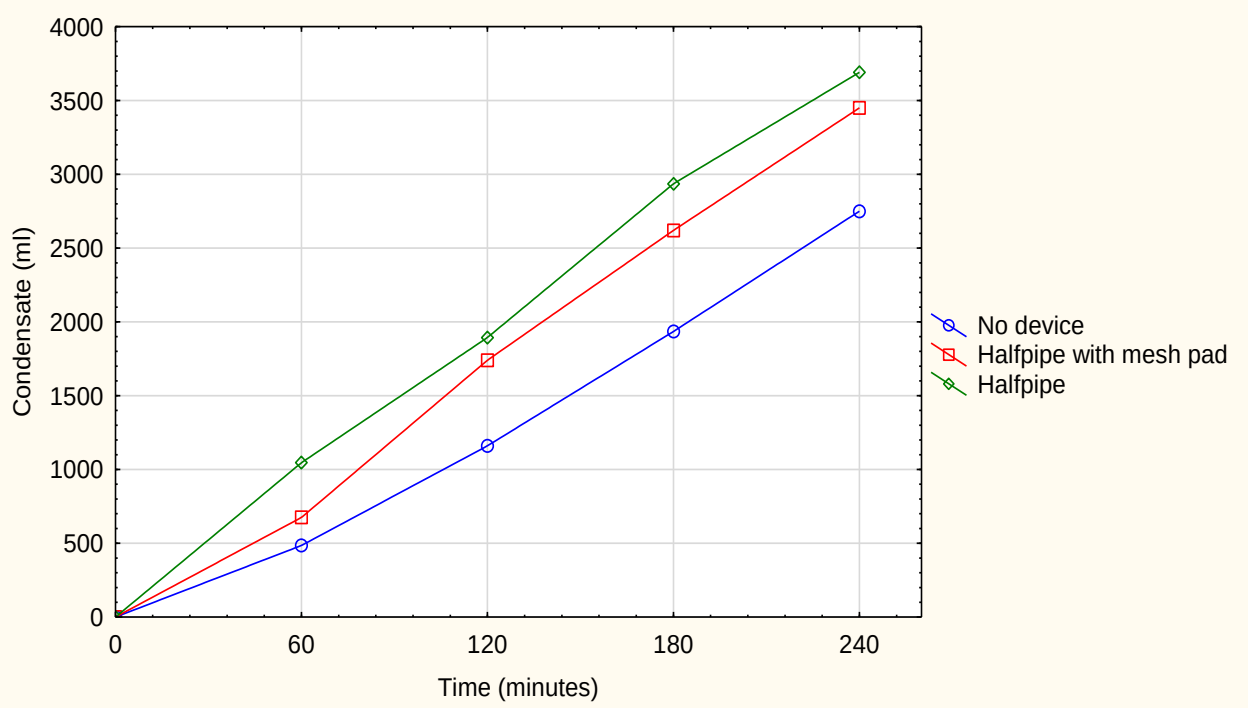

Figure 4-3: Evaporating water of different devise at the same temperature (70°C) for experiments 4, 5 and 6

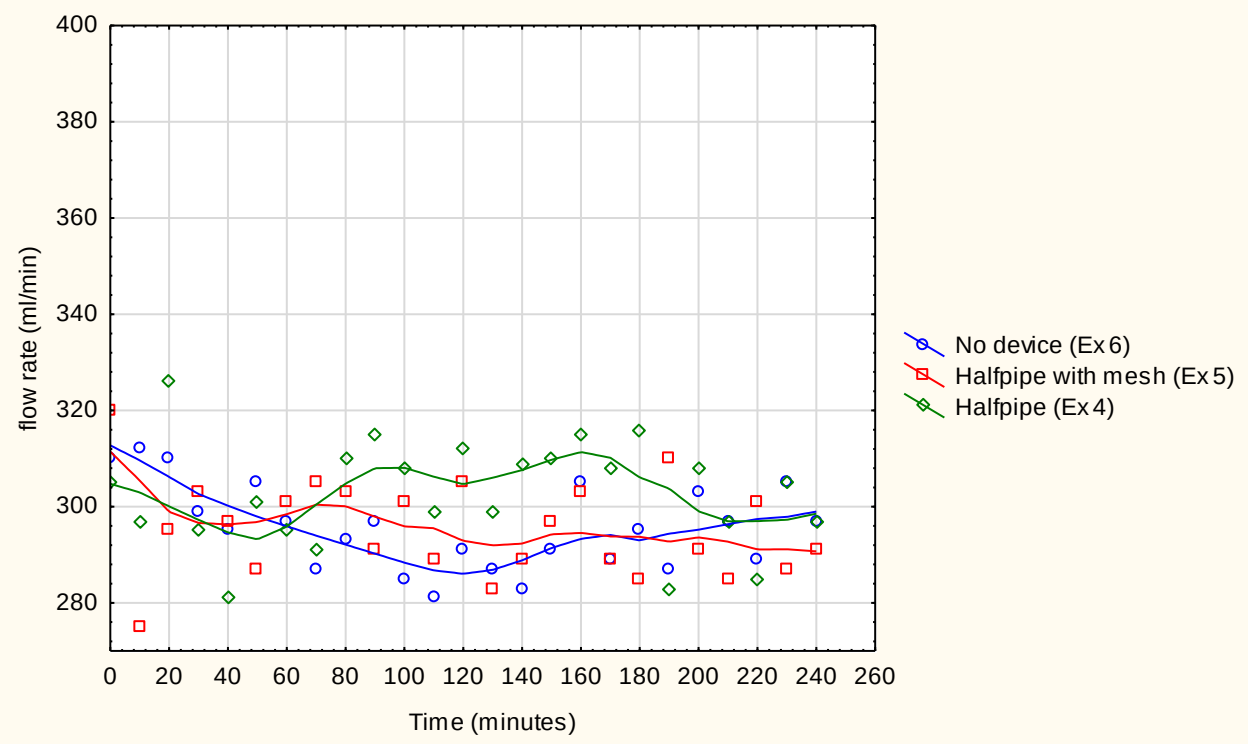

Figure 4-4: Flow rate profile of different devise at the same temperature (70°C) after modification for experiment 4, 5 and 6

4.3.2 Discussion

The condensate recovery of the VES under the three different devices conditions (half-pipe only, half-pipe with mesh, and no device) at the same feed temperature of 70^{o}C are compared for the variation of their condensate recovery with time on Figure 4-1 and 4-3. The graphs show that the condensate recovered for the half-pipe internals was higher than both the half-pipe with mesh pad and evaporation with no device. This was an expected result since the half pipe device has a higher water removal efficiency than the other two conditions, confirming the findings of Bothamley (2013a), who reported that half-pipe internals have an ability to improve the efficiency of liquid-gas separation and reasonable gas distribution. Other reseachers, like Norsok (2001) also confirmed the findings of Bothamley (2013a) and reported poor inlet separation results, with over flooding of the demisting section and hence in liquid carry-over for separators with no internal devices.

Initial design (experiments 1, 2 and 3) had higher fluctuations than modified experiments (4, 5 and 6) as shown on Figures 4-2 and 4-4 respectively. Figure 4-2 shows the fluctuations of the feed flowrate in the three experiments (1, 2 and 3) with the standard deviations of 29, 17 and 32 ml/min respectively. Experiment 3 (with no device) had the highest standard deviation, followed by experiment 1 (with a half pipe internal) and lastly experiment 2 (with a half pipe and mesh pad). The fluctuations of feed flowrate for all initial experiments were a result of dropping vacuum pressures upon opening of the vacuum valve (V-6) to allow balancing of pressure in the separator and the liquor receiver for liquor drainage. Since only one vacuum pump (VP-1) was creating vacuum, this caused variations in the operating pressure in the separating chamber, and hence fluctuations in feed flow rate.

The addition of the second vacuum pump (VP-2) created a separate vacuum line that allowed creation of vacuum in the liquor receiver without disrupting the separator, therefore minimising the feed flow rate fluctuations. The fluctuations of the feed flow rate after modifications of the initial design (Figure 4-4) dropped to give standard deviations of flow rate of 11, 9 and 8 ml/min for experiments 4 (with half a pipe), 5 (half a pipe and mesh) and 6 (no device) respectively.

4.4 EVALUATION OF FOAM ELIMINATION MODIFICATIONS

Experiment 7 (with a half-pipe and mesh pad) was run to test the VES with WPC solution, and it confirmed foaming by the solution and therefore that the system was not suitable for use with foaming solutions. Three successive modifications were then made and experiments 8 (staged mesh), 9 (multi-cyclone with staged mesh) and 10 (addition of antifoam to similar conditions as experiment 9) were undertaken to evaluate their effectiveness in foam elimination. It was only after the addition of antifoam (experiment 10) that foaming was eventually eliminated. The experimental conditions and results are presented in Table 4-5 and Table 4-6

Table 4-5: Experimental condition for foam elimination modifications.

Condition	**Experiments Number**			
	7	**8**	**9**	**10**
Initial solution concentration (wt%)	5.2	11.5	10.1	10
Initial quantity of solution (kg)	5	5	5	5
Operating temperature (°C)	70	65	60	65
Evaporator pressure (kPa abs)	21.3-21.3	15.3-21.3	15.3	12.3
Protein solution flow rate (ml/min)	300	300	300	300
Condenser water flow rate (ml/min)	750	750	750	750
Mesh pad	Yes	None	None	None
Type of internal	Half-pipe	Half-pipe	Multi-cyclone	Multi-cyclone
Stages of mesh	None	5	3	3
Anti-foam 20% use ($g/kg_{protein}$)	None	None	None	19.2

Experiment 7 was run for 30 minutes and the flash temperature dropped from 61 to 47°C due to a blocked mesh as the solution began foaming in the separator. A total of 150 ml of condensate were recovered. To eliminate blockages in the next experiment (experiment 8), a modification was done on the mesh pad by introducing stages of mesh.

Table 4-6: Experimental condition and results for foam elimination modifications

Experimental number	Run duration (minutes)	Condensate removal (ml)
7	30	150
8	30	120
9	180	500
10	180	1500

Experiment 8 was then run after the addition of mesh stages, but also lasted 30 minutes, with 120 ml of condensate being collected before foam was observed in the condenser. The run was then stopped. The mesh stages were therefore not successful in foam elimination. Another modification was done in which the half pipe was replaced with a multi cyclone device.

Experiment 9 was run after the modification and an operation temperature of 60^{o}C, lasting 180 minutes and recovering 500 ml of condensate. Foam was again observed and the experiment terminated. This run lasted longer than the previous runs by 150 minutes and more condensate was recovered (380 ml above experiment 8 and 350 ml above experiment 7). The modification managed to reduce the foam, probably because of a lower operating temperature than previous runs, which reduces the evaporation rate and therefore reduces the rate of foaming. It could however not totally eliminate the foam.

Experiment 10 was run after modification of the separator to allow addition of antifoam and to enable observation of foam whenever it started. When antifoam (0.2%) was finally added to the system in experiment 10, the foam was finally eliminated and the run lasted for 180 minutes and 1500 ml of condensate were recovered. The condensate recovery increased by 1000 ml above the previous experiment (experiment 9). The antifoam was diluted (6 g in 100 ml distilled water) before being added to the solution to break the foam whenever it was noticed.

4.4.1 Discussion

It was important in this work to eliminate foaming by physical means, avoiding addition of antifoam agents since they introduce silicone in the final products. Thus, modifications aimed at mechanically eliminating the antifoam were initially prioritised, with antifoam being used only as a last resort.

Experiments 7 – 9 had to be terminated in their early stages due to foaming. Foaming has been reported as one of the common problems in WPC solution concentration (Stewart and Arnold, 2008). Foaming can be persistent especially when the dynamic surface tension and viscosity of the solution being handled are considerably high. Foaming is also affected by the solutes molecular structure. Inorganic compounds in dilute solutions are less likely to foam, however organic compounds, owing to their hydrophilic groups (-OH, -CO, -COOH, -COO-) as well as hydrophobic groups like $-C_6H_5$ or $-C_nH2_{n+i}$ in the same molecule generally cause foaming (Yamomoto, 1968).

Whey protein foams when proteins envelop entrapped air in solution, thereby creating foam whose persistence is dependent on factors like total solids, pH, calcium concentration and presence of sucrose, lipids and other ions (Lakkis and Villota, 1990; USDEC, 2004; Zhu and Damodaran, 1994). Although foaming ability may be an important functional property in the final product, it is undesirable during the processing stages since it reduces separator efficiency in the process as evidenced by experiments 7, 8, and 9 (Paramalingam, 2004). Foam may be destroyed by various methods, which include foam breakers, liquid-level control and other physical methods like spray jets (Yamomoto, 1968). Mechanical devices such as perforated baffles could also not be fitted in this set up since foaming occurred in the flash separator and there was not enough space in the vessel. Baffles also work efficiently at high velocities (Yamamoto, 1968) whereas the velocities were very low in this study.

A combination of pH manipulation and adsorption has successfully been used for foam control before. Yamomoto (1968) reported foam control by passing the feed through a column of activated charcoal at a low pH of 4. In this study, pH control was not considered since addition of acids or alkalis to the whey protein solution may change the final characteristics and composition of the product.

The small mesh sizes of the demister (mesh pad) employed in Experiment 7 (0.28 mm) caused blockage when foaming occurred. The mesh size was thus changed to larger ones in

experiment 8 (7 mm) but still could not prevent foaming as foam bubbles passed through the holes and reached the condenser. The other way to prevent blockages caused by foaming was to equip the demister with a spray system to remove deposits (Kalis, 2004). However, due to the small lab scale of the design in this study, the spray system could also not be incorporated.

The internal device was then changed to a multi-cyclone (4 cyclone) in experiment 9, which is reported to be effective in foam prevention (Akpan, 2013). The multi-cyclone however, though managing to reduce the foam, could not totally eliminate it, and this was ascribed to the fact that the inlet momentum of the systemremained low (38 kg/m. sec^2) due to the limited capacity of the system. High inlet momentum is essential for the cyclone to be effective in foam breaking (Akpan, 2013; Bothamley, 2013a).

Since all above-mentioned attempts to avoid foaming (experiments 7–9) using physical means were unsuccessful, it was decided to employ antifoam which was applied as an additive during evaporation. Antifoam usage resulted in successfully preventing foam formation in the whey protein solutions studied (experiment 10). Food grade antifoam (AF720F, 20% food grade silicone) was however used when the physical methods had failed. The quantity of added antifoam (0.02 %) was higher than the regulations on silicone concentration in the final consumable products (maximum = 0.01%) (Silicone and Technical Products, 2016). The reason for the high antifoam usage was the difficulty in process control, but was unavoidable since the addition of antifoam proved the only successful method of eliminating foaming among the tested methods.

The findings in this section show that the use of mechanical methods to prevent foaming could not totally eliminate the foaming due to low feed flow rate, which resulted in low inlet momentum. In industrial systems, especially where product flow rates are higher, allow the mechanical methods (e.g. spraying, baffle installation, higher-momentum cyclones etc) to be effective in preventing foaming. Therefore, less antifoam would be required.

4.5 EVALUATION OF FOULING ELIMINATION MODIFICATIONS

Experiment 11 (direct heating) was run to test the VES with WPC solution, and measure the fouling on the heating element by the protein. Significant fouling on the heating element was observed, confirming that the system was not suitable for heat sensitive materials. Three successive modifications were then made and experiments 12 (direct heating with uncontrolled stirrer), 13 (direct heating controlled stirrer) and 14 (indirect heating with conditions similar to those in experiment 13) were undertaken to evaluate their effectiveness in fouling elimination. It was only after the addition of the heating jacket (experiment 14) that fouling of heating surfaces was eventually eliminated. Table 4-6 and 4-7 show the experimental conditions and results. The temperature (65^{o}C), separator pressure (12.3 - 15.3 kPa abs), condenser water supply (750 ml/min) and the initial total solution (5 kg) were maintained for all the runs. Feed flowrate was also maintained at around 300 ml/min.

Table 4-7: Experimental condition for fouling elimination modifications

Condition	**Experiments Number**			
	11	**12**	**13**	**14**
Initial solution concentration (wt%)	10.8	11.5	10.4	11.5
Initial quantity of solution (kg)	5	5	5	5
Operating temperature (^{o}C)	65	65	65	65
Evaporator pressure (kPa abs)	11.3-12.3	13.3	12.3	9.3-17.3
Protein solution flow rate (ml/min)	300	300	300	300
Condenser water flow rate (ml/min)	750	750	750	750
Heating type	Direct	Direct	Direct	Indirect
Stirrer	None	Uncontrolled	Controlled	Controlled
Multi-cyclone internals	Yes	Yes	Yes	Yes
Stages of mesh	3	3	3	3
Anti-foam 20% use (g/kg$_{protein}$)	32	9.6	None	16

Table 4-8: Results for fouling elimination modifications

Initial concentration (wt%)	Run duration (minutes)	Condensate removal (ml)	Run number
10.81	240	3070	11
11.5	60	650	12
10.45	20	0	13
11.5	300	1575	14

Experiment 11 was run for 240 minutes and a total condensate of 3070 ml were recovered, giving a final solids concentration of 13.1 wt%, as shown in Figure 4-6 and Table 4-9. The graph shows that the solids concentration initially dropped from 10.8% to 8.7 wt% after 60 minutes of heating due to fouling of the heating element (Figure 4-5). Deposits of whey solids on the heating element reduced the protein concentration in the bulk solution. The bulk solution solids concentration then started to rise as evaporation continued and ended the experiment at 13.1 wt%. The recovered condensate increased consistently throughout the evaporation run. A total of 10 g antifoam were added to the solution to break the foam whenever it was noticed.

Table 4-9: Condensate collected and solids concentration in experiments 11 and 14

	Experiment 11		Experiment 14	
Time (minutes)	Solution (wt%)	Moisture recovered (ml)	Solution (wt%)	Moisture recovered (ml)
0	10.8	0	11.54	0
60	8.6	650	12.14	185
120	9.6	1670	13.04	560
180	10.9	2495	14.77	870
240	13.1	3070	15.89	1245
300			16.78	1575

Experiment 12 was run for 60 minutes after fitting an uncontrolled stirrer (at 1250 rpm) in the feed tank. A total of 650 ml of condensate were recovered before the solution started foaming in the feed tank, possibly due to the high stirrer speed. Foaming also presented problems of pump failure, since it occupied the suction point of the centrifugal pump (in the feed tank),

causing pump cavitation. The run was then stopped when foam developed, a total of 3 g antifoam having been consumed in the experiment. The stirrer was then controlled at 200 rpm to reduce foaming due to its high speed.

Experiment 13 (with a stirrer speed of 200 rpm) lasted just 20 minutes before it was aborted due to fouling of the heating element and loss of solids. The solid deposits on the heating element (Figure 4-5) were observed and it was concluded that the low speed stirrer could not prevent fouling of the heating element in the feed tank. Direct heating using a heating element was then replaced with a heating jacket.

When the pre- heating (direct heating) was replaced with a heating jacket (indirect heating) in experiment 14 the run lasted 300 minutes, a total condensate of 1575 ml were collected and the final solids content of the solution was 16.8 wt%, as shown on Figure 4-6 and Table 4-9. Indirect heating managed to eliminate the fouling of the heating element by the solids. A total of 16 $g/kg_{protein}$ antifoam were added to the solution to break the foam whenever it was noticed.

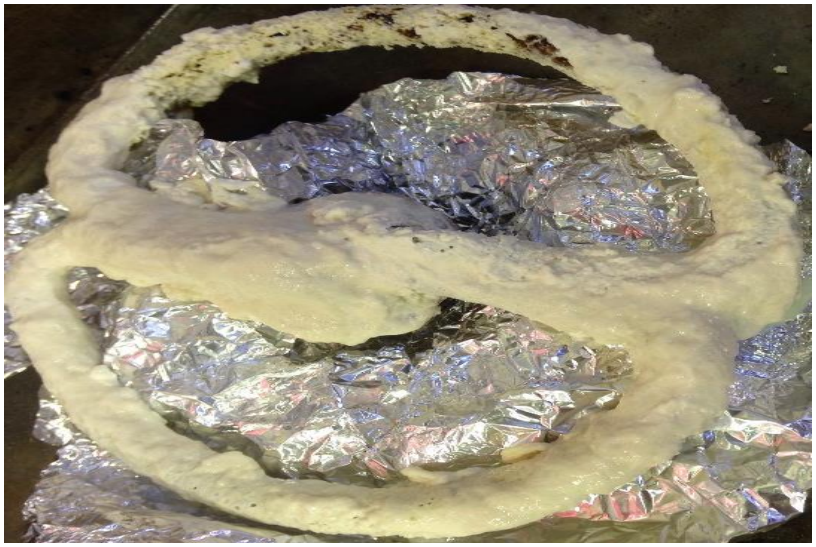

Figure 4-5: Fouling of the heating element with burnt WPC for experiments 11 and 13

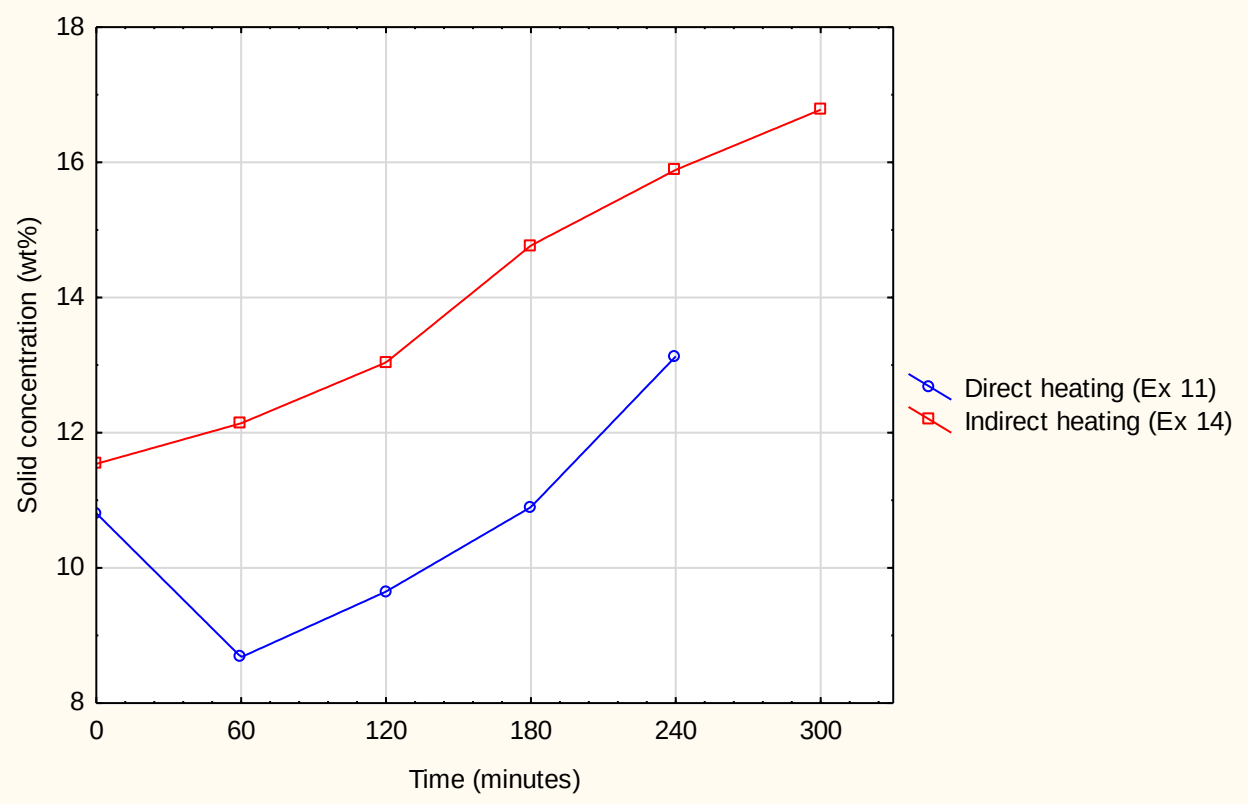

Figure 4-6: Solids concentration for direct and indirect heating evaporation for experiments (11 and 14)

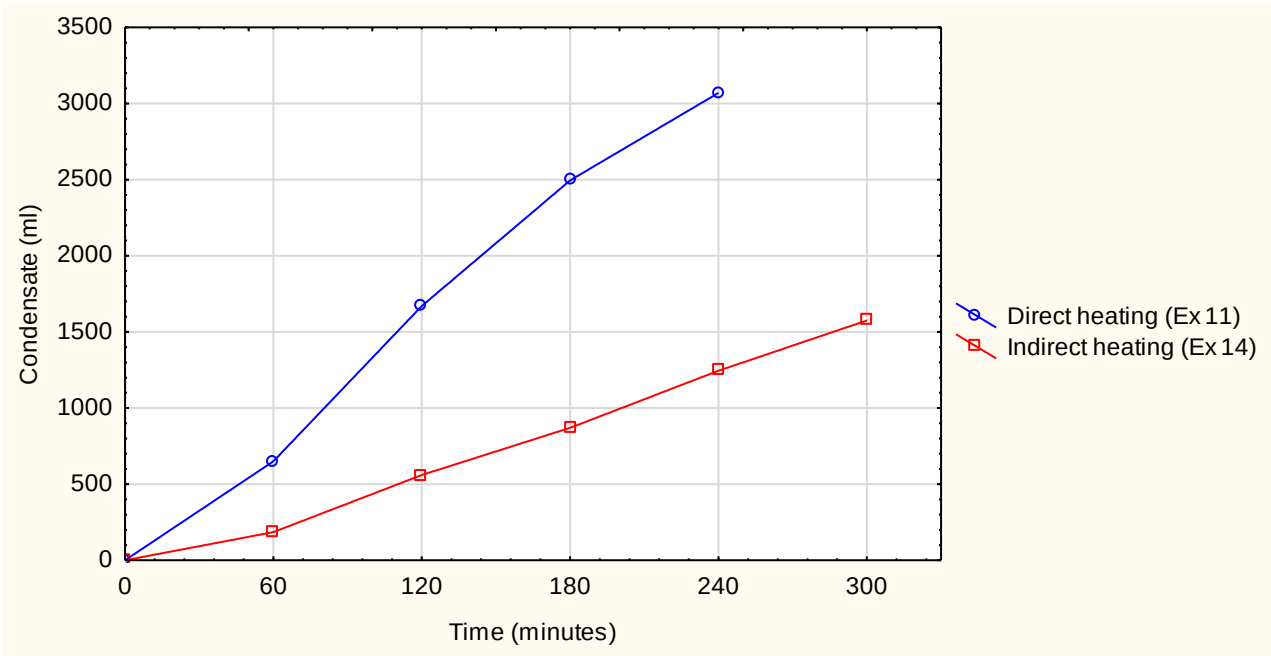

Figure 4-7: Comparing condensate removal between direct and indirect heating evaporation systems for experiments (11 and 14)

Regression analysis

In an effort to demonstrate the negative impact of protein fouling of the heating element on overall system operation, regression analysis was performed using Statistica 13 software. Results of regression analysis between solids concentration and condensate removal for the two heating systems (direct and indirect) (experiment 11 and 14) are shown on Figures 4-8 and 4-9 respectively. The graphs show that for direct heating, there was an extremely poor correlation (R^2 = 0.6404) between condensate recovered and solids concentration, whilst for indirect heating, the correlation was much higher (R^2 = 0.9942). In the case of indirect heating, therefore, the solids concentration in the solution was directly related to the condensate recovered and could therefore be predicted from the solids concentration.

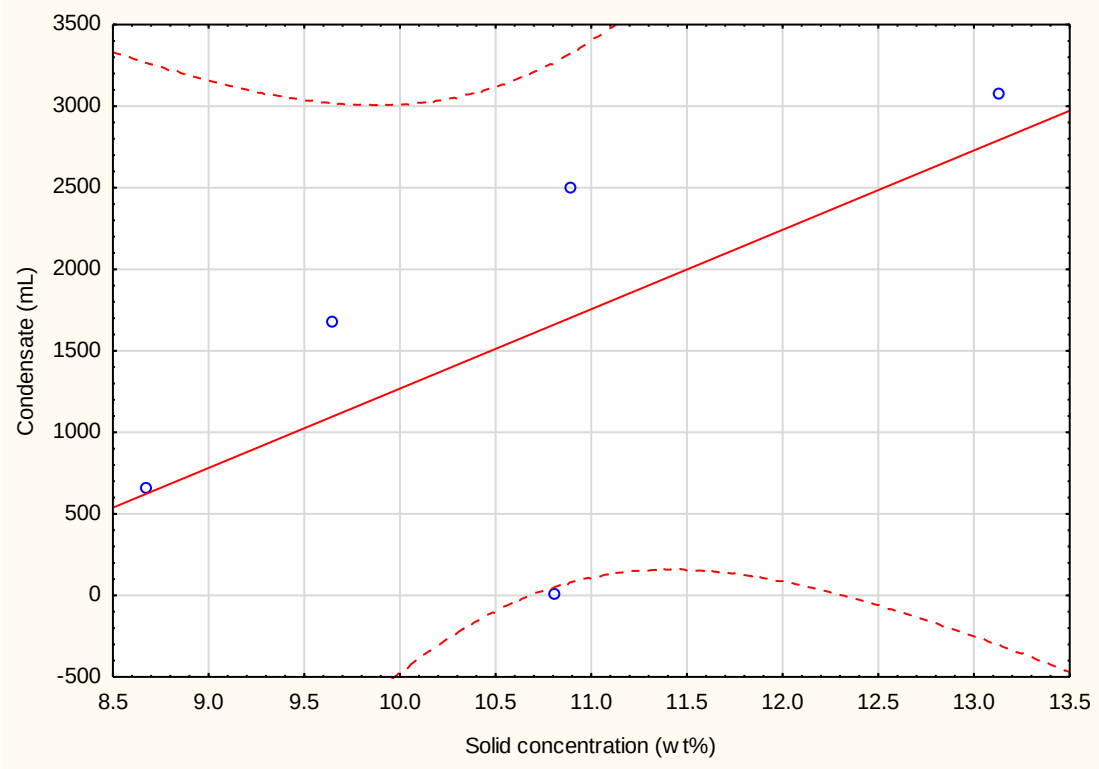

Figure 4-8: Regression analysis between condensate removal and solids concentration for the direct heating evaporation system for experiment 11

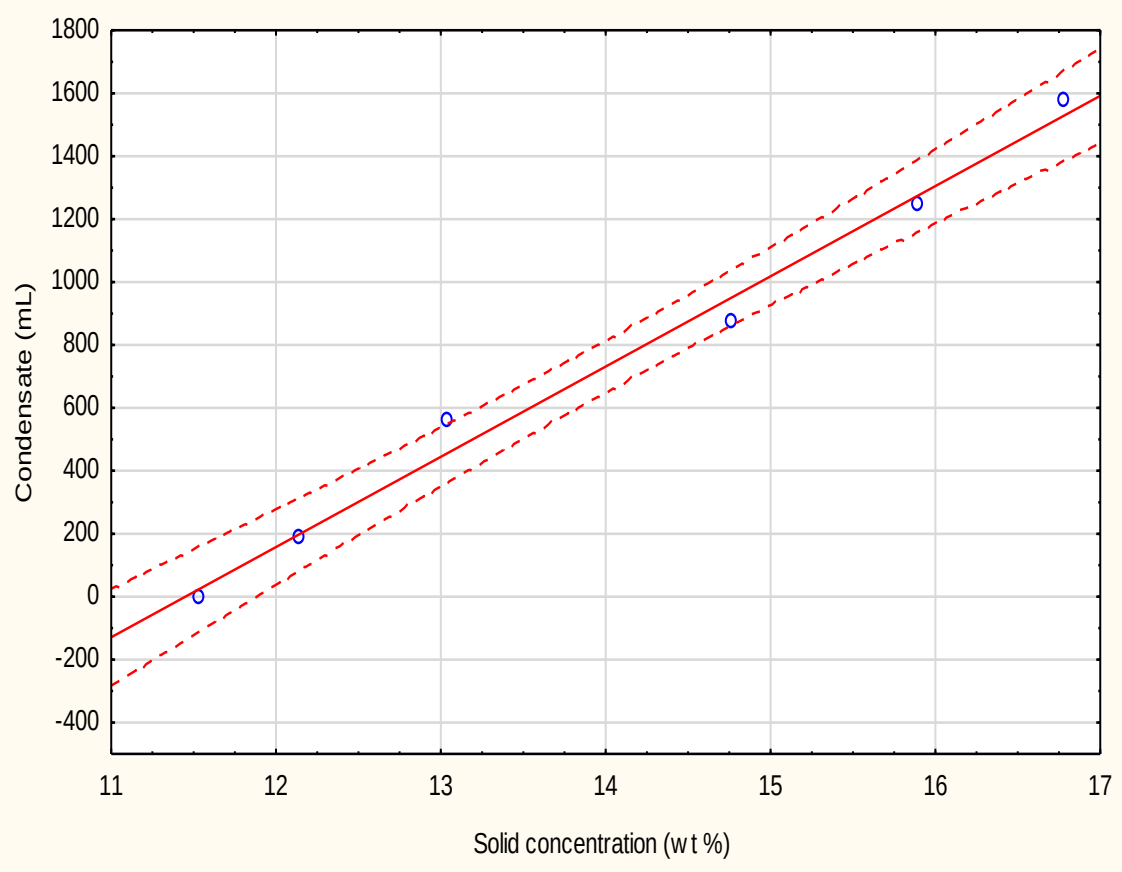

Figure 4-9: Regression analysis between condensate removal and solids concentration for the indirect heating evaporation system for experiment 14

4.5.1 Discussion

Direct heating resulted in fouling on the heating element by the WPC. This was because whey proteins comprise heat sensitive proteins (beta-lactoglobulin and alpha-lactoglobulin) which are likely to form deposits when heated (Changani *et al.,* 1997; Wijayanti *et al.,* 2014).

Figure 4-6 shows direct heating of WPC (experiment 11). It clearly shows that the concentration of WPC dropped to 8.7% for the first operation hour before it started to increase again reaching 13.1% after 240 minutes. The decrease in the WPC concentration in the first hour is attributed to the fouling on the heating element. The fouling reduced the concentration since by clogging around the heating element, the solids in the remaining fluid was lowered, resulting in lower concentrations being measured. Fouling was observed after the completion of the experiment (Figure 4-6). Figure 4-7 also indicates that maybe an insignificant amount of deposit of the WPC on heating element occurred during the remaining period, as evidenced by an increase in the concentration of the WPC in the solution. According to (Gillham *et al.,* 2000) as well as (Burton, 1968), this kind of fouling is referred to as type A fouling, since the operating temperatures of the overall solution were less than 100^{o}C, although the surface of the heating element might be over 100^{o}C.

Experiment 12 was carried out under high-speed agitation, which prevented fouling of the heating element, but the process was stopped early (after 60 minutes) because of foaming in the feed tank, which made the control of the centrifugal pump flowrate challenging. This demonstrated that using agitation could prevent fouling of the element when non-foaming solutions (e.g. NaCl or sugar) are processed. In an attempt to eliminate foaming in the feed tank while also preventing fouling of the heating element, the agitation rate was reduced to 200 rpm (Experiment 13) however, fouling was again experienced and it was decided that direct heating of the solution was not feasible.

Direct heating however had a higher condensate collection rate than indirect heating. Figure 4- 7 shows that condensate recovery in direct heating reached above 3000 ml in 180 minutes, whilst indirect heating (Experiment 14) could only reach just over 1500 ml in 300 minutes of running the process. More condensate was recovered in the direct heating process this effect was possibly due to higher heat transfer rate by direct heating is higher than indirect heating (heat jacket), thus causing more evaporation in the former

Figure 4-8 shows lack of a significant relationship between the solids concentration and the condensate recovered. The coefficient of determination is low ($R^2 = 0.6404$) and the p-value is high ($p = 0.2444$, which is much greater than 0.05). Thus, a conclusion can be made with 95% confidence that the condensate recovery is poorly predicted from the values of solution concentration. Figure 4-9 (indirect heating) on the other hand, shows a strong correlation between the condensate recovered and the solids concentration ($p << 0.05$ and $R^2 = 0.9942$), confirming the applicability of the regression model in predicting the condensate recovered from the solution concentration. The high R^2 value indicates that the model can explain more than 99% of the variance between the two variables (condensate recovery and solution concentration). This result reinforces the finding that when the WPC was being directly heated, some solids were burnt and fouled the heating element, distorting the relationship between water evaporation and solid concentration. The result of correlation between condensate recovered and solids concentration can be a useful result in industry since it proves that direct heating leads to material losses through burning, fouling and denaturation of heat sensitive material. The result confirmed indirect heating to be a better preheating choice for WPC solutions, with less fouling and burning of product.

The findings in this section confirm that the use of direct heating for WPC solution might be a challenge in the industry. This is because although it has higher evaporation rates than indirect heating, it results in product loss and deterioration, as obtained in this study. Deposits will also lead to multiple system shut down and cleaning, and therefore direct heating can be costly and time consuming. On the other hand, indirect heating resulted in negligible burning and fouling, making it more industrially applicable than direct heating.

4.6 WHEY PROTEIN CONCENTRATION

Having managed to stop foaming by addition of antifoam and eliminated the fouling of the heating element by indirect heating and controlling the agitation rate, all successive experiments were run at the same conditions. Three different solutions, WPC, sugar and NaCl solutions were employed to determine whether the system was also suitable to concentrate non-protein solutions (NaCl and sugar), and to compare the performance to the whey protein concentrations. To evaluate the effect of temperature and initial concentration on WPC, experimental runs were undertaken at different temperatures (65-70ºC) and different concentrations (5 - 10 wt%) under circulation, in closed systems.

Experiments 15, 16, 17 and 18 were run to determine the effect of initial concentration at 65ºC and 70ºC for WPC solution. The solutions of sugar (experiment 19) and NaCl (experiment 20) were used to confirm the applicability of the system in concentrating different solutions under similar conditions as experiment 15. The experimental conditions and results are presented in Table 4-10 and 4-11.

Table 4-10: Experimental condition of different solutions

Condition	**Experiments Number**					
	15	**16**	**17**	**18**	**19**	**20**
Type of the solutions	WPC	WPC	WPC	WPC	NaCl	Sugar
Initial solution concentration (wt%)	5.3	11.3	5.7	11	4.9	4.8
Initial quantity of solution (kg)	5	5	5	5	5	5
Operating temperature (ºC)	65	65	70	70	65	65
Evaporator pressure (kPa abs)	13.3	13.3	14.3	15.3	14.3	15.3
Solution flow rate (ml/min)	300	300	300	300	300	300
Condenser water flow rate (ml/min)	750	750	750	750	750	750
Indirect heating	Yes	Yes	Yes	Yes	Yes	Yes
Stirrer controlled	Yes	Yes	Yes	Yes	Yes	Yes
Multi-cyclone internals	Yes	Yes	Yes	Yes	Yes	Yes
Stages of mesh	3	3	3	3	3	3
Anti-foam 20% use ($g/kg_{protein}$)	16	16	16	16	None	None

Experiment 15 was run for 240 minutes and 2130 ml of condensate were recovered, as shown in Figure 4-10 and Table 4-11. Figure 4-10 further shows that the solids concentration increased consistently with increasing condensate recovered, to end the experiment at 10.1 wt%.

Experiment 16 lasted a total of 300 minutes and 1575 ml of condensate were recovered as shown on Table 4-11 and Figure 4-10. From the graph (Figure 4-10), the solids concentration can be observed to increase with condensate recovery, to end the experiment at 16.7 wt%. The run was stopped because the solution became too viscous, with the increased viscosity causing liquid hold-up in the equipment. Since the centrifugal pump was running, the feed tank level became too low.

After 180 minutes of evaporation, 2475 ml of condensate were recovered for experiment 17 as shown on Table 4-11 and Figure 4-12. The total solid concentration increased with condensate recovery, to end the experiment at 11.9 wt% (Figure 4-12). After 180 minutes of running, a smell characteristic of burning protein was detected and the vapour in the condenser was dark, signifying that the WPC solution was burning. The run was then stopped. Experiment 18 was stopped just after 60 minutes and 900 ml of condensate having been collected. The WPC solution had reached 12.6 wt% and started burning as in experiment 17.

Experiment 19 duration was 240 minutes and a total of 2095 ml of condensate were collected (Table 4-11). The graph (Figure 4-14) shows that the total solid concentration was increasing with condensate collected, ending at 9.6 wt%. Lastly, experiment 20 was run for 240 minutes and a total of 2535 ml of condensate were recovered. Its final solid concentration was 10.3 wt%, as shown on Figure 4-14.

.

Table 4-11: Condensate collected and solids concentration for different solutions

Time (min)	Experiments Number											
	15		16		17		18		19		20	
	Solution (wt%)	Moisture recovered (ml)	Solution (wt%)	Moisture recovered (ml)	Solution (wt%)	Moisture recovered (ml)	Solution (wt%)	Moisture recovered (ml)	Solution (wt%)	Moisture recovered (ml)	Solution (wt%)	Moisture recovered (ml)
0	5.3	0	11.5	0	5.6	0	11	0	4.9	0	4.7	0
60	6.2	440	12.1	185	6.9	765	12.6	900	5.3	320	5.2	570
120	7.3	1080	13	560	8.1	1565			6.4	1035	6.3	1290
180	8.9	1640	14.7	870	11.9	2475			7.9	1615	8.6	1960
240	10.1	2130	15.8	1245					9.6	2095	10.3	2535
300			16.7	1575								

4.6.1 Comparing evaporating conditions

Evaporating solutions of different concentration at the same temperature (65ºC)

Figures 4-10 and 4-11 show the increase in concentrations and condensate recovered for two experiments (15 and 16) at the same operating temperature (65ºC) and vacuum level (13.3 kPa abs) but different initial concentrations (5.3 wt% and 11.3 wt%) respectively. Figure 4-10 indicates a depressed rate of increase in concentration at higher starting concentrations. The 11.3 wt% solution had a lower average rate of increase in concentration than the 5.3 wt% solution as the evaporation time increased up to 240 minutes (1.0 and 1.2 wt%/hr) respectively. Figure 4-11 corroborates the results shown on Figure 4-10. It took 300 minutes to evaporate 1575 ml at an initial concentration of 11.5 wt% whilst 2130 ml were evaporated in 240 minutes at an initial concentration of 5.3 wt%. This further shows the low rate of evaporation on the 11.3 wt% solution as compared to the 5.3 wt% solution.

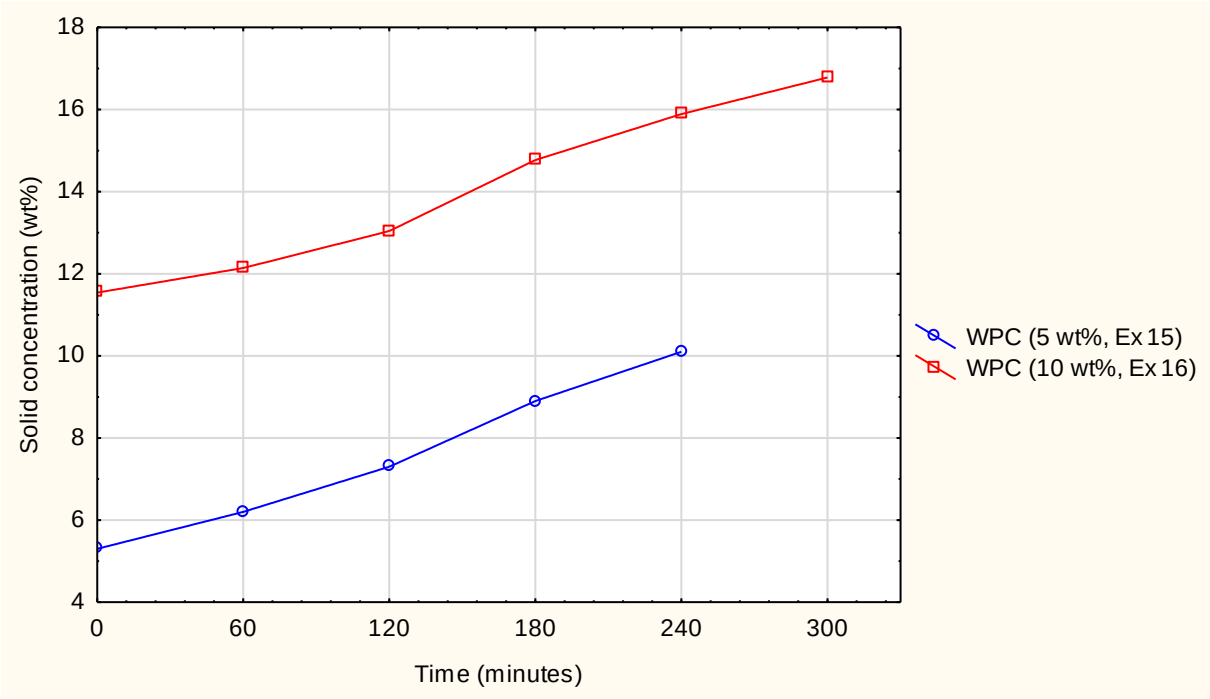

Figure 4-10: Solid concentration against time for solutions of 5% and 10% initial concentration at a temperature of 65ºC for experiments 15 and 16

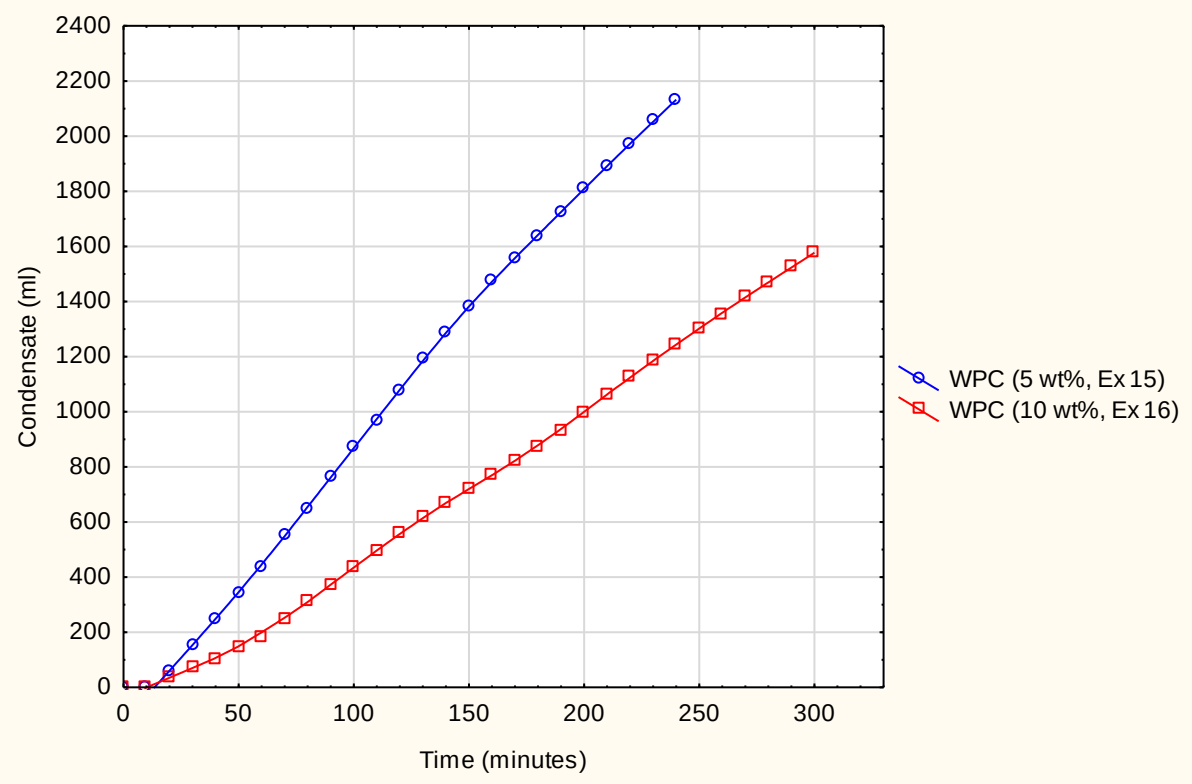

Figure 4-11: Condensate recovery against time for solutions of 5% and 10% initial concentration at a temperature of 65°C for experiments 15 and 16

Evaporating solutions of similar concentration at different temperatures (65°C and 70°C)

To evaluate the influence of feed temperature on the evaporation rate, results (increase in solids concentration with time) of experiments 15 and 17 were plotted on Figure 4-12. The solutions (5.3 wt% and 5.7 wt% respectively), were concentrated at different temperatures (65°C and 70°C). At the evaporation temperature of 65°C, the final solids concentration after 240 minutes was 10.1 wt%, giving an average rate of increase in concentration of 1.2 wt%/hr. When the evaporation temperature was then adjusted to 70°C, the final concentration reached 11.9 wt% after 180 minutes of evaporation, at an average rate of increase in concentration of 2.1 wt%/hr. The amounts of condensate recovered at each evaporation temperature are presented on Figure 4-13, where 2475 ml were recovered at 70°C whilst at 65°C, 2130 ml were recovered.

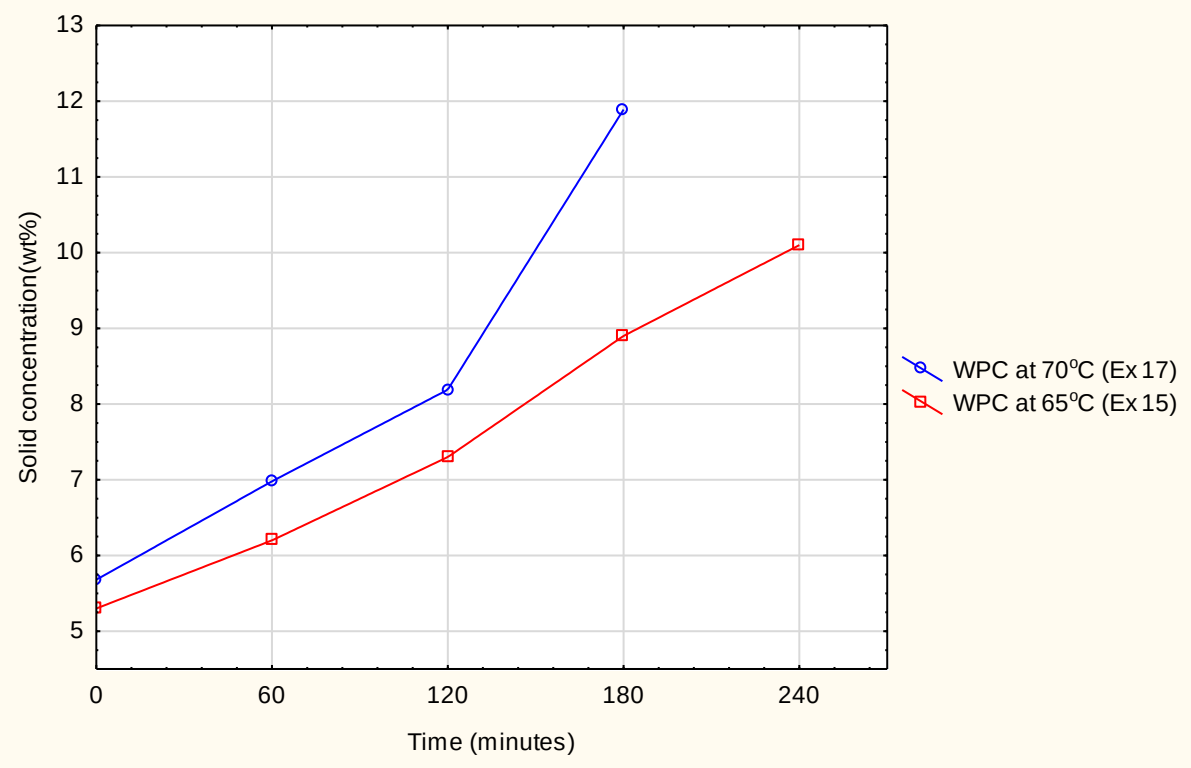

Figure 4-12: Solid concentration against time for solutions of 5% initial concentration at 65°C and 70°C (experiments 15 and 17).

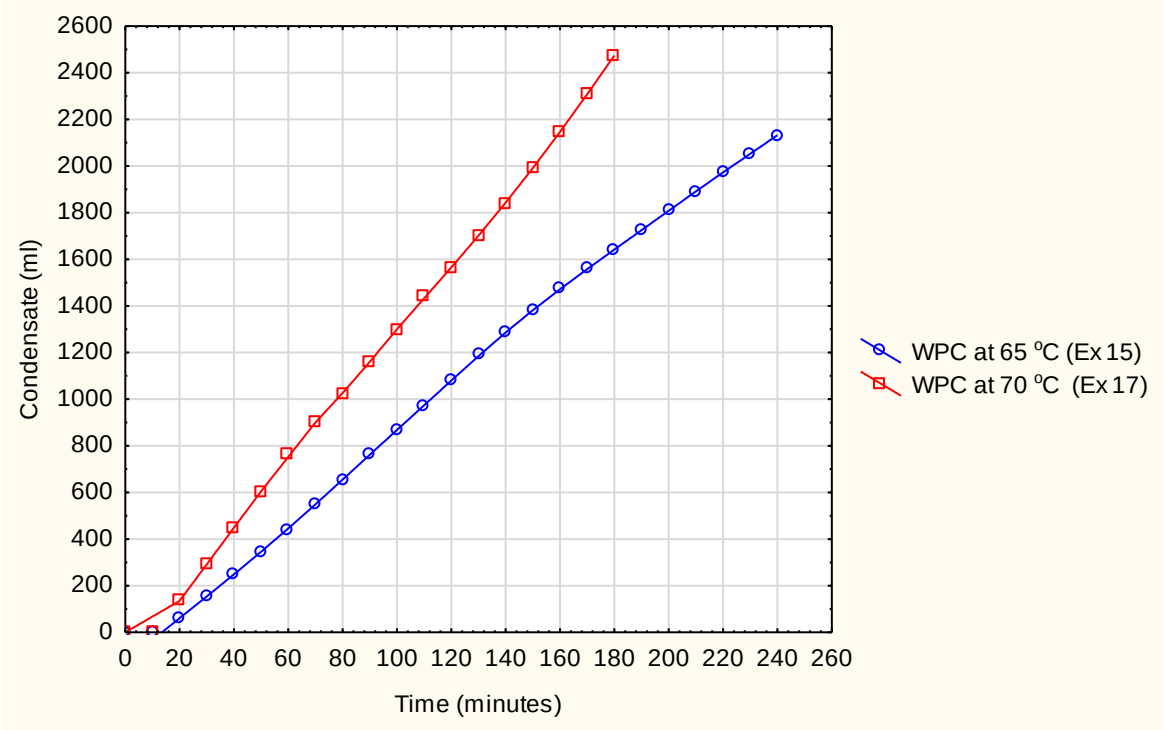

Figure 4-13: Condensate recovery against time for solutions of 5.3% and 5.7% initial concentration at a temperature of 65°C and 70°C respectively (experiments 15 and 17).

Evaporating different solutions (WPC, NaCl and sugar) of similar concentration at the same operating temperature

Figures 4-14 and 4-15 compare the condensate collected and solid concentration with time for the three solutions (WPC, sugar and NaCl). Figure 4-14 shows that the NaCl solution had the highest average rate of increase in concentration (1.4 wt%/hr), followed by the WPC solution (1.2 wt%/hr) and finally sugar solution (1.1 wt%/hr). Figure 4-15 shows that the NaCl solution gave the highest condensate (2535 ml) within 240 minutes, followed by the WPC (2130 ml in 240 minutes) and lastly the sugar solution (2095 ml) after 240 minutes. The condensate collected increased relatively linearly with time. The diagram (Figure 4-15) confirms the results observed on Figure 4-14, that as more liquid evaporates, the solution becomes more concentrated. Figure 4-14 further shows lower increases in concentration for the sugar and NaCl solutions in the first hour, which increased in the succeeding hours. This might be due to stability of evaporation pressure, which took longer to be attained when concentrating the two solutions than when concentrating the WPC solution (Table 7-23 in Appendix F).

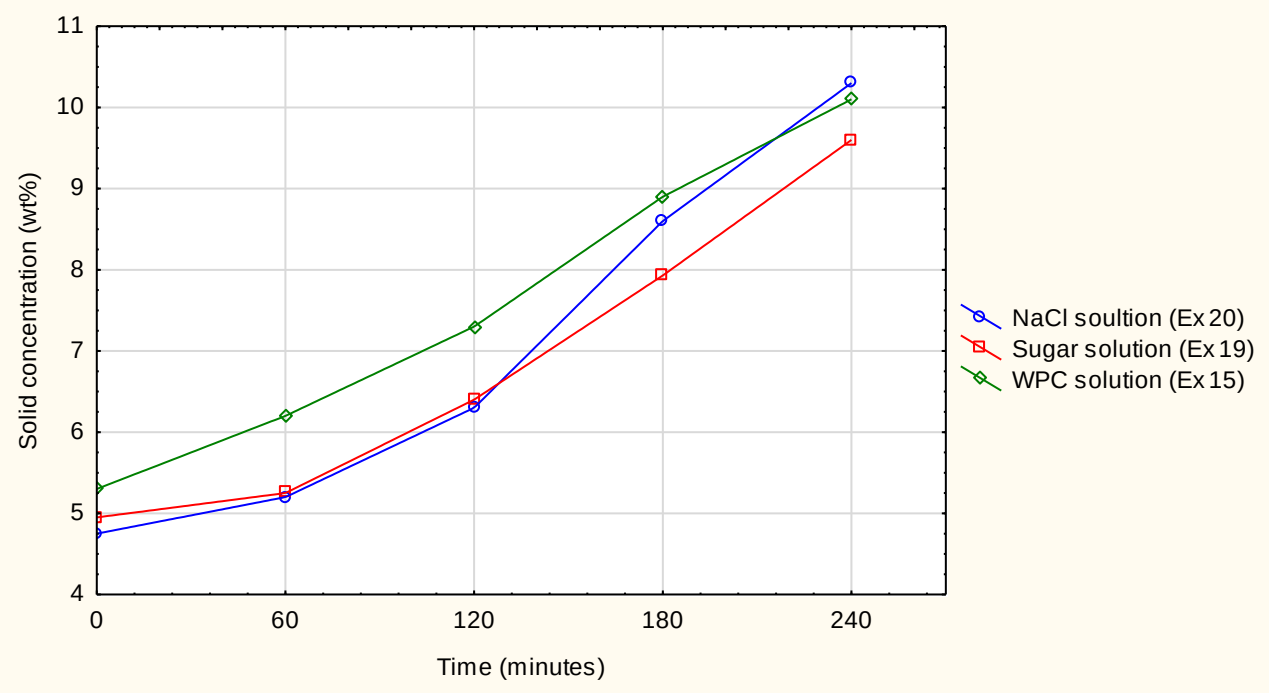

Figure 4-14: Variation of solids concentration with time for WPC, NaCl and sugar solutions during evaporation (experiments 15, 19 and 20)

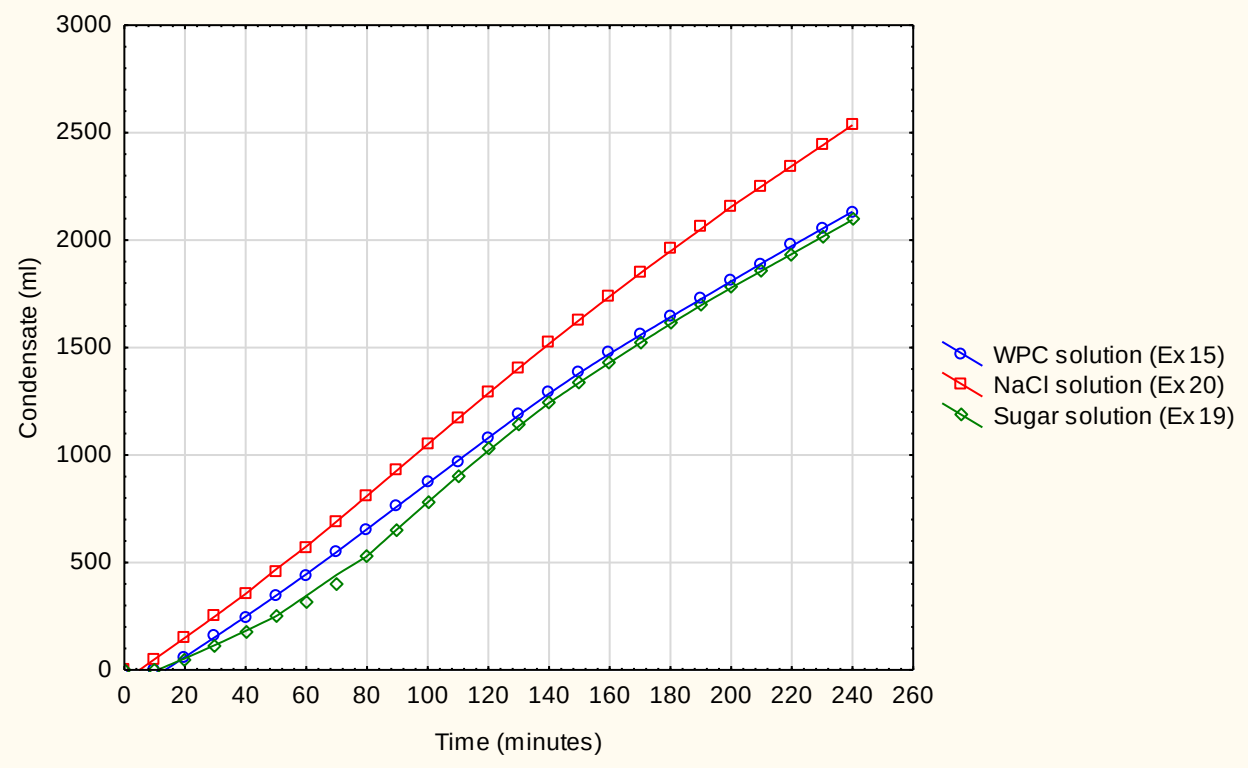

Figure 4-15: Variation of condensate collected with time for WPC, NaCl and sugar solutions during evaporation (experiments 15, 19 and 20)

4.6.1 Discussion

Figure 4-10 shows the increase in concentration of 5.3 wt% and 11.3 wt% at the same temperature (65^{o}C). This Figure illustrates the decrease in the evaporation rate with increasing solution concentration. This illustration agrees with Singh (2007), who reported decreased evaporation rate with increased solids concentration attributed to an increase in the viscosity the solution. The graph further shows that a highest WPC solution concentration of 16.8 wt% was attained before the run was stopped as the solution became too viscous to drain under gravity back to the feed tank.

Industrial operations can achieve higher concentrations by mechanically pumping the concentrated solution to the next evaporator when multi effects evaporation is used. Pumping can still be effective in recirculating the solution to the feed tank in single effect evaporators. This study worked with a single effect evaporator in which the solution drained under gravity from the evaporator to the feed tank. This limited the extent of concentration since there was a point when the concentrated solution's flow rate back to the feed tank was insufficient under gravity flow alone. This defined the concentration limit for whey protein solutions of the designed VES (at 16.8 wt%).

Increasing feed temperature results in higher moisture removal rates (Figure 4-12). Paramalingam (2004), on optimisation of the falling film evaporator, also reported concurring results, where evaporation rates increased with increasing temperatures. This agrees with the fundamental principle that higher temperatures results in higher driving forces for moisture removal. This fundamental principle was also supported by Hasan and colleagues (2011) when they investigated the heat transfer coefficient and found a linear relationship between the feed temperature and the heat transfer coefficient.

The external energy supply from the heating coil (rated 1 kW) to the bulk solution was influenced by the variance between inlet and outlet temperatures of the solution. The heating coil efficiency decreased with increasing vacuum level. Since a high vacuum level is required for low evaporation temperatures, the temperature difference for an inlet temperature of 65^{o}C was lower than that for 70^{o}C, thus more vacuum was required at 65^{o}C. Figure 4-12 and 4-13 shows that the evaporation rate at 65^{o}C is less than at 70^{o}C. This partially explains the more evaporation observed at 70^{o}C than 65^{o}C. The dependence of heat transfer coefficient on the evaporation temperature was observed in range of 65^{o}C to 70^{o}C. Since the feed enters the

evaporator at a higher temperature, then the heat transfer coefficient also increases as shown on Figure 4-18.

On Figure 4-14, three different solutions, WPC, NaCl and sugar solutions, all with an initial concentration of approximately 5 wt%, were compared for the variation of their concentrations with time. The solutions' rates of condensate collection were also compared on Figure 4-15. The Figures show that the concentration and condensate collection for the NaCl solution was higher than both the WPC and the sugar solutions. From Figures 4-14 and 4-15, the evaporation rate of the WPC was higher than the sugar solution. This result is similar to Silveira (2013) who established an evaporation rate of skim milk higher than that of water using the same experimental conditions.

The results of experiments 17 and 18, at a feeding temperature of 70^{o}C, show that the solution started burning at solids concentration of about 12 wt%. Pierre and colleagues (1977), as well as McMahon and colleagues (1993), when concentrating whey proteins six fold using ultra high temperatures, reported the denaturation of proteins which increased with increasing protein concentration. Law and Leaver (1997) also reported the similar findings.

The findings in this study suggest that the burning of the solutions might be a result of protein denaturation, which was enhanced at higher solids concentration (11.3 wt%). The WPC denaturation at 70^{o}C is critical in industry since it will probably lead to loss of final product properties especially if high solid concentration greater than 12 wt% are desired. Further concentration will therefore need to consider evaporation at lower temperatures (maximum 65^{o}C) for single effect evaporation systems, or consider employing multiple-effect evaporators.

Multiple-effect evaporators can concentrate solutions with concentrations of at most 12 wt% at 70^{o}C in the initial separator. As the concentration increases, the solution is pumped to succeeding evaporators, which will be at lower temperatures than 70^{o}C to avoid protein denaturation. Since succeeding separators will be at lower temperatures than the preceding ones, energy (vapour) from the preceding separators can be used as external energy to heat the solution in successive evaporator stages (which will be less than 70^{o}C). This can save on energy and reduce costs.

Denaturation of the WPC solution of 12 wt% was observed at 70 ^{o}C. Although, no observation of the denaturation was made at 65 ^{o}C, it could not be ascertained that there was no denaturation

since no testing of the protein structure of the final product was done. The raw material was also not tested for denaturation.

4.7 VISCOSITY MEASUREMENTS

The solution viscosity was measured for the purpose of calculating the heat transfer coefficient. The results of the WPC viscosity measurements at a constant shear rate of 23/s are presented in Figure 4-16. The graph shows that for the WPC concentration of 4.2 wt%, the viscosity remains constant at an average of 1.2 mPa.s when temperature is increased from 59^{o}C to 70^{o}C. For concentrations of 7.3 wt%, the viscosity remains constant at an average of 1.3 mPa.s when temperature is increased up to 67^{o}C, then rises by 428% from the initial 1.3 mPa.s at 67^{o}C to 6.8 mPa.s at 70^{o}C.

For concentration (9.14 and 11 wt%) the viscosities remained constant at an average of (1.7 and 2.5 mPa.s) respectively, when temperature was increased up to 63.5^{o}C, then rose from the initial 1.75 and 2.5 mPa.s at 63.5^{o}C to (22.6 and 29.7 mPa.s) respectively at 70^{o}C.

For higher concentrations of whey protein solutions (12.8 to 15.6 wt%), the viscosities rapidly increased when the heating temperature reached approximately 62^{o}C. The viscosity of the 12.8 wt% WPC rose from around 3.3 mPa.s at 63^{o}C to level at around 70 mPa.s at 70^{o}C. The 14.5 wt% solution had its viscosity rising steadily from the initial 4.5 mPa.s at 62^{o}C to 89 mPa.s at 70^{o}C. The 15.8 wt% solution viscosity also increased from 4.6 mPa.s at 62^{o}C to 91 mPa.s at 70^{o}C. Lastly, the 17.1 wt% solution viscosity also increased from 16.6 mPa.s at 59^{o}C to 136 mPa.s at 70^{o}C.

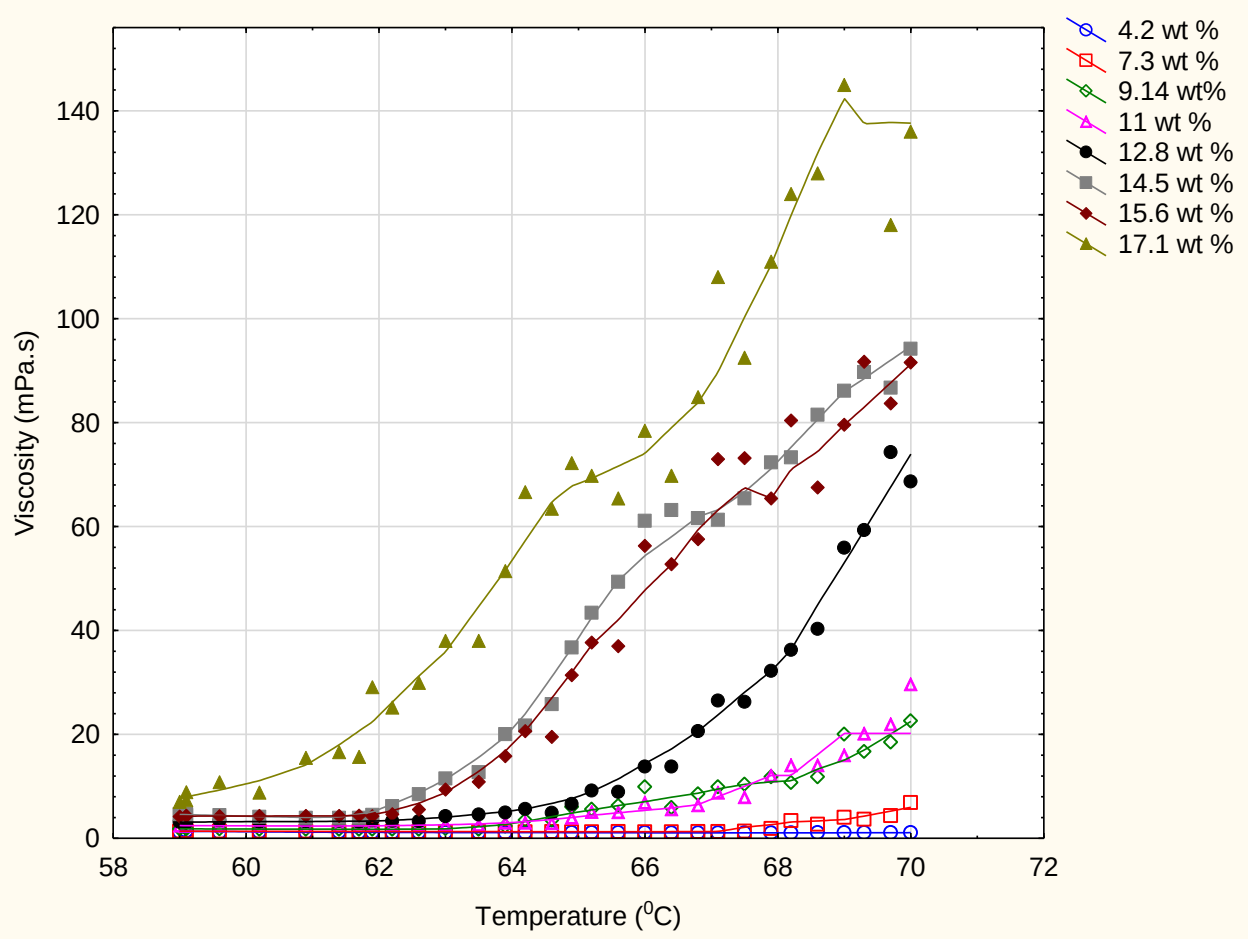

Figure 4-16: Viscosity against time for solutions of WPC as a function of temperature and concentration, at a constant shear rate of 23/s.

4.7.1 Discussion

Figure 4-16 shows that the increase in WPC solids concentration leads to an increase in viscosity. Viscosity also is observed to be influenced by temperature, more so at high concentrations. This is supported by the viscosities of lower concentrations of WPC (4.2 and 7.3 wt%), which remained almost constant with increase in temperature from 59°C to 70°C. When the WPC concentration was however raised from 9 wt% to 17 wt%, the viscosity responded to increasing temperatures by exponential increases. This result agrees with the findings of Soliman and colleagues (2010) who reported that the temperature plays a substantial role in the viscosity of WPC solution. Krešić and colleagues (2008) as well as Meza and colleagues (2009) also reported the influence of protein denaturation on the increasing viscosities with increasing temperature. This suggests that the higher concentration whey protein solutions investigated in this study (9 - 17 wt%) might be experiencing degradation

above 63^{o}C, resulting in the high increases in viscosity. Paramalingam (2004) also reported increasing viscosities of WPC solutions of concentration between 15 and 25 wt%. The increases in viscosities were observed between 55^{o}C and 60^{o}C. These results suggest the existence of a maximum temperature for each WPC concentration at which the viscosity will start to rise. It is therefore important that such temperatures be considered when selecting evaporating temperatures for evaporation systems. In this work, it can be concluded that a maximum temperature of 62^{o}C be considered when evaporating WPC solutions of up to 14.5 wt% (Figure 4-16). For higher concentrations, temperatures lower than 59^{o}C should be considered for the type of evaporation system as used in this study. Paramalingam (2004) also recommended working at temperatures less than 60^{o}C for concentration of whey proteins using a falling film evaporator.

4.8 HEAT TRANSFER COEFFICIENT

To establish the energy consumption in the evaporation system, the heat transfer coefficients of two solutions (WPC and sucrose) were calculated in the heating coil and their results are presented in the succeeding sections. The two solutions were evaluated at similar initial concentration (about 5 wt%). The heat transfer coefficients of the WPC solution at similar initial concentrations (5 wt%) and different operating temperatures (65 and 70^{o}C) were then evaluated and compared as a function temperature. Lastly, the heat transfer coefficients of the WPC solution at 65 ^{o}C and different initial concentration (5 wt% - 10 wt%) were evaluated and compared to evaluate the influence of concentration on the heat transfer coefficient. The relationship between the heat transfer and the Reynolds number as function of solid concentration was also investigated and results presented in this section.

4.8.1 Heat transfer coefficients of the WPC and sugar solutions

The heat transfer coefficients for the WPC and sugar solutions of similar concentrations at a feed temperature of 65^{o}C in a laminar flow regime, are plotted on Figure 4-17. The diagram shows higher heat transfer coefficients for the WPC than the sugar solutions, which both decrease with increasing solids concentration. The WPC solution heat transfer coefficient decreased from 431.9 W/m^2.K to 424.1 W/m^2.K as the concentration increased from 5.3 wt% to 10.1 wt%. Conversely, marginal decreases in the heat transfer coefficients for the sugar solution from 396.3 W/m^2.K at 4.95 wt% to 388.7 W/m^2.K at 9.6 wt% a solids concentration are displayed.

Figure 4-17 is a graph of Reynolds number against solids concentration for the sugar and WPC solutions for experiments 15 and 19. The Reynolds number was less than 2300 for all cases, showing that for all runs, the flow regime of operation was laminar. The graph shows that the sugar solution had higher Reynolds numbers than the WPC solution at the same solids concentration. This is a result of lower viscosities of the sugar solution than that of the WPC solutions, since lower viscosities result in higher Reynolds numbers. The graph further shows the Reynolds number decreases with increasing solids concentration for both solutions as well increasing solution viscosity and density. The WPC solution Reynolds number decreased from 402 to 232 as the concentration increased from 5.3 wt% to 10.1 wt% whilst decreases in the Reynolds number for sugar solution ranged from 680 at 4.95 wt% to 445 at 9.6 wt%.

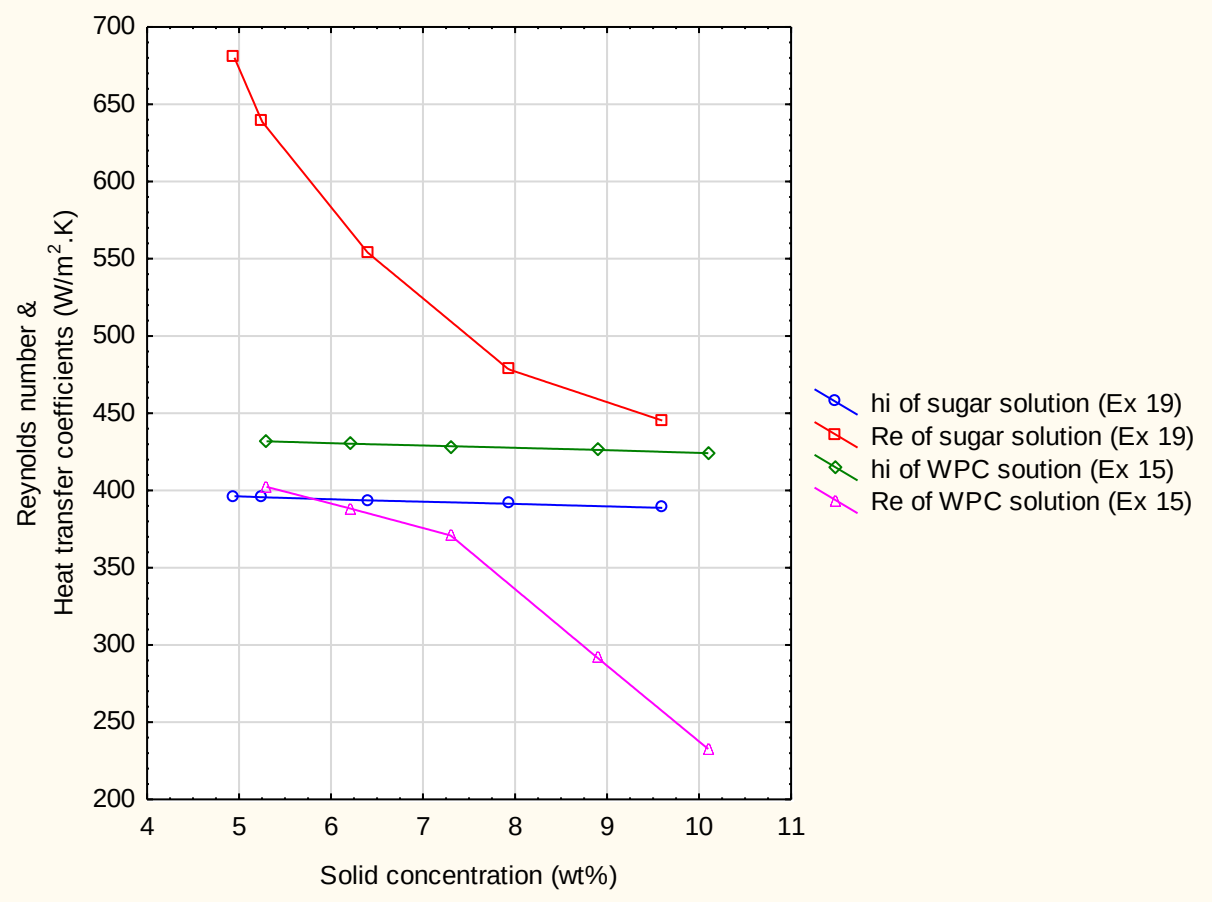

Figure 4-17: Heat transfer coefficient and Reynolds number against solid concentration of the WPC and sugar solutions for experiments 15 and 19

Where:

hi - Heat transfer coefficient inside the heating coil ($W/m^2.K$)

Re - Reynolds number

4.8.2 Heat transfer coefficient of the WPC at different feed temperatures

Figure 4-18 depicts the heat transfer coefficients for WPC solutions of similar initial concentrations (5.3 and 5.6 wt%) at 65ºC and 70ºC in the laminar flow regime. The heat transfer coefficient at 70ºC is higher than that at 65ºC (433.9 $W/m^2.K$ and 431.7 $W/m^2.K$ respectively) at similar initial concentrations. The coefficients dropped marginally (less than 1%) with increasing solids concentration, to end the evaporation process at 422.9 $W/m^2.K$ and 424.2 $W/m^2.K$ for solids concentrations of 11.9 wt% and 10.1 wt% respectively.

On Figure 4-18, the relationships between the Reynolds number and solids, concentration for the WPC solution at 65°C and 70°C is evaluated. It can be seen that the Reynolds number at 70°C is higher than that at 65°C (419 and 402 respectively). The Reynolds numbers decreased with increasing solids concentration to end the evaporation process at 117 (from 419) and 232 (from 402) for solids concentration of 11.9 wt% and 10.1 wt% respectively. The same graph further shows a rapid drop of the Reynolds number for the 70°C solution from 393 to 138 as the solids concentration increased from of 6.9 wt% and 8.1 wt%. The rapid drop in the Reynolds number is due to the increasing viscosity with increasing temperature as discussed in Section 4.6.1.

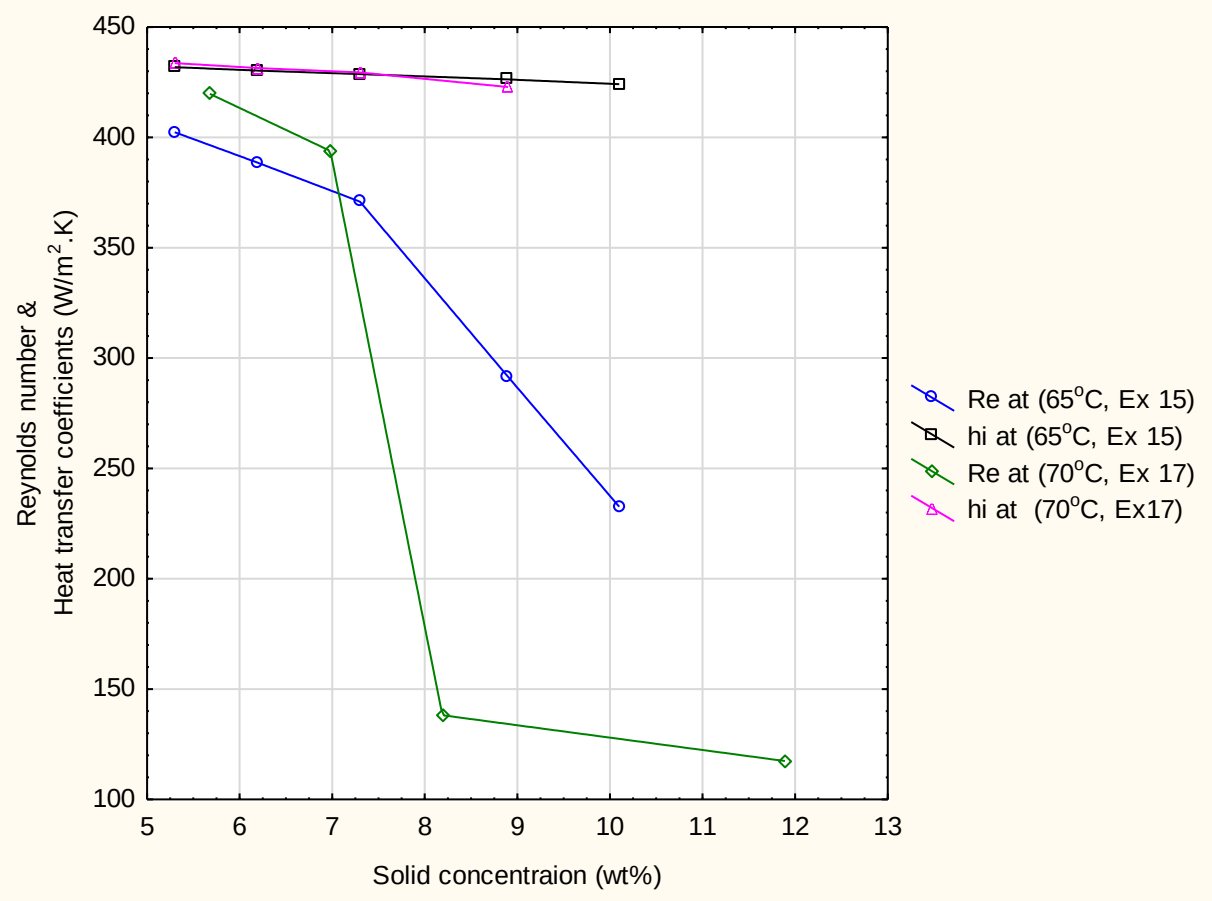

Figure 4-18: Heat transfer coefficient and Reynolds number against solid concentration of the WPC solutions at 65°C and 70°C.for experiments 15 and 17

4.8.3 Heat transfer coefficient of the WPC at different initial concentrations

Figure 4-19 shows the heat transfer coefficient for WPC solutions at 65°C with different initial concentrations (5.3 and 11.5 wt%). The solutions flow was in the laminar regime (Re < 2300). There is a marginal linear decrease in the heat transfer coefficient with increase in the amount of WPC solids. The graph further emphasises the result that increasing solids concentration reduces the heat transfer coefficient.

Figure 4.19 also shows the Reynolds numbers for the WPC solution at different initial concentrations (5.3 and 11.5 wt%). The Reynolds numbers decrease linearly with increasing solids concentration. For the weaker solution (initial concentration 5.3 wt%), the Reynolds number dropped from 402 to 232 as the concentration increased from 5.3 wt% to 10.1 wt%. On the other hand, decreases in the Reynolds number for the stronger solution (initial concentration 11.5 wt%), the Reynolds number dropped from 189 at 11.5 wt% to 75 at 16.7 wt %.

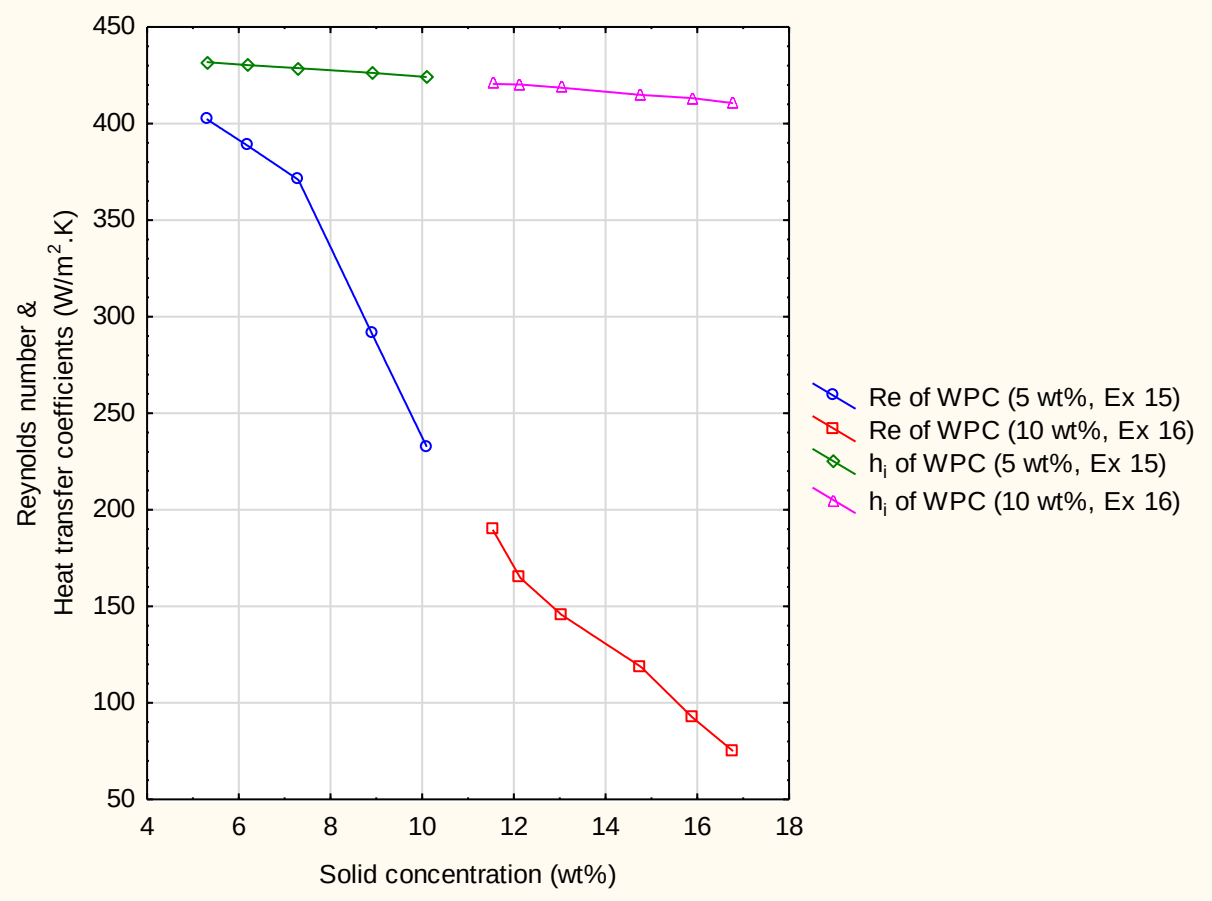

Figure 4-19: Heat transfer coefficient and Reynolds number against solid concentration of the WPC solutions at different initial concentrations for experiments 15 and 16

4.8.4 Discussion

The results of heat transfer coefficient (Figures 4-17, 4-18 and 4-19) show that the heat transfer coefficient is influenced by solids concentration and temperature, corroborating the findings of other authors (Paramalingam, 2004; Silveira, 2013; Singh, 2007; Pierre *et al.*, 1977; McMahon *et al.*, 1993). The WPC solution's heat transfer coefficient decreases with increasing solids concentration, due to an increase in viscosity (Beeby, 1966; Paramalingam, 2004). Figure 4-17 shows a higher heat transfer coefficient of WPC than that of sugar solution, which explains the results on Figures 4-14 and 4-15, which show a higher evaporation rate of WPC than that of sugar.

Figure 4-18 also shows a marginally higher heat transfer coefficient for the WPC solution at 70^{o}C than at 65^{o}C, also explaining the higher evaporation rates at higher temperatures as reported by Chen (1992). Similar results were reported by Paramalingam (2004) who, when working with casein whey protein concentrate (CWPC) and whey protein isolate (WPI), pointed out the dependency of the evaporator's evaporation capacity on the heat transfer coefficient. Figure 4-19 reinforces the result that the heat transfer coefficient decreases with increasing solids concentration, regardless of the initial concentration.

The same graphs (Figure 4.17, 4.18 and 4.19) also show that the Reynolds number, like the heat transfer coefficient, decreases with increasing solids concentration (increasing viscosity). It can therefore be concluded that the heat transfer coefficient decreases when the Reynolds number decreases. This agrees with the findings of Schwartzberg (1988) who reported a linear increase in heat transfer coefficient with an increasing Reynolds number for Reynolds numbers less than 500. The Figures 4-18 and 4-19 show a maximum Reynolds number of 419 for the WPC solution at 70^{o}C. Other authors (Hansen, 1985; Fulford, 1964) also reported increasing Reynolds numbers with decreasing viscosities, as shown on Figure 4-19.

The experiments in this study were all run under laminar conditions because the flowrate was maintained at a low constant value (about 300 ml/min). According to Yadav and colleagues (2014) as well as Pranit and colleagues (2015), turbulent flow is the preferred flow regime in industry because of its higher rates of heat transfer than laminar flow. However, due to the limiting capacity of the equipment (separator) in this study, the flow was kept laminar. From this study, the evaporation rate was increasing linearly with increasing concentration. On the other hand, the Reynolds number and the heat transfer coefficient were dropping, though

without affecting the efficiency of the system. In industrial operations, the drop in the heat transfer coefficient and Reynolds number may adversely affect the system efficiency, according to Pranit and colleagues (2015).

5. CONCLUSIONS AND RECOMMENDATIONS

5.1 CONCLUSIONS

The work undertaken resulted in the design of a functional vacuum evaporation system.

A functional laboratory scale vacuum evaporation system was successfully designed, constructed and evaluated. The results showed that the VES could be employed with certainty to non-heat sensitive material but would need some further investigation on the extent of protein denaturation, especially at temperatures at or above 65 ^{o}C for heat sensitive solutions like WPC. Depending on the findings of such investigations, its suitability for WPC concentration can be determined.

Separator efficiency was found to be increased by internal devices such as the half-pipe and multi-cyclone. The rates of evaporation for separator with and without internals, it was found that the evaporation rate for a separator with a half-pipe internals was higher than for that without.

Foaming was successfully supressed by addition of food grade antifoaming. It was partially reduced using mechanical intervention namely by multi cyclone while other mechanical means such as: half-pipe with a mesh pad and stages of mesh had no visibal effect on foaming supression.

Indirect heating in the feed tank was more preferable than direct heating. Direct preheating of the WPC solution in the feed tank by a heating element caused fouling of the element. However, by introducing a heating jacket for indirect heating, the evaporation system improved.

The viscosity is a critical parameter to consider in evaporation system design. It increases with increasing solids concentration, thereby reducing the solution recirculation and limiting the capacity of the system. In this design, the performance of the vacuum evaporation system for WPC solution was limited to a final concentration of around 17 wt%.

The viscosities of the WPC solutions in this study at constant shear rate (23/s) and solid concentrations lower than 15 wt% were negligibly affected by the operating temperature below 62^{o}C while the solution viscosities highly increased at temperature higher than 62^{o}C

The heat transfer coefficients in the heating coil for WPC and sugar solutions during the evaporation at laminar region (Re < 2300) were slightly decreased by increasing the viscosities and densities of these solutions.

The heating coil efficiency decreased with increasing vacuum level. Since a high vacuum level is required for low evaporation temperatures, the temperature difference for an inlet temperature of 65°C was lower than that for 70°C, thus more vacuum was required at 65°C. This reduced the heat transfer coefficient and ultimately the evaporation rate at 65°C. This partially explains the more evaporation observed at 70°C than 65°C. The dependence of heat transfer coefficient on the evaporation temperature was observed in the range of 65°C to 70°C.

The system evaporation efficiency was successfully evaluated using three different systems (NaCl, WPC and sugar solutions). The evaporation rate for conventional NaCl/water system (possibly due to small water/NaCl interaction) was the highest compared to lower evaporation rates for WPC and sugar/water solutions (with larger molecules and thus stronger interaction with water than NaCl). Slightly higher evaporation rate of WPC solution than that of sugar solution may partially attributed to higher heat transfer coefficient for WPC than that for sugar solution.

5.2 RECOMMENDATIONS

In this study the evaporator, feed product is heated to between 65^{o}C and 70^{o}C. It is therefore recommended that the final WPC properties during these temperatures be investigated to determine whether the system denatured the whey protein and enhanced foaming. To improve evaporator performance, optimum operating temperatures that consider temperature sensitivity of the WPC should be investigated and adopted. The substrate should also be tested to determine the exact temperature at which denaturation occurs, to determine the maximum temperature at which the system can be operated without denaturing the product.

Since the VES was limited to a maximum concentration of about 17 wt% by the increasing solution viscosity which made it difficult to drain the thick liquor from the separator, use of a recirculation pump should be considered. This will allow a further concentration of the solutions to higher concentrations.

Process control devices were manually adjusted, which allowed fluctuations in the flowrate and vacuum level, resulting in reduced accuracy. It is therefore recommended that use of an automated control system for the vacuum level and flow rate be considered, as well as replication of runs for repeatability and statistical analysis.

It is also recommended that the results of this investigation be modelled to allow application of the findings to similar process technologies.

In this study, due to the capacity of the lab scale, the flow rate was limited to the laminar region (Re < 1000). It is recommended that investigations in further work should focus on increasing the Reynolds number to achieve turbulent flow since the Reynolds numbers in most efficient commercial evaporators are above 1000.

The evaporation rate of WPC solution was higher than that of sugar solution at the same experimental conditions. However, the higher heat transfer coefficient of WPC solution is not adequate to elucidate this result. It is therefore necessary to investigate further the influence of viscosity and surface tension of the product on the efficient operation of the evaporator.

6. REFERENCES

Adib, T.A., Heyd, B. and Vasseur, J., 2009. Experimental results and modeling of boiling heat transfer coefficients in falling film evaporator usable for evaporator design. *Chemical Engineering and Processing: Process Intensification,* 48(4), pp. 961-968.

Akpan, D.G., 2013. Performance of Internals in Three-Phase Tank Separators. In: PhD thesis Norwegian University of Science and Technology.

Alizadehfard, M.R. and Wiley, D., 1996. Non-Newtonian behaviour of whey protein solutions. *Journal of Dairy Research,* 63, pp. 315-320.

Al-Najem, N., Ezuddin, K. and Darwish, M., 1998. Heat transfer analysis of preheated turbulent falling films in vertical tube evaporators. *Desalination,* 115(1), pp. 43-55.

Ammar, A.S., 2014. Food Processing Wastes: Characteristics, treatments and utilization review. *Journal of Agricultural and Veterinary Sciences,* 7(1), pp. 71-83.

Asghar, A., Rashid, H., Ashraf, M., Khan, M.H. and Chaudhry, Z., 2007. Improvement of basmati rice against fungal infection through gene transfer technology. *Pakistan Journal of Botany,* 39(4), pp. 1277-1283.

Ashurst, P.R., 2013. Production and packaging of non-carbonated fruit juices and fruit beverages. *Springer Science & Business Media.*

Atra, R., Vatai, G., Bekassy-Molnar, E. and Balint, A., 2005. Investigation of ultra-and nanofiltration for utilization of whey protein and lactose. *Journal of Food Engineering,* 67(3), pp. 325-332.

Bansal, B. and Chen, X.D., 2006. A critical review of milk fouling in heat exchangers. *Comprehensive Reviews in Food Science and Food Safety,* 5(2), pp. 27-33.

Beeby, R., 1966. Heat-induced changes in the viscosity of concentrated skim milk. 1, pp. 15- 121.

Bergman, T.L., Lavine, A.S., Incropera, F.P. and Dewitt, D.P., 2011. Fundamentals of Heat and Mass Transfer, Hoboken.

Bertsch, A.J., 1983. Surface tension of whole and skim milk between 18 and 135 ºC. 50(3), pp. 259-267.

Billet, R. and Fullarton, J., 1989. Evaporation Technology: Principles, Applications, Economics. *VCH Publishers*, Weinheim, Germany.

Blake, C., Koenig, D., Mair, G., North, A., Phillips, D. and Sarma, V., 1965. Structure of hen egg-white lysozyme: a three-dimensional Fourier synthesis at 2 Å resolution. *Nature*, 206(4986), pp. 757-761.

Bloore, C. and Boag, I., 1981. Some factors affecting the viscosity of concentrated skim milk. 16, pp. 143-154.

Bonnaillie, L.M. and Tomasula, P.M., 2008. Whey protein fractionation. *Wiley-Blackwell*, Hoboken, NJ, USA.

Borcherding, K., Lorenzen, P.C., Hoffmann, W. and Schrader, K., 2008. Effect of foaming temperature and varying time/temperature-conditions of pre-heating on the foaming properties of skimmed milk. *International Dairy Journal*, 18(4), pp. 349-358.

Bothamley, M., 2013a. Gas/Liquid separators: Quantifying separation performance-part 1. *Oil and Gas Facilities*, 2(04), pp. 21-29.

Bothamley, M., 2013b. Gas/liquids separators: Quantifying separation performance-part 2. *Oil and Gas Facilities*, 2(05), pp. 35-47.

Bothamley, M., 2013c. Gas/liquids separators: Quantifying separation performance-part 3. *Oil and Gas Facilities*, 2(05), pp. 34-47.

Bough, W. and Landes, D., 1978. Treatment of food processing wastes with chitosan and nutritional evaluation of coagulated by-products, Proceedings of the First International Conference on Chitin and Chitoswan. Cambridge*:* MIT SEA Grant Program, pp. 218-230.

Božanić, R., Barukčić, I. and Lisak, K., 2014. Possibilities of whey utilisation. *Austin Journal Nutr.Food Science.*, 2(7), pp. 1036.

Branan, C., 1994. Rules of Thumb for Chemical Engineers: A Manual of Quick, Accurate Solutions Everyday Process Engineering Problems. *Gulf Publishing Company,* Houston.

Brans, G., Schroën, C., Van Der Sman, R. and Boom, R., 2004. Membrane fractionation of milk: state of the art and challenges. *Journal of Membrane Science,* 243(1), pp. 263-272.

Brennan, J.G., 2006. Food Processing Handbook: Evaporation and Dehydration. *Wiley Online Library*, pp. 71-124.

Brennan, J.G., Butters, J., Cowell, N. and Lilly, A., 1990. Food Engineering Operations. 3th edn. *Elsevier Applied Science*, London.

Buma, T., 1980. Viscosity and density of concentrated lactose solutions and of concentrated cheese whey. 34(1), pp. 65-68.

Burton, H., 1968. Reviews of the progress of dairy science. Section G. Deposits from whole milk in heat treatment plant-A review and discussion. *Journal Dairy Research,* 35, pp. 317-330.

Bylund, G., 1995. Dairy Processing Handbook: Tetra Pak Processing Systems AB. *S-221,* 86.

Campbell, D., Brown, N. and Cox, J., 2015. Centrifugal Pumps.

Campbell, J.M., 2014. Gas Conditioning and Processing: The Equipment Modules. 9th edn. *Campbell Petroleum Series*, 2, Norman, Oklahoma.

Changani, S., Belmar-Beiny, M. and Fryer, P., 1997. Engineering and chemical factors associated with fouling and cleaning in milk processing. *Experimental Thermal and Fluid Science*, 14(4), pp. 392-406.

Chen, H., 1992. Factors Affecting Heat Transfer in the Falling Film Evaporator. In: Master Thesis, Massey University, Palmerston North, New Zealand.

Choi, Y., 1986. Effects of temperature and composition on the thermal properties of food. *Food Engineering and Process Applications,* 1, pp. 93-101.

Cohn, E.J. and Edsall, J.T., 1965. Proteins, Amino Acids and Peptides as Ions and Dipolar Ions. In: E.J. Cohn and J.T. Edsall, ed. *Hafner Publishing Company*, New York, pp. 506-542.

Couper, J.R., 2012. Chemical Process Equipment: Selection and Design. 3th edn. *Elsevier/Butterworth-Heinemann,* Amsterdam; Boston, pp. 655-675.

Damodaran, S., 1997. Food proteins and their applications. *CRC Press.*

Dannenberg, F. and Kessler, H., 1988. Reaction kinetics of the denaturation of whey proteins in milk. *Journal of Food Science,* 53(1), pp. 258-263.

Darros-Barbosa, R., Balaban, M.O. and Teixeira, A.A., 2003. Temperature and concentration dependence of density of model liquid foods. *International Journal of Food Properties,* 6(2), pp. 195-214.

De Wit, J., 1998. Nutritional and functional characteristics of whey proteins in food products. *Journal of Dairy Science,* 81(3), pp. 597-608.

De Wit, J., 1989. The use of whey protein products. *Developments in Dairy Chemistry,* 4, pp. 323-345.

Delplace, F., Leuliet, J. and Tissier, J., 1996. Fouling experiments of a plate heat exchanger by whey proteins solutions. *Fouling and Cleaning in Food Processing Conference Notes*, pp. 1-8.

Duranti, M., Pagani, S., Iametti, S. and Carpen, A., 1989. Heat-induced changes of milk proteins: Rocket immunoelectrophoretic detection of α-lactalbumin. *Milchwissenschaft,* 44(3), pp. 142-144.

Dutta, B.K., 2006. Heat Transfer: Principles and Applications. 1st edn. *PHI Learning Pvt. Ltd,* New Delhi, pp. 361-420.

Evans, F.L., 1974. Equipment Design Handbook for Refineries and Chemical Plants. *Gulf Publishing Company*.

Fabian, P., Cusack, R., Hennessey, P. and Neuman, M., 1993. Demystifying the selection of mist eliminators. *Chemical engineering,* 100(11), pp. 148.

Fergusson, P., 1989. Developments in the Evaporation and Drying of Dairy Products. 42(4), pp. 94-101.

Fernandez-Martin, F., 1972. Influence of temperature and composition on some physical properties of milk and milk concentrates. 39(1), pp. 75-82.

Fischer, K., 1935. Neues verfahren zur maßanalytischen bestimmung des wassergehaltes von flüssigkeiten und festen körpern. *Angewandte Chemie,* 48(26), pp. 394-396.

Foegeding, E. A., and P. J., Luck, 2011. Whey Protein Products: In Encyclopaedia of Dairy Sciences. In: H. Roginski, P.F. Fox, and J.W. Fuquay, ed. *Academic Press*, London, UK, pp. 873-878.

Frankel, A., 1960. Flash evaporators for the distillation of seawater. *Proceedings of the Institution of Mechanical Engineers*, 174(1), Pp. 312-361.

Freese, H. and Glover, W., 1979. Mechanically agitated thin-film evaporators. 75(1), pp. 52- 58.

Frid, A.H., Nilsson, M., Holst, J.J. and Bjorck, I.M., 2005. Effect of whey on blood glucose and insulin responses to composite breakfast and lunch meals in type 2 diabetic subjects. *The American Journal of Clinical Nutrition*, 82(1), pp. 69-75.

Fryer, P. and Belmar-Beiny, M., 1991. Fouling of Heat Exchangers in the Food Industry: A Chemical Engineering Perspective. 2, pp. 33-37.

Fulford, G.D., 1964. The flow of liquids in thin films. *Advances in Chemical Engineering*, 5, pp. 151-236.

Gerunda, A., 1981. How to size liquid-vapor separators. *Chemical Engineering,* 88(9), pp. 81- 84.

Gillham, C., Fryer, P., Hasting, A. and Wilson, D., 2000. Enhanced cleaning of whey protein soils using pulsed flows. *Journal of Food Engineering*, 46(3), pp. 199-209.

Glover, W.B., 2004. Selecting evaporators for process applications. *Chemical Engineering Progress*, 100(12), pp. 26-33.

GPSA, G., 2004. Engineering Data Book. 12th edn. *Gas Processors Suppliers Association*, Tulsa, Oklahoma.

Green, D.W. and Perry, R.H., 1973. Chemical Engineers Handbook. 5th edn. *McGraw-Hill*, New York, pp. 11-27.

Green, D.W. and Perry, R.H., 2008. Perry's Chemical Engineers' Handbook. 8th edn. *McGraw-Hill*, New York.

Guimarães, P.M., Teixeira, J.A. and Domingues, L., 2010. Fermentation of lactose to bio- ethanol by yeasts as part of integrated solutions for the valorisation of cheese whey. *Biotechnology Advances*, 28(3), pp. 375-384.

Ha, E. and Zemel, M.B., 2003. Functional properties of whey, whey components, and essential amino acids: mechanisms underlying health benefits for active people. *The Journal of Nutritional Biochemistry*, 14(5), pp. 251-258.

Hall, S., 2012. Rules of Thumb for Chemical Engineers. 5th edn. *Butterworth-Heinemann: Elsevier*.

Hansen, R., 1985. Evaporation, Membrane Filtration and Spray Drying in Milk Powder and Cheese Production. *North European Dairy Journal*, Denmark, pp. 25-43.

Harker, J.H., Backhurst, J.R. and Richardson, J., 2013. Chemical Engineering. *Butterworth-Heinemann.*

Hasan, S.N.U., Ali, S., Qureshi, L.A., Ahmed, S., Farooq, S.H., Ilyas, M., Qazi, A., Haydar, S., Bari, A. and Tanwari, A., 2011. Experimental investigation of heat transfer coefficient in vertical tube rising film evaporator. *Journal of Engineering and Technology*, 30(4), pp. 539-548.

Hat_International, H., 2008. Feature: Inlet Distributor Selection.

Herceg, Z., Lelas, V. and Škreblin, M., 2002. Influence of tribomechanical micronisation on the rheological properties of whey proteins. *Food Technology and Biotechnology*, 40(2), pp. 145-155.

Hermansson, A., 1975. Functional properties of proteins for foods-flow properties. *Journal of Texture Studies,* 5(4), pp. 425-439.

Hillier, R.M. and Lyster, R.L., 1979. Whey protein denaturation in heated milk and cheese whey. *Journal of Dairy Research,* 46(1), pp. 95-102.

Housˇka, M., Adam, M., Celba, J., Havlicˇek, Z., Jeschke, J. and Kubesˇova, A., 1994. Milk, milk products and semi products. Thermophysical and rheological properties of food. *Institute of Agricultural and Food Information*, Prague.

Hyde, W. and Glover, W., 1997. Evaporation of difficult products-Agitated thin-film evaporation overcomes common problems. *Chemical Processing*, 60(2), pp. 59-&.

Jeewanthi, R.K., Lee, N.K. and Paik, H.D., 2015. Improved Functional Characteristics of Whey Protein Hydrolysates in Food Industry. *Journal for Food Science of Animal Resources,* Korea (South), 35(3), pp. 350-359.

Jeurnink, T.J. and De Kruif, K.G., 1993. Changes in milk on heating: viscosity measurements. *Journal of Dairy Research,* Cambridge University Press, 60(2), pp. 139-150.

Jovanović, S., Barać, M. and Maćej, O., 2005. Whey proteins-properties and possibility of application. *Mljekarstvo,* 55(3), pp. 215-233.

Kalis, B., 2004. Cure liquid carryover from compressor suction drums. *Hydrocarbon Process.* 83(10), pp. 77-84.

Kandlikar, S.G., 1990. A general correlation for saturated two-phase flow boiling heat transfer inside horizontal and vertical tubes. *ASME Journal of Heat Transfer*, 112(1), pp. 219-228.

Kendrew, J., Watson, H., Strandberg, B., Dickerson, R., Phillips, D. and Shore, V., 1961. A partial determination by x-ray methods and its correlation with chemical data. *Nature, Springer,* 190(4777), pp. 666-670.

Kessler, H., 1981. Food Engineering and Dairy Technology. *Verlag A. Kessler*. Germany

Kirkwood, J.G., Buff, F.P. and Green, M.S., 1949. The statistical mechanical theory of transport processes. III. The coefficients of shear and bulk viscosity of liquids. *The Journal of Chemical Physics*, 17(10), pp. 988-994.

Klarenbeek, G., 1984. Effects of various heat treatments on structure and solubility of whey proteins. *Journal of Dairy Science*, 67(11), pp. 2701-2710.

Koch-Glitsch-Lp, 2007. Mist elimination. *Koch-Otto York Separations Technology*.

Koretsky, M.D., 2004. Engineering and Chemical Thermodynamics. *Wiley Hoboken*, New Jersey.

Krešić, G., Lelas, V., Jambrak, A.R., Herceg, Z. and Brnčić, S.R., 2008. Influence of novel food processing technologies on the rheological and thermophysical properties of whey proteins. *Journal of Food Engineering*, 87(1), pp. 64-73.

Lakkis, J. and Villota, R., 1990. A study on the foaming and emulsifying properties of whey protein hydrolysates. Food Emulsion and Foams: Theory and Practice, 86, pp. 87-101.

Laleh, A.P., Svrcek, W.Y. and Monnery, W.D., 2012. Design and CFD studies of multiphase separators a review. *The Canadian Journal of Chemical Engineering*, 90(6), pp. 1547- 1561.

Law, A.J. and Leaver, J., 1997. Effect of protein concentration on rates of thermal denaturation of whey proteins in milk. *Journal of Agricultural and Food Chemistry*, 45(11), pp. 4255- 4261.

Lewis, M., 1993. Physical Properties of Dairy Products. In: R. K. Robinson, ed, *Elsevier Applied Science Publishers*, London, New York, pp. 261-306.

Litchfield, J.H., 1987. Microbiological and enzymatic treatments for utilizing agricultural and food processing wastes. *Food Biotechnology*, 1(1), pp. 29-57.

Lopez-Toledo, J., 2006. Heat and Mass Transfer Characteristics of a Wiped Film Evaporator. In: PhD thesis. The University of Texas at Austin.

Lu, Y., Greene, J.J. and Agrawal, M., 2009. CFD Characterization of Liquid Carryover in Gas/Liquid Separator with Droplet Coalescence due to Vessel Internals, SPE Annual Technical Conference and Exhibition, Society of Petroleum Engineers.

Lyons, W.C. and Plisga, G.J., 2005. Standard Handbook of Petroleum and Natural Gas Engineering. *Gulf Professional Publishing*, Burlington.

Maćej, O., 1983. Prilog proučavanju koprecipitata radi potpunijeg iskorišćavanja belančevina mleka. *Magistarski Rad*, Univerzitet u Beogradu.

Mackereth, A.R., Trinh, K.T. and Woohall, M.C., 2003. Mlik Powder Technology. *New Zealand Dairy Research Institute.*

Manning, F.S. and Thompson, R.E., 1995. Oilfield Processing of Petroleum, Crude Oil. *Pennwell Books.*

Mccabe, W.L., Smith, J.C. and Harriott, P., 1993. Unit Operations of Chemical Engineering. 5th edn. *McGraw-Hill*, New York.

Mcginnis, R.A., 1971. Beet-Sugar Technology. 2nd edn. Fort Collins: Beet Sugar Development Foundation.

Mcintosh, G.H., Royle, P.J., Le Leu, R.K., Regester, G.O., Johnson, M.A., Grinsted, R.L., Kenward, R.S. and Smithers, G.W., 1998. Whey Proteins as functional food ingredients? *International Dairy Journal*, 8(5-6), Pp. 425-434.

Mcmahon, D.J., Yousif, B.H. and Kaláb, M., 1993. Effect of whey protein denaturation on structure of casein micelles and their rennet ability after ultra-high temperature processing of milk with or without ultrafiltration. *International Dairy Journal*, 3(3), pp. 239-256.

Meade, G. and Chen, J., 1977. Cane Sugar Handbook. 10th edn. *John Wiley and Sons*, New York.

Meza, B., Verdini, R.A. and Rubiolo, A.C., 2009. Viscoelastic behaviour of heat-treated whey protein concentrate suspensions. *Food Hydrocolloids*, 23(3), pp. 661-666.

Middleton, J., 1996. Physical Properties of Dairy Products. *MAF Quality Management*, Ministry of Agriculture Wellington, New Zealand.

Miller, G., Jarvis, J. and Mcbean, L., 2000. The Importance of Milk and Milk Products in The Diet, Handbook Of Dairy Foods And Nutrition. 2nd edn. *CRC Press*, Boca Raton, Florida, USA.

Minton, P.E., 1986. Handbook of Evaporation Technology. New Jersey, Noyes.

Miranda, V. and Simpson, R., 2005. Modelling and simulation of an industrial multiple effect evaporator: tomato concentrate. *Journal of Food Engineering*, 66(2), pp. 203-210.

Mokhatab, S. and Poe, W.A., 2012. Phase Separation, Handbook of Natural Gas Transmission and Processing. 2rd edn. *Gulf Professional Publishing*, pp. 195-238.

Morr, C.V., 1989. Developments in Dairy Chemistry: Functional Milk Proteins. In: P.F. Fox, ed. *Applied Science Publishers*, New York, pp. 245-284.

Moss, D.R. and Basic, M.M., Eds, 2013. Pressure Vessel Design Manual. 4th edn. *Butterworth-Heinemann: Elsevier*, Oxford.

Mulvihill, D., 1992. Production, functional properties and utilization of milk protein products. *Advanced Dairy Chemistry*, 1, pp. 369-404.

Murakami, E. and Okos, M., 1989. Measurement and prediction of thermal properties of foods. *Food Properties and Computer-Aided Engineering of Food Processing Systems.* Springer, pp. 3-48.

Nelson, P.E. and Tressler, D.K., 1980. Fruit and Vegetable Juice Processing Technology. 3rd edn. *AVI Publishing Company*, West Port.

NiroInc., 2005. Evaporation Technology. Available on: http://www.niroinc.com/html/evaporator/etech.html,

Norsok., 2001. P-100 Engineering Standard for Process Systems. pp. 10-16.

Oldfield, D.J., Singh, H., Taylor, M.W. and Pearce, K.N., 1998. Kinetics of denaturation and aggregation of whey proteins in skim milk heated in an ultra-high temperature (UHT) pilot plant. *International Dairy Journal,* 8(4), pp. 311-318.

Oldfield, D.J., 1996. Heat-Induced Whey Protein Reactions in Milk: Kinetics of Denaturation and Aggregation as Related to Milk Powder Manufactur*e*. In: PhD thesis. Massey University.

Oldfield, D., Taylor, M. and Singh, H., 2005. Effect of preheating and other process parameters on whey protein reactions during skim milk powder manufacture. *International Dairy Journal,* 15(5), pp. 501-511.

Pabby, A.K., Rizvi, S.S. and Sastre, A.M., 2008. Handbook of Membrane Separations: Chemical, Pharmaceutical. *Food and Biotechnological Applications, CRC*,USA.

Paramalingam, S., 2004. Modelling, Optimisation and Control of a Falling-Film Evaporator, In: PhD thesis. Massey University.

Parker, N.H., 1963. How to Specify Evaporators. *Chemical Engineering*, pp. 135-140.

Patterson, F., 1969. Vortexing can be prevented. *Oil and Gas Journal.*

Perry, R., Green, D. and Maloney, J.,1984. Perry's Chemical Engineers' Handbook. 6th edn. *McGraw-Hill,* New York.

Pierre, A., Brule, G., Fau1mt, J. and Piot, M., 1977. The influence of thermal treatments on the physicochemical properties of retentates obtained by ultrafiltration of milk of the cow and goat. *Lait*, pp. 569-570-646-662.

Pintado, M.E., Pintado, A.E. and Malcata, F.X., 1999. Controlled whey protein hydrolysis using two alternative proteases. *Journal of Food Engineering*, 42(1), pp. 1-13.

Pranit, M., Yadav, A.P. and Patil, P.A., 2015. Comparative study between heat transfer through laminar flow and turbulent flow. *International Journal of Innovative Research in Science*, 4(4), pp. 2223-2226.

Rektor, A. and Vatai, G., 2004. Membrane filtration of Mozzarella whey. *Desalination, Elsevier,* 162, pp. 279-286.

Renner, E. and Abd-El-Salam, M., 1991. Application of ultrafiltration in the dairy industry. *Elsevier Science Publishers Ltd.*

Saxena, A., Tripathi, B.P., Kumar, M. and Shahi, V.K., 2009. Membrane-based techniques for the separation and purification of proteins: an overview. *Advances in Colloid and Interface Science,* 145(1), pp. 1-22.

Scheiman, A.D., 1963. Size Vapor-Liquid Separators Quickly by Nomograph. *Hydrocarbon Process and Petroleum Refiner.*

Schwartzberg, H., 1989. Food Property Effects in Evaporation. In: R.P. Singh and A.G. Medina, ed. *Food Properties and Computer-Aided Engineering of Food Processing Systems*, pp. 443-470.

Silveira, A.C.P., 2013. Pilot-scale investigation of effectiveness of evaporation of skim milk compared to water. *Dairy Science & Technology,* 93(4-5), pp. 537-550.

Simion, A., Grigoraş, C., Rusu, L., Dabija,A., 2017. Modeling of the thermo-physical properties of aqueous sucrose solutions ii. Boiling point, specific heat capacity and thermal conductivity. *Food and Environment Safety Journal,* 10(4).

Singh, H., 2007. Interactions of milk proteins during the manufacture of milk powders. *EDP Sciences*, 87(4-5), pp. 413-423.

Singh, H. and Creamer, L.K., 1991. Denaturation, aggregation and heat stability of milk protein during the manufacture of skim milk powder. *Journal of Dairy Research,* 58(3), pp. 269- 283.

Singh, R.P. and Heldman, D.R., 2001. Introduction to Food Engineering. *Gulf Professional Publishing*, New Jersey:

Sinnott, R.K., 2005. Equipment Selection, Specification and Design, Coulson and Richardson's Chemical Engineering Chemical Engineering Design. 4th edn. *Elsevier*, pp. 461-465.

Slettebø, E.S., 2009. Separation of Gas from Liquids in Viscous Systems. In: Master's thesis Norwegian University of Science and Technology.

Smith, P., 2011. Evaporation and Drying: Introduction to Food Process Engineering. *Springer*, pp. 299-334.

Smithers, G.W., 2008. Whey and whey proteins from 'gutter-to-gold'. *International Dairy Journal*, 18(7), pp. 695-704.

Smithers, G.W., Ballard, F.J., Copeland, A.D., De Silva, K.J., Dionysius, D.A., Francis, G.L., Goddard, C., Grieve, P.A., Mcintosh, G.H. and Mitchell, I.R., 1996. New opportunities from the isolation and utilization of whey proteins. *Journal of Dairy Science*, 79(8), pp. 1454-1459.

Snoeren, T., Damman, A. and Klok, H., 1982. The viscosity of skim-milk concentrate. *Milk Dairy Journal*, Netherlands, 36, pp. 305-316.

Soares, C., 2002. Process Engineering Equipment Handbook. *McGraw-Hill*. New York:

Soliman, T., Farrag, A., Shendy, A. and El-Sayed, M., 2010. Denaturation and viscosity of whey proteins solutions as affected by frozen storage. *Journal America Science*, 6, pp. 49- 62.

Spellman, D., Kenny, P., O'cuinn, G. and Fitzgerald, R.J., 2005. Aggregation properties of whey protein hydrolysates generated with Bacillus licheniformis proteinase activities. *Journal of Agricultural and Food Chemistry*, 53(4), pp. 1258-1265.

Standiford, F.C., 2005. Kirk-Othmer Encyclopedia of Chemical Technology. 4th edn. Elastomers, Synthetic-Expert Systems, *John Wiley and Sons*, New York, pp. 472-493.

Standiford, 1983. Production of concentrated alcohol and distillery slop. U.S. Patent 4,381,220. edn.

Stanic, D., Radosavljevic, J., Stojadinovic, M. and Velickovic, T.C., 2012. Application of Ion Exchanger in the Separation of Whey Proteins and Lactin from Milk Whey. *Ion Exchange Technology II. Springer*, Netherlands, pp. 35-63.

Stewart and Arnold, K., 2008. Gas-Liquid and Liquid-Liquid Separators. *Elsevier*.

Suryanarayana, N.V., 1995. Engineering Heat Transfer. *West Publishing Company*, St.Paul, MN, pp. 291-428.

Svrcek, W. and Monnery, W., 1994. Design 2-phase separators within the right limits (Vol 80, pg 53, 1993). *Chemical Engineering Progress*, 90(7), pp. 9-9.

Swaisgood, H. and Fox, P., 1992. Advanced Dairy Chemistry-Proteins. *Elsevier Science Publishers Ltd*, England, 1.

Taborek, J., Aoki, T., Ritter, R., Palen, J. and Knudsen, J., 1972. Fouling: the major unresolved problem in heat transfer.

Talavera, P., 1990. Selecting gas/liquid separators. *Hydrocarbon Processing*, USA, 69(6),.

Tamm, F., Sauer, G., Scampicchio, M. and Drusch, S., 2012. Pendant drop tensiometry for the evaluation of the foaming properties of milk-derived proteins. *Food Hydrocolloids*, 27(2), pp. 371-377.

Tang, Q., Munro, P.A. and McCarthy, O.J., 1993. Rheology of whey protein concentrate solutions as a function of concentration, temperature, pH and NaCl concentration. *Journal of Dairy Research*, 60(3), pp. 349-361.

Todaro, C.M. and Vogel, H.C., 2014. Fermentation and Biochemical Engineering Handbook. *William Andrew*.

Uki, T., Sarda, S.T. and Mathew, T., 2012. Design of Gas-Liquid Separator for Complete Degasing. *International Journal of Chemical Engineering and Applications*, 3(6), pp. 477- 480.

USDEC, 2004, Reference manual for U.S. whey and lactose products. Available on: http://www.usdec.org.

Vélez-Ruiz, J. and Barbosa-Cánovas, G., 1998. Rheological properties of concentrated milk as a function of concentration, temperature and storage time. *Journal of Food Engineering*, 35(2), pp. 177-190.

Wenten, I. and Chandranegara, A.S., 2008. Improving Mist Eliminator Performance in Gas-Liquid Separators.

Whitney, R.M., 1988. Proteins of Milk: Fundamentals of Dairy Chemistry. *Springer*, New York, USA, , pp. 81-169.

Wiencke, B., 2011. Fundamental principles for sizing and design of gravity separators for industrial refrigeration. *International Journal of Refrigeration*, 34(8), pp. 2092-2108.

Wijayanti, H.B., Bansal, N. and Deeth, H.C., 2014. Stability of whey proteins during thermal processing: A review. *Comprehensive Reviews in Food Science and Food Safety*, 13(6), pp. 1235-1251.

Wilde, P., 2000. Interfaces: their role in foam and emulsion behaviour. *Current Opinion in Colloid & Interface Science*, 5(3), pp. 176-181.

Woodshead, 1997. The Lactose Company of New Zealand.

Yamomoto, Y., 1968. Design and Operation of Evaporators for Radioactive Wastes.

Yadav, A.P., Pranit, M. and Patil, P.A., 2014. The Effect of insertion of different geometries on heat transfer performance in circular pipe-a review. *International Journal of Modern Engineering Research*, 4(11), pp. 47-53.

Younger, A., 1955. How to Size Future Process Vessels. *Chemical Engineering.*

Younger, A. and Eng, P., 2004. Natural Gas Processing Principles and Technology-part 2. *Gas Processors Association*, Tulsa Oklahoma.

Zeman, L.J., 1996. Microfiltration and Ultrafiltration: Principles and Application. *Marcel Dekker, Inc*., New York.

Zhu, H. and Damodaran, S., 1994. Effects of calcium and magnesium ions on aggregation of whey protein isolate and its effect on foaming properties. *Journal of Agricultural and Food Chemistry*, 42(4), pp. 856-862.

7. APPENDIX

7.1 APPENDIX A

7.1.1 Centrifugal pump sizing calculations

The pump design was done according to the method of Perry (Green and Perry, 2008). The initial assumption requirement of the pump was to pump 500 kg/hr of water. The water stream was available from feed tank, which operated at atmospheric pressure and 25°C. Minimum liquid level in the feeder tank above pump suction nozzle was kept at 0.2 m. The suction line was a copper pipe, 12.3 mm inside diameter and 0.4 m long to the centrifugal pump. On the pump discharge line, at a height of 1.3 m was a throttling device (a needle valve). There was no control valve in the discharge line up to throttling device. The discharge line, consisting of all the fittings and valves, was assumed to be 1.9 m long. Pump efficiency and motor efficiency were assumed to be 70% and 90% respectively.

Step 1: Determination of the important physical properties of given fluid (water)

Physical properties of water were determined at atmospheric pressure:

- water density at 25°C = 994.72 kg/m^3
- water viscosity at 25°C = 0.90 mPa.s

Step 2. Calculation of pressure drop

The suction and discharge line pressure drop was calculated as follows:

The Reynolds number

$$Re = \frac{\rho D u}{\mu} \qquad \text{Equation 7-1}$$

Re - Reynolds number of the motion

ρ – Fluid density (kg/m^3)

μ - Fluid viscosity (cP)

D - Inner dimeter of pipe (m)

Average velocity

$$u = \frac{Q}{A}$$ Equation 7-2

where;

u - Mean velocity of the flow (m/sec)

Q - Discharge volumetric flowrate (m^3/sec)

A - Cross sectional area of discharge line (m^2)

Friction loss

The total length of section line and discharge line was 2.3 m. The line was made from a copper pipe and the pipe roughness, ε was 0.046 mm.

Table 7-1: Minor Loss Coefficients for the fittings used in the design.

Fitting	Number	Coefficient per each
Elbows 90^o	4	1.5
Tee, standard	4	1
Gate valve ,open	3	0.17
Gate valve , 1/4 open	1	24
Sharp edged, K	1	1

Friction factor equations were calculated as follows:

For Laminar Flow:

By using Moody friction factor (f):

$$f = \frac{Re}{64}$$ Equation 7-3

For Turbulent flow:

By using the Churchill Equation:

$$f = [-2\,log(0.27\varepsilon/D) + (7/Re)0.9]^{-2}$$ Equation 7-4

Where;

ε - Pipe Roughness (mm)

For Transitional Flow

By using the formula Colebrook Equation:

$$f = 2(\left\{\left(\frac{8}{Re}\right)^{12}\right\} + \frac{1}{(A+B)^{\frac{3}{2}}})^{1/12} \qquad \text{Equation 7-5}$$

$$A = (2.457ln(\frac{1}{(7/Re)^{0.9}} + 0.27\left(\frac{\varepsilon}{D}\right))^{16} \qquad \text{Equation 7-6}$$

$$B = (37530/Re)^{16} \qquad \text{Equation 7-7}$$

Step 3: The overall head loss

The two head losses (major and minor) of the pipe system were determined from which the overall head loss was then calculated as follows:

$$h_L = h_{L\,major} + h_{Lminor} \qquad \text{Equation 7-8}$$

Where;

h_L - Total head loss

h_{Lminor} - Minor head loss

h_{Lmajor} - Major head loss

Major Losses

The Darcy-Weisbach Equation

$$h_{L\,major} = \frac{f_L}{D}\ \frac{V^2}{2g} \qquad \text{Equation 7-9}$$

Where;

f_L - Friction factor.

Minor Losses

The additional components such as valves and bends contributes to the overall system head losses, as shown in Equation 7-10.

$$h_{L\,minor} = K_L\ \frac{V^2}{2g} \qquad \text{Equation 7-10}$$

Where;

K_L - Loss coefficient.

Overall, head loss

$$h_L = \frac{f_L}{D} \frac{V^2}{2g} + K_L \frac{V^2}{2g}$$ Equation 7-11

Step 4: Total Dynamic Head (TDH)

The total dynamic head is calculated using Equation 7-12.

TDH = Static Height + overall head loss

$$TDH = (Z_2 - Z_1) + h_L$$ Equation 7-12

Where Z_2 is the height from the pump to the throttling device and Z_1 is the liquid level in the feeder tank.

7.1.2 Calculations Result

Table 7-2: System curve calculation.

Q (m^3 /hr)	u (m/sec)	R_e	R_e Fluid Type	f_L	h_L	TDH
0.01	0.023	288	Laminar Flow	0.223	0.002	0.70
0.05	0.117	1438	Laminar Flow	0.045	0.031	0.73
0.09	0.210	2588	Transitional Flow	0.050	0.102	0.80
0.20	0.468	5751	Turbulent Flow	0.041	0.487	1.19
0.25	0.584	7189	Turbulent Flow	0.039	0.754	1.45
0.30	0.701	8626	Turbulent Flow	0.038	1.080	1.78
0.35	0.818	10064	Turbulent Flow	0.037	1.463	2.16
0.40	0.935	11502	Turbulent Flow	0.036	1.904	2.60
0.45	1.052	12939	Turbulent Flow	0.035	2.402	3.10
0.5	1.169	14377	Turbulent Flow	0.035	2.958	3.66

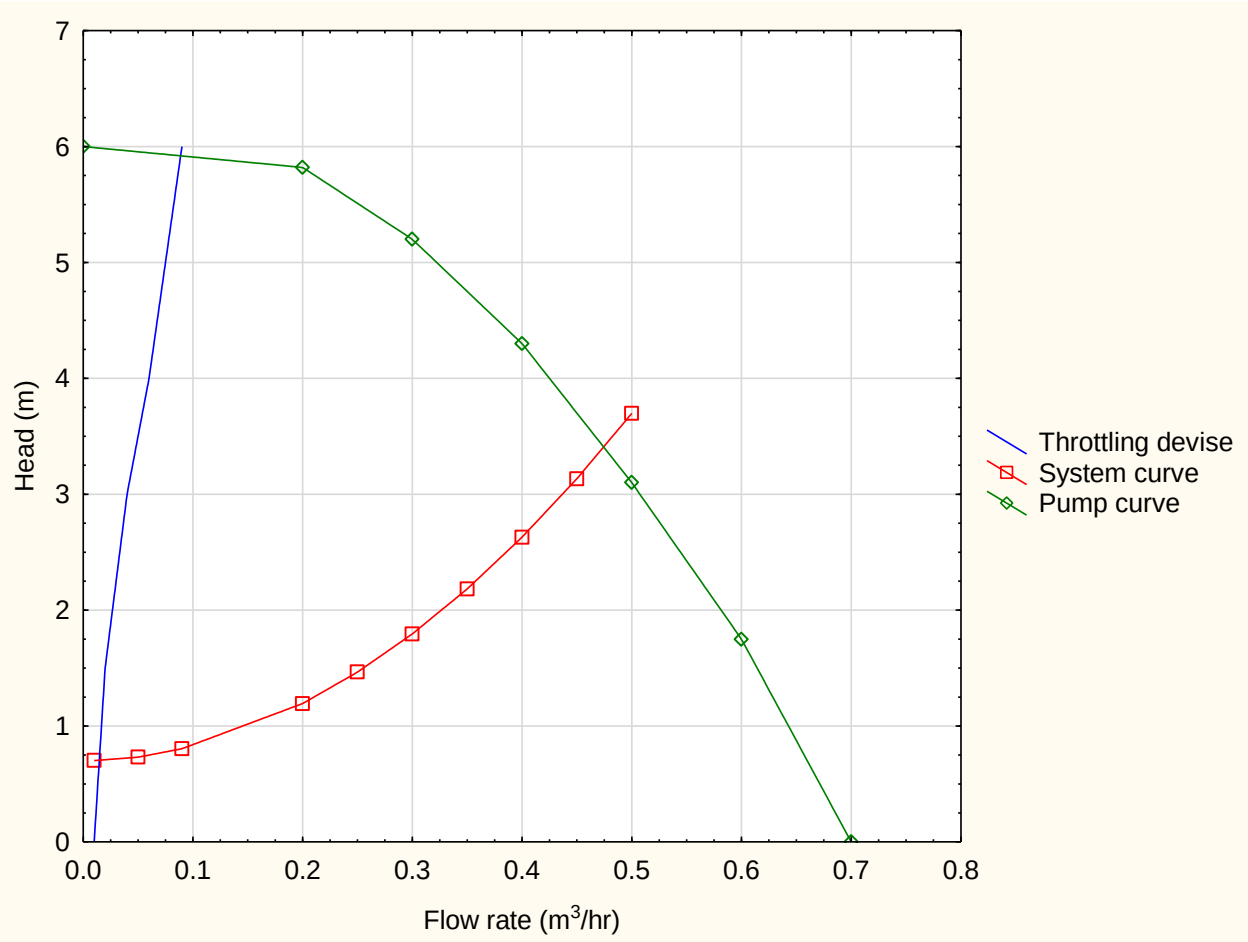

Figure 7-1: Centrifugal pump curve against system design curve as a function flowrate.

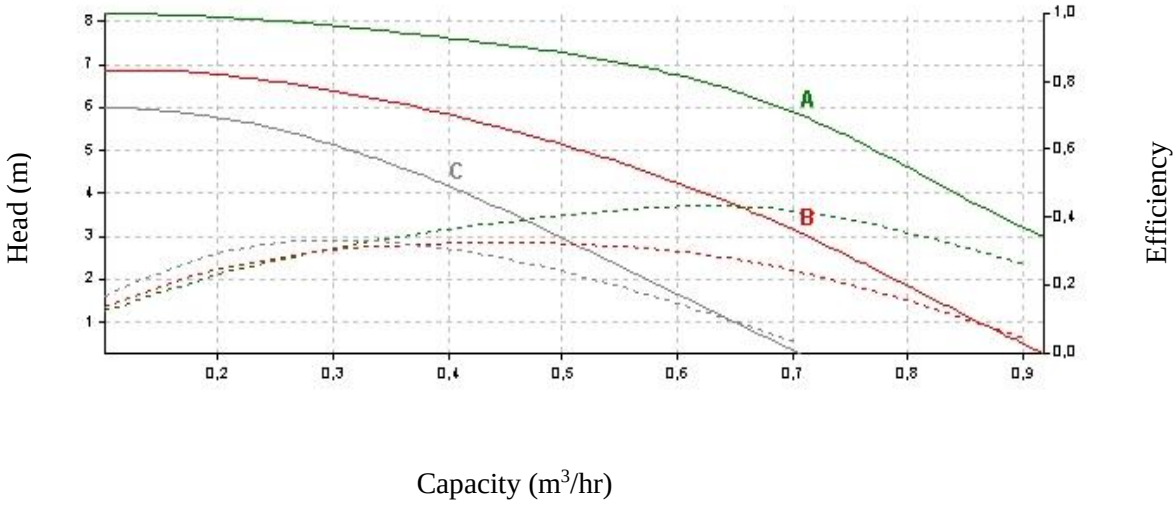

Figure 7-2: Pump curve

7.2 APPENDIX B

7.2.1 Details of design calculation of the vertical flash separator

7.2.1.1 Design procedures

The design of the vertical two phase separator procedures was done by following (Sinnott, 2005).

1. Calculation of the vertical terminal vapour velocity

$$u_g = 0.07\sqrt{\frac{(\rho_l - \rho_g)}{\rho_g}} \qquad \text{Equation 7-13}$$

Where;

u_g - Settling velocity, m/sec

ρ_L – Density of liquid, kg/m^3

ρ_g – Density of vapour, kg/m^3

If a mesh pad is not used, the settling velocity shown in Equation 7-1 must be multiplied by 0.15.

Typical proportions of a vertical separator of the vapour-liquid are presented in Figure 7-3.

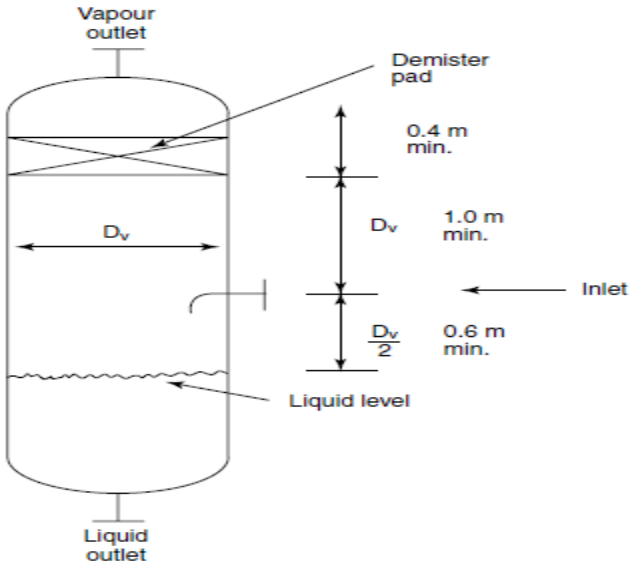

Figure 7-3: Vertical two-phase separator

2. Calculation of the vapour volumetric flow rate.

$$Q_v = \frac{m_v}{\rho_v}$$ Equation 7-14

Where;

Qv - Volumetric flowrate of vapour (m^3/sec)

m_v - Mass flowrate of vapour, (kg/hr)

ρ_g – Density of vapour, kg/m^3

3. Calculation of the vessel inside diameter

The vessel diameter should be big enough to slow down the flow of the gas to a velocity below the particle settling velocity. Therefore, the minimum allowable diameter is shown in Equation 7-15.

$$D_v = \sqrt{\frac{4Q_v}{\pi u_s}}$$ Equation 7-15

Where;

D - Minimum diameter of the separator (m)

Q_v - Volumetric flowrate of vapour (m^3/s)

The liquid level largely depends on the hold-up time needed for effectual operation and control.

4. Calculation of the liquid volumetric flow rate

$$Q_l = \frac{m_l}{\rho_l}$$ Equation 7-16

Where;

Q_L - Volumetric flowrate of the liquid (m^3/sec)

m_L - Mass flowrate of the liquid, (kg/hr)

ρ_l - Density liquid (kg/m^3)

5. Calculation of the holdup volume by select holdup time

$$V_H = (T_h)(Q_l)$$ Equation 7-17

Where: V_H is the volume held in vessel (m^3)

T_h is the holdup times (minutes)

6. Calculation of the liquid depth required

$$h_H = \frac{V_H}{A_v}$$ Equation 7-18

$$A_v = \frac{\pi}{4} D_v^2$$ Equation 7-19

Where: h_H is the liquid depth required (m)

A_v is the vessel cross-sectional area (m^2)

7. Calculation of the height from the liquid depth to inlet vessel. From Figure 8-2.

$$h_{hl} = \frac{D_v}{2}$$ Equation 7-20

Where;

h_{hl} - Height from the liquid depth to inlet vessel (m)

8. Calculation of the height from the inlet vessel to mesh pad

A height equal to or greater than the separator diameter should be used, as shown in Figure 7-3.

$$h_{hh} = D_V$$ Equation 7-21

Where;

h_{hh} - Height from the inlet vessel to mesh pad (m)

9. The minimum height from mesh pad to out let vapour:

   From the figure = 0.4 m

10. Calculation of the total height of vessel

$$h_T = h_H + h_{hl} + h_{hh} + 0.4 \qquad \text{Equation 7-22}$$

7.2.1.2 Calculation of design

The design for the two phase vertical flush separator was done in a ratio (L/D) of 4.8. The design was done based on the physical properties of water, but was applicable to other solutions.

Assumption of design

A preliminary design of a liquid / gas separator

From saturation water, courtesy of Koretsky (2004)

Operation pressure 4 kPa abs

From steam Table saturation temperature is 45.8°C,

ρ_l = 990.09 kg/m3, ρ_g = 0.068 kg/m^3, m_L =14.4 kg/h and m_v = 3.6 kg/h

Vertical terminal vapour velocity

$$u_g = 0.07 \times 0.15 \sqrt{\frac{(990.09 - 0.068)}{0.068}} = 1.27 \text{m/sec}$$

$$Q_v = \frac{3.6}{3600 \times 0.068} = 0.0147 \text{ m}^3/\text{sec}$$

$$D_v = \sqrt{\frac{4 \times 0.0147}{\pi \times 1.27}} = 0.122 \text{ m} \cong 0.125 \text{ m}$$

$$Q_l = \frac{14.4}{990.09 \times 3600} = 0.000004 \text{ m}^3/\text{sec}$$

Allow a minimum of 3 minutes hold-up

$$V_H = 3 \times 60 \times 0.000004 = 0.0007 \text{ m}$$

$$A_v = \frac{\pi}{4} 0.125^2 = 0.0122 \text{ m}^2$$

$$h_H = \frac{0.0007}{0.0122} = 0.059 \text{ m}$$

$$h_{hl} = \frac{0.125}{2} = 0.0625\text{m}$$

$$h_{hh} = 0.125 \text{ m}$$

$$h_T = 0.059 + 0.0625 + 0.125 + 0.35 = 0.5965 \cong 0.6 \text{ m}$$

The total height was reduced to give the main design part (the L/D ratio) of 4.8 using mesh pad (therefore lying between 3 and 5) as recommended in Section 2.4.8 for a vertical separator design. The main reasons for the height reduction was to reduce the equipment cost without affecting the separator efficiency.

7.3 APPENDIX C

7.4 THERMAL PROPERTIES OF SOLUTIONS

7.4.1 WPC solution

The model used for WPC was developed from the thermal property data for food (protein, fat, water, Carbohydrate and ash) (Choi, 1986; Murakami and Okos, 1989). The regression model is applicable for temperature range (-40°C – 150°C).

7.4.1.1 Density

$$\frac{1}{\rho} = \sum \frac{w_i}{\rho_i} \qquad \text{Equation 7-23}$$

Where: w_i is the mass fraction of the component in the solutions (kg/kg)

ρ_i is the density of component in the Solutions. (kg/m^3)

ρ is the density of the total solution. (kg/m^3)

Choi 1986 has given the following models

$$\rho_{protein} = 1.3299 \times 10^3 - 5.1840 \times 10^{-1} T \qquad \text{Equation 7-24}$$

$$\rho_{fat} = 9.2559 \times 10^2 - 4.1757 \times 10^{-1} T \qquad \text{Equation 7-25}$$

$$\rho_{ash} = 2.4238 \times 10^3 - 2.8063 \times 10^{-1} T \qquad \text{Equation 7-26}$$

$$\rho_{carbohydrate} = 1.5991 \times 10^3 - 3.1046 \times 10^{-1} T \qquad \text{Equation 7-27}$$

$$\rho_{water} = 9.9718 \times 10^2 + 3.1439 \times 10^{-3} T - 3.7574 \times 10^{-3} T^2 \qquad \text{Equation 7-28}$$

7.4.1.2 Thermal conductivity

Thermal conductivity can be estimated using the following equations as developed by (Murakami and Okos, 1989**)**

$$K = \sum \emptyset_i \, K_i \qquad \text{Equation 7-29}$$

$$\emptyset_i = \frac{w_i}{\rho_i \sum \frac{w_i}{\rho_i}} = \frac{w_i \, \rho}{\rho_i} \qquad \text{Equation 7-30}$$

Where: Ki is the thermal conductivity of the component in the solutions (W/m.K)

$\emptyset_i$ is the volume fraction of the component in the solutions (kg/kg)

K is the thermal conductivity of the solutions (W/m.K)

ρ_i is the density of component in the Solutions. (kg/m^3)

ρ is the density of the total solution. (kg/m^3)

The density of the solutions is determined using the equation earlier the thermal conductivity are given by following equations Choi (1986).

$$\rho_{protein} = 1.7881 \times 10^{-1} + 1.1958 \times 10^{-3}T - 2.7178 \times 10^{-7}\,T^2 \quad \text{Equation 7-31}$$

$$\rho_{mositure} = 5.7109 \times 10^{-1} + 1.7625 \times 10^{-3}T - 6.7036 \times 10^{-6}\,T^2 \quad \text{Equation 7-32}$$

$$\rho_{fat} = 1.8071 \times 10^{-1} - 2.7604 \times 10^{-4}T - 1.7749 \times 10^{-7}\,T^2 \quad \text{Equation 7-33}$$

$$\rho_{ash} = 3.2962 \times 10^{-1} + 1.4011 \times 10^{-3}T - 2.9069 \times 10^{-6}\,T^2 \quad \text{Equation 7-34}$$

$$\rho_{carbohydrate} = 2.0141 \times 10^{-1} + 1.3874 \times 10^{-3}T - 4.3312 \times 10^{-6}\,T^2 \quad \text{Equation 7-35}$$

7.4.1.3 Heat capacity

The heat capacity of the ideal mixture is given by Equation 8-36 (Murakami and Okos, 1989).

$$C_p = \sum w_i\, C_{pi} \quad \text{Equation 7-36}$$

C_p is the heat capacity of the solution (kJ/kg·K)

The heat capacity of the solution components are given by the following equations (Choi, 1986)

$$\rho_{protein} = 2.0082 + 1.2089 \times 10^{-3}T - 1.3129 \times 10^{-6}\,T^2 \quad \text{Equation 7-37}$$

$$\rho_{water} = 4.1289 + 9.0864 \times 10^{-5}T + 5.4731 \times 10^{-6}\,T^2 \quad \text{Equation 7-38}$$

$$\rho_{fat} = 1.9842 + 1.4733 \times 10^{-3}T - 4.8008 \times 10^{-6}\,T^2 \quad \text{Equation 7-39}$$

$$\rho_{ash} = 1.0926 + 1.8896 \times 10^{-3}T - 3.6817 \times 10^{-6}\,T^2 \quad \text{Equation 7-40}$$

$$\rho_{carbohydrate} = 1.5488 + 1.9625 \times 10^{-3}T - 5.9399 \times 10^{-6}\,T^2 \quad \text{Equation 7-41}$$

7.4.2 Sugar solution (sucrose)

7.4.2.1 Density

Density data for each binary solution as a function of temperature and concentration were fitted to the following model (Darros-Barbosa, *et al.*, 2003);

$$\rho = (a_1 + b_1 S + c_3 S^2) + T(a_2 + b_2 S + c_2 S^2) + T^2(a_3 + b_3 S + c_3 S^2) \quad \text{Equation 7-42}$$

Where: ρ is the density of the solution (g cm^{-3})

S is the solute concentration (g solute 100 ml-solution^{-1})

T is the temperature (^oC)

a_i, b_i, c_i are the regression coefficients.

Table 7-3: Density predictive equation parameters for aqueous sucrose

Regression Coefficients	Value
a_1 (g/cm^3)	1.00042
b_1 (10^2g/g solute)	0.004056
c_1 (10^2 cm^3 g/g $solute^2$)	-4.058e-6
a_2 (g/cm^3 ^oC)	-2.294e-6
b_2 (10^2g/g solute)	-1.332e-5
c_2 (10^2 cm^3 g/^oC g $solute^2$)	2.661e-7
a_3 (g/cm^3 $^oC^2$)	-4.646e-6
b_3 (10^2g/g solute)	1.254e-7
c_3 (10^2 cm^3 g/$^oC^2$ g $solute^2$)	-3.043e-9

7.4.2.2 Thermal conductivity

The model used for thermal conductivity was developed from modelling of the thermo-physical properties of aqueous sucrose solutions (Simion, *et al.*, 2017):

$$K = a + bX + \frac{c}{T} + dX^2 + \frac{e}{T^2} + \frac{fX}{T} + \frac{h}{T^3} + \frac{iX}{T^2} + \frac{jX^2}{T} \quad \text{Equation 7-43}$$

Where: X is the sucrose concentration (wt%) and K is the thermal conductivity, (W/m K), at temperatures T, (K)

The coefficients of the fitted polynomial equation are presented in Table 7-4.

Table 7-4: Thermal conductivity polynomial equation for aqueous sucrose.

Coefficient	Value
a	-0.84385948
b	-0.0051670655
c	1602.2814
d	2.3609905e-06
e	-528571.74
f	0.45271455
h	53598501
i	42.375474
j	-0.0020785223

7.4.2.3 Heat capacity

The model used for sucrose solution was developed from modelling of the thermo-physical properties of aqueous sucrose solutions (Simion, *et al*., 2017):

$$C_p = a + b\,InT + cX + d(InT)^2 + eX^2 + fXInT \qquad \text{Equation 7-44}$$

Where: C_p is the specific heat capacity (J/kg. K), at temperatures T, (K)

X is the sucrose concentration (wt%)

The coefficients of the fitted polynomial equation are presented in Table 7-5:

Table 7-5: Coefficients for equation of sucrose solution

Coefficient	Value
a	25132.56
b	-7267.3551
c	-161.21331
d	630.05763
e	-0.0010015742
f	24.255336

7.5 APPENDIX D

7.5.1 Calculation data of thermal properties of solutions.

7.5.1.1 Thermal property of WPC solution (experiment 15).

Table 7-6: Thermal property of WPC solution (experiment 15)

Concentration (wt%)	Temperature (ºC)	Density (Kg /m^3)	Heat capacity (J/kg. K)	Thermal conductivity (W/m. K)	Viscosity (mPa.s)
5.3	62	995	4013	0.738	1.2
6.2	61.9	997	3994	0.735	1.2
7.3	62.1	999	3971	0.732	1.3
8.9	62.4	1003	3937	0.728	1.6
10.1	62.1	1006	3912	0.723	2.1

7.5.1.2 Thermal property of WPC solution (experiment 16)

Table 7-7: Thermal property of WPC solution (experiment 16)

Concentration (wt%)	Temperature (ºC)	Density (Kg /m^3)	Heat capacity (J/kg. K)	Thermal conductivity (W/m. K)	Viscosity (mPa.s)
11.5	60.6	1010	3881	0.715	2.6
12.1	61.4	1011	3869	0.715	3
13	61.2	1013	3850	0.712	3.4
14.7	60.2	1018	3813	0.704	4.2
15.8	60.5	1021	3789	0.701	5.4
16.7	59.1	1023	3770	0.695	6.6

7.5.1.3 Thermal property of WPC solution (experiment 17)

Table 7-8: Thermal property of WPC solution (experiment 17)

Concentration (wt%)	Temperature (°C)	Density (Kg /m^3)	Heat capacity (J/kg. K)	Thermal conductivity (W/m. K)	Viscosity (mPa.s)
5.6	65.3	994	4005	0.744	1.1
6.9	65.1	997	3978	0.739	1.2
8.1	65	1000	3952	0.735	3.5
11.8	64.3	1009	3874	0.722	4.2

7.5.1.4 Thermal property of Sugar solution (experiment 19)

Table 7-9: Thermal property of Sugar solution (experiment 19)

Concentration (wt%)	Temperature (°C)	Density (Kg /m^3)	Heat capacity (J/kg. K)	Thermal conductivity (W/m. K)	Viscosity (mPa.s)
4.9	63.1	999	4078	0.639	0.7
5.2	62.5	1001	4072	0.637	0.7
6.4	61.9	1005	4048	0.632	0.8
7.9	62.8	1010	4018	0.628	1
9.6	62.9	1016	3984	0.622	1.1

7.5.1.5 Thermal property of Sugar solution (experiment 19)

Carbohydrate properties determined by a model developed by Choi (1986).

Table 7-10: Thermal property of Sugar solution (experiment 19) by using carbohydrate properties.

Concentration (wt%)	**Temperature (ºC)**	**Density (Kg /m^3)**	**Heat capacity (J/kg. K)**	**Thermal conductivity (W/m. K)**	**Viscosity (mPa.s)**
4.9	63.1	1001	3998	0.629	0.7
5.2	62.5	1002	3991	0.628	0.7
6.4	61.9	1007	3963	0.626	0.8
7.9	62.8	1012	3925	0.623	1
9.6	62.9	1019	3883	0.620	1.1

7.5.1.6 Viscosity of WPC

Table 7-11: Viscosity experiment data of WPC solution

Meas. Pts.	T (ºC)	4.2 (wt%)	7.3 (wt%)	9.14 (wt%)	11 (wt%)	12.82 (wt%)	14.56 (wt%)	15.68 (wt%)	17.1 (wt%)
	Viscosity (mPa.s)								
1	59.1	1.41	1.38	1.86	2.48	3.09	4.61	4.3	7.34
2	59	1.2	1.35	1.82	2.47	3.13	4.61	4.22	7.02
3	59.1	1.3	1.38	1.8	2.41	3.03	4.48	4.32	8.85
4	59.6	1.1	1.36	1.82	2.45	3.42	4.44	4.25	10.8
5	60.2	1.2	1.34	1.77	2.39	3.13	4.17	4.34	8.77
6	60.9	1.1	1.34	1.79	2.35	3.21	3.93	4.29	15.5
7	61.4	1.2	1.33	1.75	2.4	3.37	3.95	4.28	16.6
8	61.7	1.1	1.32	1.74	2.37	3.14	3.95	4.39	15.7
9	61.9	1.1	1.31	1.77	2.39	3.42	4.52	4.24	29.1
10	62.2	1.13	1.32	1.73	2.45	3.36	6.18	4.65	25.2
11	62.6	1.18	1.29	1.74	2.48	3.31	8.52	5.55	29.9
12	63	1.1	1.28	1.86	2.65	4.27	11.5	9.36	38
13	63.5	1.11	1.31	1.77	2.58	4.56	12.7	10.9	38
14	63.9	1.12	1.28	2.34	3.04	4.96	20	15.8	51.4
15	64.2	1.09	1.27	3.48	3	5.69	21.7	20.6	66.6
16	64.6	1.12	1.3	3.49	2.93	4.91	25.8	19.5	63.4
17	64.9	1.09	1.27	6.05	4.01	6.61	36.7	31.4	72.2
18	65.2	1.08	1.25	5.6	5.1	9.21	43.4	37.7	69.8
19	65.6	1.09	1.29	6.3	5	8.98	49.4	37	65.4
20	66	1.07	1.27	9.94	6.92	13.8	61.1	56.3	78.4
21	66.4	1.05	1.24	5.93	5.6	13.8	63.2	52.8	69.8
22	66.8	1.05	1.29	8.54	6.38	20.6	61.6	57.6	84.9
23	67.1	1.06	1.31	9.9	8.81	26.5	61.3	73	108
24	67.5	1.05	1.37	10.4	7.91	26.3	65.4	73.2	92.5
25	67.9	1.06	1.91	11.8	12.1	32.2	72.3	65.4	111
26	68.2	1.05	3.41	10.7	14.1	36.3	73.3	80.4	124
27	68.6	1.07	2.74	11.8	14.1	40.3	81.5	67.5	128
28	69	1.07	4.08	20	16	55.9	86.1	79.6	145
29	69.3	1.07	3.68	16.7	20.2	59.3	89.7	91.7	163
30	69.7	1.09	4.36	18.5	22	74.3	86.7	83.7	118
31	70	1.1	6.86	22.6	29.7	68.7	94.2	91.6	136

7.5.1.7 Viscosity of sugar solution

Table 7-12: Viscosity experiment data of sugar solution

	Viscosity (mPa.s)			
Meas.Pts	**T (ºC)**	**4.8 (wt%)**	**7.5 (wt%)**	**9.8 (wt%)**
1	59.1	0.76	1.24	0.93
2	59.1	0.75	1.06	0.97
3	59.2	0.74	1.1	1.04
4	59.6	0.72	1.07	1.07
5	60.2	0.73	1.02	1.06
6	60.8	0.72	1.02	1.08
7	61.3	0.71	0.996	1.07
8	61.7	0.72	1	1.09
9	62	0.71	1.01	1.1
10	62.3	0.71	0.99	1.07
11	62.6	0.71	1.05	1.08
12	63	0.70	0.98	1.13
13	63.4	0.70	1.02	1.14
14	63.8	0.69	0.97	1.13
15	64.2	0.6	0.98	1.1
16	64.6	0.69	0.97	1.09
17	64.9	0.68	1.01	1.12
18	65.3	0.68	0.95	1.13
19	65.6	0.68	1.03	1.12
20	66	0.67	0.96	1.11
21	66.4	0.67	1	1.1
22	66.8	0.66	0.97	1.1
23	67.1	0.65	0.96	1.12
24	67.5	0.66	0.99	1.12
25	67.9	0.65	0.96	1.12
26	68.2	0.64	0.97	1.14
27	68.6	0.65	0.98	1.15
28	68.9	0.64	1.05	1.16
29	69.3	0.64	1.01	1.17
30	69.7	0.64	1	1.17
31	70.1	0.63	1.05	1.19

7.6 APPENDIX E

7.6.1 Heat transfer coefficient calculation

7.6.1.1 Heat transfer coefficient of WPC solution (experiment 15)

Table 7-13: Heat transfer coefficient of WPC solution (experiment 15)

wt%	T(°C)	R_e. Num	Pr. Num	Nu. Num	h_i (W/m^2.K)
5.3	62	402.3	6.5	7.6	431.8
6.2	61.9	388.4	6.8	7.6	430.2
7.3	62.1	370.8	7.1	7.6	428.6
8.9	62.4	291.4	9.1	7.6	426.2
10.1	62.1	232.6	11.4	7.6	424.1

7.6.1.2 Heat transfer coefficient of WPC solution (experiment 16)

Table 7-14: Heat transfer coefficient of WPC solution (experiment 16)

wt%	T(°C)	Re. Num	Pr. Num	Nu. Num	h_i (W/m^2.K)
11.5	60.6	189.6	14.1	7.6	420.5
12.1	61.4	164.7	16.2	7.6	420.2
13	61.2	145.5	18.4	7.6	418.5
14.7	60.2	118.6	22.7	7.6	414.8
15.8	60.5	92.5	29.1	7.6	413.1
16.8	59.1	75.3	36.0	7.6	410.5

7.6.1.3 Heat transfer coefficient of WPC solution (experiment 17)

Table 7-15: Heat transfer coefficient of WPC solution (experiment 17)

wt%	T(ºC)	Re. Num	Pr. Num	Nu. Num	h_i (W/m^2.K)
5.6	65.3	419.6	6.2	7.5	433.6
6.9	65.1	393.8	6.6	7.5	431.4
8.1	65	138.1	19	7.5	429.4
11.8	64.3	117.4	22.5	7.6	422.8

7.6.1.4 Heat transfer coefficient of Sugar solutions (experiment 19)

Table 7-16: Heat transfer coefficient of Sugar solutions (experiment 19)

wt%	T(ºC)	Re. Num	Pr. Num	Nu. Num	h_i (W/m^2.K)
4.9	63.1	680	4.5	8.06	396.3
5.2	62.5	638.8	4.9	8.06	395.6
6.4	61.9	553.9	5.6	8.08	393.5
7.9	62.8	478.4	6.6	8.09	391.4
9.6	62.9	445.2	7.1	8.11	388.7

7.6.1.5 Heat transfer coefficient of Sugar solutions (experiment 19)

Table 7-17: Heat transfer coefficient of Sugar solutions (experiment 19) by using carbohydrate properties.

wt%	T(ºC)	Re. Num	Pr. Num	Nu. Num	h_i (W/m^2.K)
4.9	63.1	681	4.5	8.05	389.9
5.2	62.5	639.7	4.8	8.05	389.5
6.4	61.9	554.8	5.6	8.05	388.2
7.9	62.8	479.6	6.5	8.05	386.73
9.6	62.9	446.7	6.9	8.06	384.9

7.7 APPENDIX F

7.7.1 Experimental data

Table 7-18: Experiment 15 data of WPC solution

Time (min)	Q (ml/min)	Th_8 (°C)	Th_7 (°C)	Th_1 (°C)	Th_2 (°C)	Th_3 (°C)	Th_4 (°C)	Th_5 (°C)	Th_6 (°C)	Pressure kPa abs	(ml)
0	308	65	20	21.1	20	20.3	9.4	20	72	21.3	0
10	301	66.5	64.4	59.7	59.3	58.8	9.6	21	69	17.3	0
20	314	64.9	64.7	59.8	63.5	61.2	11.1	22.1	66	15.3	60
30	297	64.5	64.6	58.8	63.6	60.3	12.5	21.8	66.7	15.3	155
40	295	63.8	64.8	58.8	63.5	60.8	11.1	22	65	15.3	245
50	297	64.1	64.3	59.1	62.9	60.3	11.6	22.4	65.3	13.3	345
60	293	64.1	64.5	59.3	63.1	60	13	22.6	65.6	13.3	440
70	295	64.9	65	59.8	63.6	59	12.3	22.9	66.1	13.3	550
80	287	64.1	64.3	59.3	63.5	60.9	9.5	22.6	64.8	13.3	650
90	316	64.2	64	59.7	63.3	59.3	9.8	22.6	65.5	13.3	765
100	307	64.1	64.2	59.3	63.4	58.6	11.3	23	67.8	13.3	870
110	301	65	64.6	59.4	63.6	58.9	12.1	22.9	67.8	13.3	970
120	299	64.5	64.5	59.8	63.6	61	11.4	23	65.9	13.3	1080
130	295	64.6	64.3	59.6	64	60.1	12.1	22.9	66.1	13.3	1190
140	285	64.7	64.2	60.1	63.5	60.5	12.7	23.1	67.7	13.3	1290
150	289	64.3	64.3	59.6	63.5	60.7	11.1	23.1	71.3	13.3	1385
160	301	64.6	64.3	60.3	63.4	60.8	10.8	23.1	68.4	13.3	1475
170	314	65	64.5	61	63.8	60	11.6	23.2	70.2	13.3	1560
180	314	64.7	64.8	60	64.3	60	12.6	23.3	71.6	13.3	1640
190	310	64.2	65.2	60.5	64.6	60	12.8	23.1	69.7	13.3	1725
200	295	64.6	65	60.4	64.5	61.6	11.4	22.4	70.1	13.3	1810
210	305	64.1	65	60.4	64	61	10	22	70	13.3	1890
220	301	64.1	64.8	60.5	64.5	60.3	10.4	21.8	69.9	13.3	1975
230	297	63.9	65	60.5	64.3	60.5	10.6	22	69.3	13.3	2055
240	285	64.1	64.2	60.1	63.8	58.8	10.6	22.1	70.8	13.3	2130

Table 7-19: Experiment 16 data of WPC solution

Time (min)	Flow rate (ml/min)	Th_8 (°C)	Th_7 (°C)	Th_1 (°C)	Th_2 (°C)	Th_3 (°C)	Th_4 (°C)	Th_5 (°C)	Th_6 (°C)	pressure kPa abs	(ml)
0	275	65	14.3	15.2	14.2	14.7	6.5	14.1	75.3	17.3	0
10	308	64.5	54.5	56.3	48.2	47.3	6.8	15.8	79	11.3	0
20	303	65.4	64.2	56.7	60.1	59.1	7.9	16.4	69.5	16.3	35
30	326	65.2	64.7	57	61.5	59	8.1	16.6	72.3	16.3	70
40	314	65.4	65	58.1	62	59.7	7.9	16.8	71.3	15.3	105
50	299	65.5	65.3	57.6	62.2	58.9	7.8	17.1	71.4	15.3	145
60	295	66.5	65.1	58.2	62.3	59.5	8.1	17.1	72.8	15.3	185
70	291	66.5	64.8	58.4	61.8	58.5	8.8	17.4	74	15.3	245
80	306	65.1	64.8	58.1	61.9	58.1	9.5	17.6	73	15.3	310
90	285	64.8	65	58.1	62.3	58.7	10	17.4	72.5	15.3	375
100	318	65	64.5	58.1	61.9	58.8	9.7	17.9	74.9	14.3	435
110	314	65.8	63.8	59.1	60.8	58.3	9.5	18.1	74.9	13.3	495
120	316	65.1	64	58.5	61.1	57.4	9.6	18.1	76.7	13.3	560
130	299	65.8	64.1	56.8	60.5	55.4	11	17.8	74	13.3	620
140	291	65	64	58.2	60.6	57	11.4	17.9	71.3	13.3	670
150	303	65.6	64.2	58.2	60.8	56.3	10.9	18	73.5	13.3	720
160	285	66.5	64.4	58.6	60.8	57.3	10.7	18.1	75.3	13.3	770
170	307	65.3	64	57.7	60.6	57.8	9.1	18.2	71.8	12.3	820
180	314	64.8	63.8	56.6	60.3	57.7	8.8	18.3	70.9	11.3	870
190	301	65.8	63.3	57.5	59.8	57.9	8.8	18.5	75.6	11.3	935
200	332	64.9	63.3	57.6	59.7	57	9.3	18.6	77.1	11.3	1000
210	289	65.6	63.5	58	60	56.8	9.8	18.6	72.8	11.3	1065
220	310	66.2	63.6	57.9	60	55.7	10.3	18.7	76	11.3	1125
230	314	67.3	63.4	57.4	59.8	57.1	10.3	18.6	76	11.3	1185
240	301	66.5	63.5	57.5	59.9	56.9	10.5	18.9	74.8	11.3	1245
250	297	64.8	62.3	55.6	58.5	56.3	10.3	18.9	78.3	11.3	1305
260	285	67	62.6	57	58.8	55.6	10.8	19.4	79.1	9.3	1355
270	307	65.5	62.6	55.6	59	55	11.3	19.4	75.3	9.3	1420
280	316	64.5	62.8	55.1	59	54	11.3	19.3	79	9.3	1470
290	287	66.7	62.8	55.7	59	54.8	11.1	19.2	82.8	9.3	1525
300	310	65.3	62.2	55.2	58.8	54.9	11.2	19.4	79	9.3	1575

Table 7-20: Experiment 17 data of WPC solution

Time (min)	Flow rate ml/min	Th_8 (°C)	Th_7 (°C)	Th_1 (°C)	Th_2 (°C)	Th_3 (°C)	Th_4 (°C)	Th_5 (°C)	Th_6 (°C)	pressure kPa abs	(ml)
0	320	65	15.9	17.4	15.8	16.1	6.7	15.4	71.2	21.3	0
10	305	71.2	63	57.2	17.6	45	6.1	16.5	84.3	15.3	0
20	295	70.2	69	61.6	62.1	53	6.3	16.9	79.7	14.3	135
30	281	70.3	68	60.8	64	55.8	11.1	19.1	74	14.3	290
40	291	70.3	68.5	60.9	64.5	59.4	12.1	19.5	76.8	14.3	450
50	287	70.5	68.5	61.2	64.8	59.6	10.4	19.6	78	14.3	605
60	316	69.5	69	61.2	64.1	57.9	11.5	19.5	76.1	14.3	765
70	326	70.9	69.1	60	64.9	56.3	12.2	19.8	81.4	14.3	900
80	322	70.3	69.2	62.2	64.1	58	12.3	19.8	79	14.3	1025
90	305	70.1	69.5	61	64.3	60.2	11.6	19.9	82.4	14.3	1155
100	293	69.2	68.8	60.3	64.2	59.5	10.6	19.8	81.8	14.3	1300
110	316	70.1	68.7	61.1	64.3	59.8	10.2	19.8	79.5	14.3	1445
120	314	70.1	69	61.1	64.2	58.7	11.1	19.9	81.9	14.3	1565
130	326	69.8	69.2	60.5	64.3	58.3	13.6	20.2	83.3	14.3	1700
140	310	70	69.3	59.3	64.4	57.9	11.1	20.2	84	14.3	1840
150	291	71.3	69.5	59.3	64.1	57.6	12.9	20.3	77.8	14.3	1990
160	295	65.2	68.6	57.4	64.7	59	12	20.3	80.9	14.3	2145
170	301	71.3	68.7	60.3	63.3	57.1	12.7	20.3	84.4	14.3	2305
180	275	69.5	69.3	59.3	63.6	58.8	12.3	20.5	82.3	14.3	2475

Table 7-21: Experiment 19 data of sugar solution

Time (min)	Flow rate (ml/min)	Th_8 (ºC)	Th_7 (ºC)	Th_1 (ºC)	Th_2 (ºC)	Th_3 (ºC)	Th_4 (ºC)	Th_5 (ºC)	Th_6 (ºC)	pressure kPa abs	(ml)
0	320	65	18	19.4	17.9	18.2	9.5	17.5	68.8	22.3	0
10	295	65.5	65.5	60.8	45	60.3	7.4	18.8	67	15.3	0
20	285	64.8	65.5	60.4	64.1	60.8	9.6	19.6	65	15.3	50
30	301	64	65.5	59.3	64.1	60.9	10.4	19.8	64.4	15.3	115
40	285	64.6	65.5	59.8	64.5	62.1	10.6	20.1	65.5	15.3	180
50	303	64.5	64.8	60	63.3	60.5	9	20.3	65.5	15.3	250
60	287	64	64.8	59.4	63.6	60	9.6	20.3	65.9	15.3	320
70	283	64.4	64.6	60.3	63.5	60.1	11.3	21.2	65.7	15.3	400
80	291	64.1	65.1	59.8	63.8	61.4	10	20.8	65.8	14.3	530
90	303	64.7	65.3	59.8	64	60.1	10.6	21.1	68.1	14.3	655
100	297	64.5	65.6	60	64.3	60.8	9.5	21	67	14.3	785
110	301	64.1	65.6	60	64.5	62.3	9.3	20.8	64.8	14.3	900
120	316	64.1	64.6	59.3	63.4	61	10	21	68.9	14.3	1035
130	301	64.3	64.7	60.1	63.8	59.8	10.2	21.6	67.6	14.3	1145
140	305	64.1	65	60.1	63.9	61.6	9.1	21.3	65.8	14.3	1245
150	297	64.4	65	60.3	64	61.5	10	21.2	67	14.3	1340
160	293	64.3	66.2	60.1	64.5	60.8	10	21.5	68.1	14.3	1430
170	295	64.3	66	60.1	64.1	62	9	20.7	68.7	14.3	1520
180	303	65.1	65	60.6	63.9	61.8	9.9	21.9	69.7	14.3	1615
190	308	64.2	65.5	60.3	64.4	59.3	10.3	22.1	67.6	14.3	1700
200	332	63.7	65.7	60.2	64.5	60.2	10.6	22.1	67.1	13.3	1780
210	316	64.6	66.2	61	65	62.9	9	22	68	13.3	1855
220	310	64.4	66.3	60.5	65	62.1	8.8	22	67.5	13.3	1935
230	291	64.5	66.6	60.6	65	62.8	9.3	22	68	13.3	2015
240	283	63.5	65.5	60.4	64.6	60.8	9.4	22.2	67.5	13.3	2095

Table 7-22: Experiment 14 data of NaCl solution

Time (min)	Flow rate (ml/min)	Th_8 (°C)	Th_7 (°C)	Th_1 (°C)	Th_2 (°C)	Th_3 (°C)	Th_4 (°C)	Th_5 (°C)	Th_6 (°C)	pressure kPa abs	(ml)
0	305	65	17.8	19.2	17.6	18	7.7	17.2	74.3	21.3	0
10	291	65	63.4	59	48	55.1	7.3	18.3	68.6	17.3	50
20	324	64.7	64.8	59.1	63.5	59.5	11.2	19.8	64.8	15.3	150
30	281	64.1	64.7	58.1	62.8	59.5	10.3	20.3	65.2	15.3	250
40	299	64.1	64.9	59.1	63.3	60.3	10.6	20.1	65	15.3	350
50	307	64	65.1	58.8	63.5	61.6	11.3	20.1	65.7	15.3	460
60	287	64	64	59	62.3	60.8	10.1	20.4	64.8	15.3	570
70	330	64.1	64.2	59.3	62.6	60.6	11.1	20.5	65.9	15.3	690
80	328	63.6	64.8	59.1	63.3	60.1	11.2	20.4	66.1	15.3	810
90	303	64.5	64.9	59.5	63	61.8	10.5	20.6	65.8	15.3	930
100	301	64.4	65.1	59.1	63.3	62	11.1	20.5	65.6	15.3	1050
110	301	64.1	65.5	59.1	63.5	60.9	11.7	20.3	67.3	15.3	1170
120	295	64.3	64.5	59.5	62.8	60.8	10.3	20.4	67.8	15.3	1290
130	301	64.8	64.3	60	62.5	61.1	11.1	20.5	69.8	15.3	1405
140	297	63.5	64.8	59.3	63	61.1	10	20.7	69.1	15.3	1520
150	295	63.9	65.1	59.9	63.4	60.8	10	20.4	68.6	15.3	1630
160	285	64.5	65.3	59.6	63.7	61.6	11.1	20.6	66.6	15.3	1740
170	289	64.8	65.5	59.8	63.6	59.6	11.7	20.5	69.1	15.3	1845
180	293	64.3	64.2	60.1	62.8	58.8	11.1	20.8	69.9	15.3	1960
190	281	64	65.1	59.8	63.3	60.2	13.1	21	69.3	15.3	2060
200	293	64.5	65.5	59.8	63.5	62.1	10.5	20.8	70.5	15.3	2155
210	291	64.1	65.6	59.7	63.5	61	10.6	20.8	69.3	15.3	2250
220	283	64.1	66.1	59.6	63.6	61.3	11	20.9	68.6	15.3	2345
230	289	64.8	65.2	60	63	60.7	11.3	21.3	70.5	15.3	2440
240	303	64.1	65.6	59.6	63.1	60.2	12	21.1	70.5	15.3	2535

Table 7-23: Comparing evaporating conditions between of (WPC, sugar Solution, NaCl solution)(experiments 15, 19 and 20)

	WPC solution			**Sugar solution**			**NaCl solution**		
Time (min)	**T_{Feed} (C°)**	**T_{flash} (C°)**	**pressure (kPa abs)**	**T_{Feed} (C°)**	**T_{flash} (C°)**	**pressure (kPa abs)**	**T_{Feed} (C°)**	**T_{flash} (C°)**	**pressure (kPa abs)**
0	20	20	21.3	18	17.9	22.3	17.8	17.6	21.3
10	64.4	59.3	17.3	65.5	45	15.3	63.4	48	17.3
20	64.7	63.5	15.3	65.5	64.1	15.3	64.8	63.5	15.3
30	64.6	63.6	15.3	65.5	64.1	15.3	64.7	62.8	15.3
40	64.8	63.5	15.3	65.5	64.5	15.3	64.9	63.3	15.3
50	64.3	62.9	13.3	64.8	63.3	15.3	65.1	63.5	15.3
60	64.5	63.1	13.3	64.8	63.6	15.3	64	62.3	15.3
70	65	63.6	13.3	64.6	63.5	15.3	64.2	62.6	15.3
80	64.3	63.5	13.3	65.1	63.8	14.3	64.8	63.3	15.3
90	64	63.3	13.3	65.3	64	14.3	64.9	63	15.3
100	64.2	63.4	13.3	65.6	64.3	14.3	65.1	63.3	15.3
110	64.6	63.6	13.3	65.6	64.5	14.3	65.5	63.5	15.3
120	64.5	63.6	13.3	64.6	63.4	14.3	64.5	62.8	15.3
130	64.3	64	13.3	64.7	63.8	14.3	64.3	62.5	15.3
140	64.2	63.5	13.3	65	63.9	14.3	64.8	63	15.3
150	64.3	63.5	13.3	65	64	14.3	65.1	63.4	15.3
160	64.3	63.4	13.3	66.2	64.5	14.3	65.3	63.7	15.3
170	64.5	63.8	13.3	66	64.1	14.3	65.5	63.6	15.3
180	64.8	64.3	13.3	65	63.9	14.3	64.2	62.8	15.3
190	65.2	64.6	13.3	65.5	64.4	14.3	65.1	63.3	15.3
200	65	64.5	13.3	65.7	64.5	13.3	65.5	63.5	15.3
210	65	64	13.3	66.2	65	13.3	65.6	63.5	15.3
220	64.8	64.5	13.3	66.3	65	13.3	66.1	63.6	15.3
230	65	64.3	13.3	66.6	65	13.3	65.2	63	15.3
240	64.2	63.8	13.3	65.5	64.6	13.3	65.6	63.1	15.3

7.8 APPENDIX G

7.8.1 Operating procedure of equipment

7.8.1.1 Starting

1) Turn on the temperature recorder (LCD display)
2) Turn on the cooling finger in the condenser water container and add some ice blocks to maintain the temperature as low as possible.
3) Close all process valves except the feed recirculation gate valve, which should be fully opened.
4) Adjust the feeder tank temperature to the set point as required by the experiment run.
5) Turn on the water supply to the condenser.
6) Switch on vacuum pump (V1).
7) Check the sealing of the vacuum trap and evaporating side (ensure that the vacuum pressure P = 10.3 kPa abs), and adjust the vacuum level inside flash separator until the correct pressure is obtained.
8) Start the feed pump, ensure that the product enters the flash separator, and adjust the feed flow rate to the desired value.
9) Turn on the heating coil and set the temperature by adjusting the temperature controller.
10) Start the second vacuum pump (V2) and adjust the vacuum level of the concentrate liquid receiver.
11) Open the drain valve of the flash separator to drain the liquor concentrate to the liquor receiver and then close the valve.
12) Drain the liquor concentrate from the liquor receiver to the feeder tank.
13) Drain the condensate from the vacuum receiver to vacuum trap (TR3) and then close the drain valve.

7.8.1.2 Cleaning

1) Release the vacuum in the evaporating side.
2) Rinse the equipment with tap water for 20 minutes.
3) Rinse the equipment with 0.2 % NaOH for 20 minutes.
4) Rinse the equipment with tap water for 20 minutes.

7.8.1.3 Stopping

1) Switch off the heating coil and the heating element in a heating jacket.
2) Stop the first vacuum pump.
3) Release the vacuum in the evaporating side.
4) Stop the feed pump and the second vacuum pump.
5) Close the cooling water supply to condenser.
6) Switch off the temperature recorder.
7) Allow the solution in the feeder tank to cool down then drain it.

7.8.1.4 Operating caution

1) Never run the centrifugal pump without liquid. If allowed to run dry, the pump may be destroyed.
2) Never switch the heating coil on without liquid flowing inside it, if it is switched on then the coil will burn.
3) The condenser should be supplied with enough cooling water to keep the outgoing water temperature below the evaporation temperature.
4) Always keep eyes on the temperature recorder and flow rate recorder whilst running, to make sure that the flowrate or the heating do not go too high or too low.
5) Always keep eyes on the level indicator of the separator whilst running, so as to drain the liquid when the level rises too high.